universität wien

MASTERARBEIT | MASTER'S THESIS

Titel | Title

Arguments for and against the essentiality of recombinases RadA, RadB in N. magadii and newly identified ϕCh1 nucleocapsids

verfasst von | submitted by

Roland Trieu Hau Ha BSc

angestrebter akademischer Grad | in partial fulfilment of the requirements for the degree of

Master of Science (MSc)

Wien | Vienna, 2025

Studienkennzahl lt. Studienblatt | Degree programme code as it appears on the student record sheet:	UA 066 830
Studienrichtung lt. Studienblatt | Degree programme as it appears on the student record sheet:	Masterstudium Molecular Microbiology, Microbial Ecology and Immunobiology
Betreut von | Supervisor:	ao. Univ.-Prof. Dipl.-Biol. Dr. Angela Witte

Acknowledgement

I want to express my deepest gratitude's and thanks to my supervisor Angela Witte. Not only did she gave me the opportunity to work in her lab, she also supported me through the whole time. No matter if the problems regarded science or life.

Further, I want to show my gratitude to my colleagues Ermirë Jerliu and Helene Eliaćik with whom I had a great time during the lab.

Next, I would like to show my gratitude to Hena Comić and Elisa Husting from the Moll Lab. They provided me with incredible warm support. Another member I want to address and give a special thanks to is Armin Resch for his guidance when I struggled.

In addition, I would like to thank Reinhard Klein and his colleagues from IMC University of Applied Sciences Krems for performing the mass spectrometry.

Furthermore, I want to thank my family. My loving mother, Thuy Lien, and father, Dat Nam Ha, made my study possible. My sisters, Martina Ha and Christine Ströbitzer, provided me with their support and believed in me.

Lastly, I want to thank Dominik Jobst, to whom I would like to dedicate this work. He showed me how beautiful life can be. Without his incredible support, encouragement and belief in me, my study would not have been possible.

Abstract

The temperate archaeal virus ϕCh1 infects *Natrialba magadii*, its only known host. The virus contains an invertible region comprising open reading frame (ORF) 34, *int*1 and ORF36, which could determine the host range. This study aimed to show the influence of the putative responsible recombinases RadA and RadB on the ϕCh1 invertible region. However, attempts to delete either all chromosomal *radA* or *radB* in *N. magadii* have not been successful. Consequently, this study tried to answer whether these genes are essential to this organism. Hence, this thesis analysed the time kinetics of transformants harbouring inducible antisense *radA* or *radB* RNA codon plasmids. Furthermore, a spot test was performed. Unfortunately, the results do not support this hypothesis.

In addition, this thesis aspired to identify further structural components of ϕCh1. Mass spectroscopy analysis of purified virus particles showed that nine ORFs encoded potentially for nucleocapsid proteins. Of these, six could be identified as ϕCh1 nucleocapsids through Western Blot. These newly discovered viral-structure proteins-coding ORFs are located at the beginning and centre of the viral genome.

Zusammenfassung

Der temperate Archaea Virus ϕCh1 infiziert *Natrialba magadii*, seinen bislang einzig bekannten Wirt. Das Virusgenom enthält eine invertierbare Region bestehend aus dem offenen Leserahmen (ORF) 34, *int*1 und ORF36, die den Wirtskreis definieren könnte. Diese Arbeit versucht die Auswirkung der dafür vermeintlich verantwortlichen Rekombinasen RadA und RadB auf die Inversionsregion von ϕCh1 zu zeigen. Allerdings konnte weder *radA* noch *radB* erfolgreich aus allen Chromosomen in *N. magadii* deletiert werden. Auf diesem Ergebnis aufbauend versucht diese Arbeit zu beantworten, ob diese Gene essentiell für diesen Organismus sind. Folglich wurden Zeitreihen von Transformanten analysiert, die induzierbare antisense kodierende *radA* oder *radB* RNA Plasmide enthielten. Weiters wurde ein Spot Test durchgeführt. Bedauerlicherweise stützen die Erkenntnisse diese Hypothese nicht.

Ein weiterer Teil dieser Arbeit fokussierte sich auf die Identifizierung neuer ϕCh1 Strukturproteine. Die Auswertung der Massenspektroskopien von aufgereinigten Virenpartikeln gaben Rückschluss auf neun ORFs, die potentiell für Kapside kodieren. Sechs davon konnten als ϕCh1 Kapside mittels Western Blot nachgewiesen werden. Die neu entdeckten viralen Strukturproteine kodierenden ORFs befinden sich am Anfang und in der Mitte des viralen Genoms.

Contents

1. Introduction

1.1. Archaea

Archaea are the third domain of life besides Bacteria and Eukarya (Woese et al., 1990). For a long time the classification among life was only divided into *Prokaryotae* and *Eukaryotae*, a classification which was not according to their phylogeny although it was treated as such (Woese & Fox, 1977). Williams et al. (2020) proposed a two-domain tree of life, claiming that eukaryotes originate from an archaeal branch. They identified *Heimdallarchaeota* as the current best candidate for the closest relative between Archaea and Eukarya.

Archaea are found in most ecosystems and predominantly in extreme environments (Cavicchioli et al., 2003). It was thought that this domain only included (i) extreme thermophiles with growth conditions at 80 °C or above, (ii) halophiles which require at least 2 M NaCl and (iii) strictly anaerobic methanogens (Cavicchioli & Thomas, 2000). This changed when sequencing analysis together with culturing studies showed that Archaea can also be found in environments which are aerobic, cold or temperate (DeLong, 1998; Karner et al., 2001). Interestingly, no pathogenic Archaea could be identified so far (Cavicchioli et al., 2003). However, there are indications that methanogenic Archaea, such as *Methanobrevibacter smithii,* are associated with diverticulosis (Weaver et al., 1986).

1.1.1. Haloarchaea

Halophilic Archaea are classified within the superphylum of Euryarchaeota (Woese et al., 1990). These extremely halophilic organisms grow in environments which exceed salt concentration of 250 – 300 g L^{-1} (Oren, 1994). The most dominant cellular life form among these appears to be Haloarchaea (Grant et al., 2001). The high-saline environment requires strategies to maintain a turgor pressure or at least an isoosmotic condition as membranes are permeable to water (Oren, 2002). Sodium ions are toxic for the cell, so they are generally expelled via Na^+/H^+ antiporters from the cell interior (Oren, 1999). Haloarchaea have high intracellular concentrations of KCl with 4 M (Grant, 2004). The use

of inorganic ions such as KCl is only used by Haloarchaea and anaerobic Bacteria of the order Haloanaerobiales as osmoprotectant (Grant, 2004; Kushner, 1978). Furthermore, the proteins of such organisms require modifications as well. It was suggested that the protein surfaces may be protected by high levels of cations to promote stability (Mevarech et al., 2000). It appears that proteins of Haloarchaea have fewer hydrophobic amino acid residues because salt may maintain the protein structure by stabilising the otherwise weak hydrophobic interactions (Grant, 2004). Generally, it is accepted that the proteins of halophiles are acidic (Lanyi, 1974; Larsen, 1967). If salt concentrations decrease below 1 M most enzymes are denatured and, therefore, inactive (Adams & Kelly, 1995). Taken together, it can be challenging to work with halophilic Archaea, especially proteins isolation and purification.

1.1.2. Natrialba magadii

Natrialba magadii is a haloalkaliphilic Archaea and was first isolated from a soda lake in Africa. Tindall et al. (1984) described this organism as obligate aerobe and rod-shaped appearance with a length of 0.5 – 0.7 µm. Further, the authors mention that the growth of *N. magadii* is sensitive to low temperature and that it grows at best between 37 – 42 °C. As a haloalkaliphilic organism it needs sodium chloride concentrations of 4 to 5 M (Tindall et al., 1984), Mg^{2+} concentrations below 10 mM, and pH between 8.5 and 11 (Kamekura et al., 1997).

Aerobic halophilic archaea are the main microbial biomass component in soda lakes (Oren, 2002). High concentrations of C-50 carotenoid pigments are found in most of these members in the cell membrane and this contributes to the red colour of the lakes (Oren, 1994). This explains why cultures or colonies of *N. magadii* can also appear in red or pink.

A study from 2006 showed that halophilic organisms have multiple copies of chromosomes as *Halobacterium salinarum* contains 25 copies of chromosomes during the exponential phase and 15 copies in the early stationary phase (Breuert et al., 2006). The same study obtained similar results for *Haloferax volcanii*. Accordingly, it is assumed that *N. magadii* has multiple chromosomes as well, containing around 50 copies of the

chromosome during the exponential phase (A. Witte, personal communication, February 3, 2025).

There are two laboratory strains used. Witte et al. (1997) obtained the strains *N. magadii* L11, which carries the genome of the virus ϕCh1, from isolation of a single plaque and L13, which has lost the genetic information of the virus by continuous passaging. They showed that L13 can be reinfected with ϕCh1 again, making it suitable as an indicator strain.

1.2. Recombinases

The repair of the DNA is a basic feature and its fundamental mechanisms were first described through the discovery of RecA by Clark & Margulies (1965). Double-strand DNA (dsDNA) breaks can occur due to several environmental factors such as reactive chemicals or ion radiation (Wu et al., 2004). Homologous recombination can repair these breaks, so it is no surprise that this mechanism is found in all three kingdoms of domains (Cromie et al., 2001). Consequently, the DNA strand exchange through homologous recombination is performed by different enzymes such as RecA in Bacteria (Clark & Margulies, 1965), RadA or Rad51 (RadB) in Archaea (Sandler et al., 1996), Rad51 in Eukarya (Shinohara et al., 1992) and meiosis specific DMC1 (Bishop et al., 1992). Although amino-acid sequence alignments among these showed weak similarities, Yang, VanLoock, et al. (2001); Yang, Yu, et al. (2001) and Yu et al. (2001) suggested a two right-handed helical structure, one of which is extended and active while the other is compact and inactive (Wu et al., 2004). Further, these studies suggested from performed neuron scattering, atomic force microscopy and electron microscopy experiments that the filament of recombinase together with single-stranded DNA (ssDNA) and ATP has a pitch of ~90 to 110 Å with about six recombinase subunits. Egelman (2001) argued that this conserved helical structure could be driven from the DNA performing an intrinsic stretch to allow the strand exchange. All recombinases of all domains have a short polymerisation motif followed by an ATPase core (Pellegrini et al., 2002). Nevertheless, they have different N- and C-terminals. Hence, RadA, Rad51 and DMC1 show a fairly conserved N-terminal domain while for RecA the comparison shows these similarities for the C-terminus (Yang,

VanLoock, et al., 2001). They are, therefore, referred to as a superfamily (Wu et al., 2004). Yang, Yu, et al. (2001) showed that archaeal RadA exists in octameric rings and helical filaments. Further, they describe that both of these can bind DNA. Interestingly, the ATP-driven formation of helical RadA nucleoprotein filaments on the DNA resembles the filament formation driven by RecA in *Escherichia coli* (Yu & Egelman, 1993). Sequences analysis showed that RadB proteins are similar to *E. coli* RecA domain II (Friedberg et al., 1995; Rashid et al., 1996), also known as mCor named by Sandler et al. (1996). Komori et al. (2000) suggested from biochemical properties that RadB is not a recombinase. They explain that the ATP turnover of *Pyrococcus furiosus* RadB is not potent and that it is unable to perform strand exchange reactions. Nevertheless, RadB can bind to ssDNA as well as dsDNA (Komori et al., 2000), to polymerase D of the DNA exonuclease subunit (Hayashi et al., 1999), to RadA and Hjc resolvase (Komori et al., 2000). RadB could act as an inhibitor of Hjc and upon ATP binding, RadB may dissociate, enabling Hjc to cleave the Holiday junction (Komori et al., 2000). However, the knowledge of recombination relies mostly on studies performed in bacterial or eukaryotic organisms (Haldenby et al., 2009).

1.3. Shuttle vector and selection markers

Shuttle vectors are a suitable tool for transformation into haloalkaliphilic organisms because they can be produced in a sufficient amount by *E. coli* prior to the transformation. RepH with an AT-rich region functions as minimal origin of replication for plasmids of halophilic archaea (Ng & DasSarma, 1993). The virus-ϕCh1 open reading frame (ORF) 53 and ORF54 sequences have similarities to the gene *repH*. Mayrhofer-Iro et al. (2013) cloned the mutated *gyrB* of *Haloferax alicantei* into pKSII+ resulting in plasmid pNov-1. Further, the authors described the cloning of different parts of ORF53 and ORF54 into pNov-1, which gave rise to plasmids pRo-1 to pRo-11. They reported that of these eleven vectors, pRo-5 showed a high transformation efficiency and was suitable for future experiments with ϕCh1 and *N. magadii*. The copy number of pRo-5 with 1 to 5 was determined by Ladurner (2008). Another shuttle vector is pNB102, which was driven from plasmid pNB101 by the insertion of ColE1, the origin of replication of *E. coli*, and genes

mediating ampicillin (Amp) and mevinolin (Mev) resistance (Zhou et al., 2004). This shuttle vector has a copy number of around 20 (A. Witte, personal communication).

Novobiocin (Nov) inhibits DNA gyrase by binding to the β-subunit and blocks the binding site of ATP. Resistance against novobiocin is mediated by *H. alicantei gyrB* since it contains 3 point mutations compared to the wildtype *gyrB* (Holmes et al., 1991). The antibiotic Mev targets the lipid synthesis. Isoprenoid lipids need mevalonate (Brown & Goldstein, 1980), but its synthesis is prevented by the inhibition of 3-hydroxy-3-methylglutaryl-coenzyme A (HMG-CoA) reductase through Mev (Lam & Doolittle, 1992). The resistance against it is mediated through Mev^R because it likely cause increased synthesis of HMG-CoA reductase (Cabrera et al., 1986). In addition, Lam & Doolittle, 1992, showed by comparison of the wildtype mev^S (sensitive) and mutated mev^R (resistant) sequences that the transition from G to T, 29 bp upstream of the translation initiation site, leads to the destroying of *Mlu*I-site and this may cause the resistance.

1.4. Tryptophan inducible promoter

To study genes of interest, it is common to clone them under the control of an inducible promoter such as the commonly used *lac* promoter from *E. coli* (Donovan et al., 1996). Unfortunately, these systems cannot be applied to halophilic organisms. In an ideal world, a promoter used for induction experiments would be completely inactive during repression, highly induced in the presence of the substrate or condition and would not interfere with other genes (Large et al., 2007). In 2007, inducible promoters were analysed using DNA microarray (Large et al., 2007; Zaigler et al., 2003). Therefore, Large et al. (2007) could identify that the tryptophanase (*tna*) gene was hardly expressed if tryptophan was absent. Further, the authors pointed out that transcription levels were very low in media with casamino acids and that activity was considerably higher if yeast extract or peptone was added to media. Moreover, they performed a β-galactosidase (BgaH) activity assay and showed that tryptophan concentrations of 4 mM achieved maximum induction. Accordingly, the authors concluded that the *tna* promoter is suitable for transcription induction in *H. volcanii*. The inducibility of the *tnaA* promoter of *N. magadii* was also demonstrated using the *bgaH* gene (Selb et al., 2017).

1.5. Viruses of Archaea

Through all life forms viruses seem to be ubiquitous (Koonin et al., 2006). Although viruses can infect all three domains of life, viruses of Archaea have not been studied extensively (Pina et al., 2011). The first ever isolated archaeal virus derived from *H. salinarum* was reported by Torsvik & Dundas (1974). Most archaeal viruses were found in extreme habitats like hypersaline water or geothermal environments (Pina et al., 2011). As a consequence, viruses have adapted to these environments. Thus, viruses of acidophilic hyperthermophiles require high temperature (above 80 °C) (Prangishvili, Forterre, et al., 2006) and extreme pH values below 3 (Prangishvili, Vestergaard, et al., 2006). Accordingly, it is not surprising that haloarchaeoviruses need salt concentrations of 3 – 5 M to be stable and become inactive in media with low ionic strength (Witte et al., 1997). Currently, there are 33 families of archaeal viruses with two distinctive groups: (i) viruses with morphology unique to archaea, therefore, named archaea-specific viruses and (ii) viruses which share structural similarities to their bacterial and eukaryotic family, namely cosmopolitan archaeal virus (Iranzo et al., 2016). Archaea-specific viruses have a huge range of morphologies, such as spindle-shaped, bottle-shaped, droplet-shaped virions and filamentous-shaped virions (Baquero et al., 2020; Krupovic et al., 2018; Liu et al., 2023; Rensen et al., 2016). Interestingly, all currently isolated archaeal viruses infect only two major phyla, either Thermoproteota or Euryarchaeota (Sensevdi et al., 2024).

1.5.1. ϕCh1

Virus ϕCh1 was first isolated by Witte et al. (1997). They described that the virus consists of a head with approximately 70 nm and a tail with approximately 130 nm length. The contractible tail contains an internal shaft and altogether, they have a width of approximately 20 nm (Witte et al., 1997). Consequently, ϕCh1 is classified as *Myoviridae* due to its morphology. Remarkably, the latter-mentioned characterisation resembles other described halophilic viruses (Schnabel et al., 1982; Torsvik & Dundas, 1974; Wais et al., 1975). The genetic information of the virus is chromosomally integrated into the *N. magadii* genome (Witte et al., 1997). Since it contains a linear dsDNA and several 50 – 700 nucleotides RNA sequences (Witte et al., 1997), allocation according to the Baltimore

classification is not possible (Lostroh, 2019). It was hypothesised that the RNA could be involved in DNA packaging (Witte et al., 1997). However, their function remains unclear. Klein et al. (2002) determined the viral genome with a length of 58,498 bp and a G+C content of 61.9 %. They predicted 98 ORFs as genes, containing at least 30 nucleotides. Moreover, they revealed that the majority are predicted to start with the ATG codon and four ORFs are predicted to begin with GTG codon. Further, they state that the codon usage of ϕCh1 appears to be similar to halophilic archaea's. According to them, the organisation of the ORFs indicates that transcriptional units (operons) are formed (Figure 1). Taking a closer look at the map, it can be observed in the left and right part that the ORFs are organised in a rightward transcribed way while the middle part contains a mixture of left- and rightward transcribed genes (Klein et al., 2002). As the map further shows, the genes encoding for predicted structural components, such as the four major and five minor structural components of the virus, are located on the left part (Klein et al., 2002; Witte et al., 1997). The middle part harbour genes predicted for the inversion (ORF34, *int*1, ORF36) and DNA replication (Klein et al., 2002). On the right side, some genes are predicted for DNA modifications such as methyltransferases. This is remarkable as the virus contains partially methylated adenine residues (Witte et al., 1997). These Dam-like methylation (5'-GATC-3') were unexpected because no such methylation was found in *N. magadii* (Lodwick et al., 1986). Baranyi et al. (2000) could isolate the ϕCh1 Dam-like methyltransferase (M.ϕCh1) and showed that its expression could be determined during the late phase of virus development in *N. magadii*.

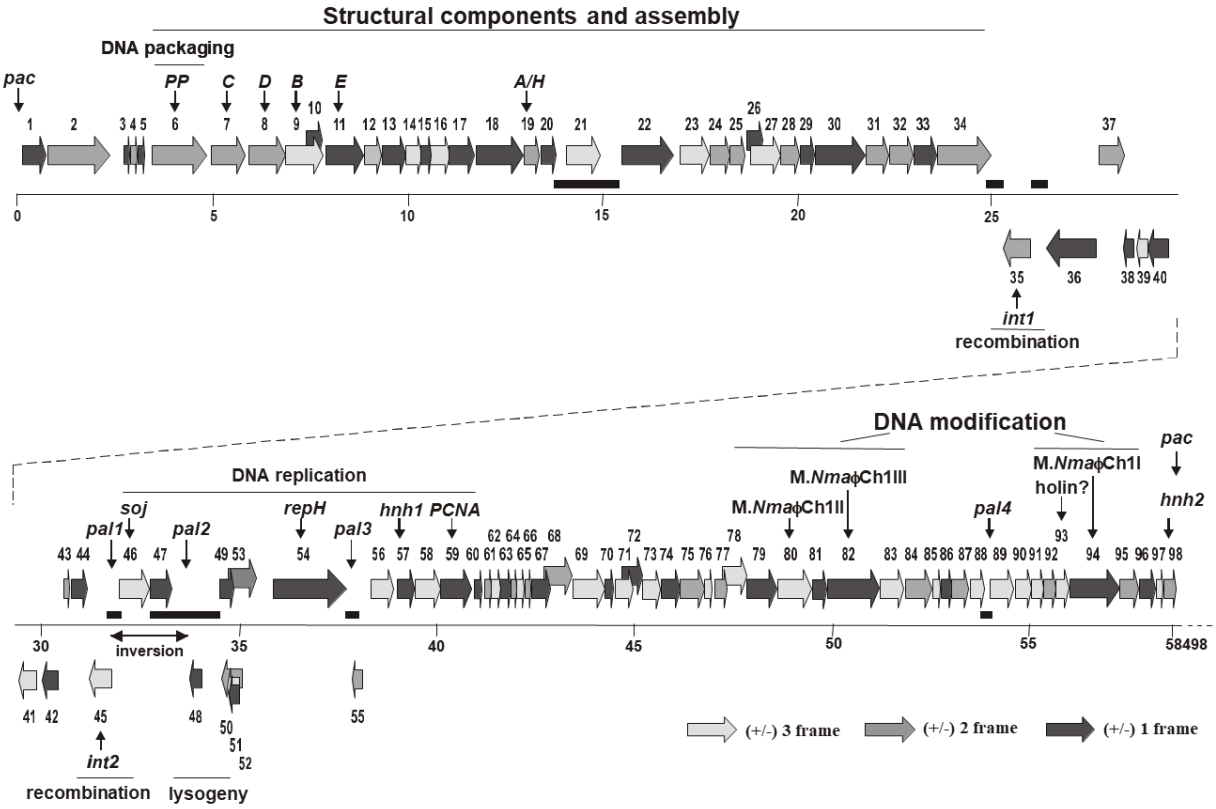

Figure 1: Gene map of ϕCh1 with length of 58,498 bp. ORFs with corresponding frame shifts are indicated with grey arrows (light grey third reading frame, mid-grey second reading frame and dark grey first reading frame). Black bars illustrate sequences with low G and C content. Adapted from Klein et al. (2002).

As the virus is adapted to its host, salt concentrations below 2 M lead to either dissociation of the virus particle or changes in the conformation of the nucleocapsids (Witte et al., 1997). Interestingly, low salt concentrations and the presence of Mg^{2+} are also not tolerated, as reported for ϕH (Schnabel et al., 1982). *N. magadii* appears to be the only known host of virus ϕCh1 (Witte et al., 1997). It remains unclear if the virus can infect other (haloalkaliphilic) organisms.

1.5.1.1. The invertible region of ϕCh1

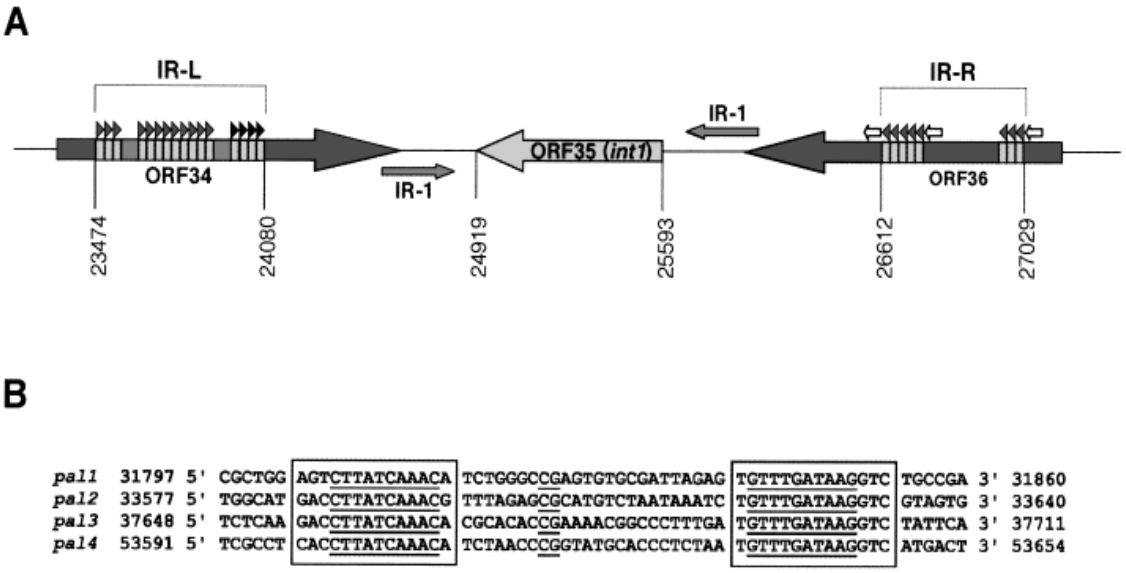

Figure 2: Invertible region of ϕCh1. (**A**) IR Direct repeats are indicated with small arrows in the IR-L and IR-R regions. Similar sequences within ORF36 are indicated with white arrows and are flanking the region of IR-R. Numbers indicate the position in the ϕCh1 nucleotide sequence. (**B**) Alignments of ϕCh1 nucleic acid sequence of the putative invertible region. From Klein et al. (2002).

The invertible region of ϕCh1 consists of ORF34, ORF35 (*int*1) and ORF36 (Figure 2, A). As Klein et al. (2012) showed, ORF34 and ORF36 encode for a putative tail fibre protein while *int*1 encodes for a putative site-specific recombinase. Furthermore, they compared DNA and amino acid level sequences between ORF34 and ORF36, which showed high similarities and direct repeats of 30 bp or 10 amino acids. These clusters of direct repeats, named IR-L and IR-R, are located in the inverse direction to each other. This resembles the tail proteins of other bacteriophages, where the shaft domain, part of the central section, often contains inalterable sequence motifs with a conserved pattern of hydrophobic amino acids (George et al., 1983; Montag et al., 1990; Sandmeier, 1994). In addition, Klein et al. (2002) demonstrated that *int*1, which is associated with the bacteriophage λ Int family, is also flanked by two nearly identical repeats with a length of 267 bp (IR-1) (Figure 2, A). Expression of *int*1 in ϕCh1 showed to be constitutively over the life cycle. Why is this invertible region so interesting? The host range of some bacteriophages can be changed by site-specific recombination of sequences that determine the host range (Hiestand-Nauer & Iida, 1983; Plasterk et al., 1983). The fact that not only the invertible

region resembles the latter mentioned fact but also its similar morphology and function to other dsDNA viruses infecting Bacteria or Archaea leads to the conclusion that rearrangement of ORF34 and ORF36 could determine the host . In fact, Klein et al. (2012) claim that reorganisation of ORF34 and ORF36 drives C-terminal rearrangement of these proteins and this could be used as adaptation for different hosts. Further, they compared the two proteins, gp34 and gp36, and found similarities of around 33 % with nearly identical and unchanging stretches of amino acids. The authors also stated that the antiserum produced against $gp36_1$ could not discriminate between these two proteins. Hence, it was unclear if either both or only one protein was synthesised. Therefore, they performed transcriptional analysis by using specific internal primers for ORF34 and ORF36 and revealed that only ORF34 is transcribed, while no RNA could be detected for ORF36. To investigate this further, they transformed vectors harbouring ORF34 and ORF36 into *Haloferax volcanii* and could elucidate that only proteins encoded by ORF34 could be detected by using α-ϕCh1 antibodies but none for ORF36 (Klein et al., 2012).

The C-terminal of ORF34 encoded proteins appeared to have similarities with galactose binding domains (Klein et al., 2012). However, only one protein called $gp34_{52}$ carries an amino acid conserved region able to form the binding pocket for α-D-galactose. The purpose of such domains is to bind to the cell surface via carbohydrate-ligands (Ito et al., 1991). Klein et al. (2012) concluded from the following findings that only one protein of ORF34/36 variants, namely $gp34_{52}$, was able to bind to the surface of *N. magadii*: (i) $gp34_{52}$ was found only in *N. magadii* pellets but not in supernatant, (ii) deletion of conserved tryptophan residue of $gp34_{52}$ averted virus binding to the surface and (iii) addition of 10 mM α-D-galactose inhibited ϕCh1 infection unambiguously.

1.6. Thesis aim

Certain bacteriophages can adapt to different hosts by site-specific recombination of sequences encoding for the host range (Hiestand-Nauer & Iida, 1983; Plasterk et al., 1983). The archaeal virus ϕCh1 contains an invertible region with ORF34, *int*1 and ORF36. While *int*1 is thought to encode for a site-specific recombinase, ORF34 and ORF36 encodes putatively for tail fibre proteins (Klein et al., 2002, 2012). It was elucidated that

only ORF34 was transcribed (Klein et al., 2012). However, both ORFs contain direct repeats of 30 bp, which are named IR-L and IR-R (Klein et al., 2002). Therefore, the recombination of ORF34 and ORF36 leads to the transcription and synthesis of different proteins. One of these proteins ($gp34_{52}$) was shown to be crucial for binding to the surface of *N. magadii* and thus causing an infection (Klein et al., 2012). The question arose: Who was responsible for this site-specific recombination? As a logical consequence, it was first thought that Int1 would catalyse this reaction. However, previous attempts to determine if Int1 interferes with the inversion could not provide any concludable hints (Beer, 2024). Nevertheless, there are two more candidates which could be responsible, recombinases RadA and RadB. Thus, the first part of this study aimed to construct *N. magadii* L13-Δ*radA* and L13-Δ*radB* deletion mutants to analyse its putative influence on the invertible region.

The second part of this thesis focused on the nucleocapsids of ϕCh1. Witte et al. (1997) could identify and describe four major and five minor structural components of the virus. Klein et al. (2002) reported that the N-terminal amino acid sequence of protein A and H were similar to the protein encoded by ORF19. They could detect a band with a size of around 80 kDa as Witte et al. (1997) and concluded that this is due to formation of a stable or covalently joined homo- or heteromultimer comprising of at least ORF19. A list including all previously known ORFs encoding nucleocapsids is provided in Table 1. Today, bioinformatic analysis allows us to examine potential ORFs as their analysis conclude that they are part of the nucleic envelope. Thus, this part of the study aimed to identify novel ϕCh1 nucleocapsids.

part of ϕCh1 capsid
ORF7 or *C*
ORF8 or *D*
ORF9 or *B*
ORF11 or *E*
ORF18
ORF19 or *A*/*H*
ORF34

Table 1: List of recently identified ORFs encoding nucleocapsids (Klein et al., 2000, 2002, 2012; Witte et al., 1997)

2. Material and Methods

2.1. Material

2.1.1. Archaeal and bacterial strains

Natrialba magadii

strain	genotype	source
L11	contains provirus ϕCh1	Witte et al., 1997
L13	ϕCh1 cured	Witte et al., 1997
L13 pKS$_{II+}$-Δ*radA*F	with suicide plasmid carrying Nov cassette (*gyrB)* in forward direction	This study
L13 pKS$_{II+}$-Δ*radA*R	with suicide plasmid carrying Nov cassette (*gyrB)* in reverse direction	This study
L13 pKS$_{II+}$-Δ*radB*F	with suicide plasmid carrying Nov cassette (*gyrB)* in forward direction	This study
L13 pKS$_{II+}$-Δ*radB*R	with suicide plasmid carrying Nov cassette (*gyrB)* in reverse direction	This study
L13 RadA^{-}(Nov$^{R\text{-}fw}$)	*radA* absent in some chromosomes and exchanged by Nov cassette (*gyrB)* in forward direction	This study
L13 RadA^{-}(Nov$^{R\text{-}rv}$)	*radA* absent in some chromosomes and exchanged by Nov cassette (*gyrB)* in reverse direction	This study
L13 RadB^{-}(Nov$^{R\text{-}fw}$)	*radB* absent in some chromosomes and exchanged by Nov cassette (*gyrB)* in forward direction	This study
L13 RadB^{-}(Nov$^{R\text{-}rv}$)	*radB* absent in some chromosomes and exchanged by Nov cassette (*gyrB)* in reverse direction	This study
L13 pNB102-ptnaN	plasmid with tryptophan inducible promoter	This study
L13 pNB102-ptnaN-a_*radA*	plasmid carrying antisense *radA* under tryptophan inducible promoter	This study
L13 pNB102-ptnaN-a_*radB*	plasmid carrying antisense *radB* under tryptophan inducible promoter	This study
L13 pRo-5-ptnan-a_*radA*	plasmid carrying antisense *radA* under tryptophan inducible promoter	This study

Escherichia coli

strain	genotype	source
BL21(DE3)	F– *ompT hsdSB* (rB– mB–) *gal dcm* Δ(*srl*–*rec*A)306::Tn10 (TcR) (DE3)	Novagen
BL21(DE3) pRSET-A	with plasmid	This study
BL21(DE3) pRSET-A-ORF12	plasmid carrying ORF12	This study
BL21(DE3) pRSET-A-ORF14	plasmid carrying ORF14	This study
BL21(DE3) pRSET-A-ORF16	plasmid carrying ORF16	This study
BL21(DE3) pRSET-A-ORF24	plasmid carrying ORF24	This study
BL21(DE3) pRSET-A-ORF25	plasmid carrying ORF25	This study
BL21(DE3) pRSET-A-ORF28	plasmid carrying ORF28	This study
BL21(DE3) pRSET-A-ORF29	plasmid carrying ORF29	This study
BL21(DE3) pRSET-A-ORF61	plasmid carrying ORF61	This study
BL21(DE3) pRSET-A-ORF71	plasmid carrying ORF71	This study
XL1-Blue	*end*A1, *gyr*A96, *hsd*R17 (rk^-mK^+), *lac*, *rec*A1, *rel*A1, supE44, *thi* (F´, *lac*Iq, *lac*ZΔM15, *pro*AB^+, *tet*)	Stratagene
XL1-Blue pNB102-ptnaN	plasmid with tryptophan inducible promoter	This study
XL1-Blue pNB102-ptnaN-a_*radA*	plasmid carrying antisense *radA* under tryptophan inducible promoter	This study
XL1-Blue pNB102-ptnaN-a_*radB*	plasmid carrying antisense *radB* under tryptophan inducible promoter	This study
XL1-Blue pRo-5-ptnaN	plasmid with tryptophan inducible promoter	This study
XL1-Blue pRo-5-ptnaN-a_*radA*	plasmid carrying antisense *radA* under tryptophan inducible promoter	This study
XL1-Blue pRo-5-ptnaN-a_*radB*	plasmid carrying antisense *radB* under tryptophan inducible promoter	This study
XL1-Blue pRSET-A	with plasmid	This study
XL1-Blue pRSET-A-ORF12	plasmid carrying ORF12	This study
XL1-Blue pRSET-A-ORF14	plasmid carrying ORF14	This study
XL1-Blue pRSET-A-ORF16	plasmid carrying ORF16	This study
XL1-Blue pRSET-A-ORF24	plasmid carrying ORF24	This study
XL1-Blue pRSET-A-ORF25	plasmid carrying ORF25	This study
XL1-Blue pRSET-A-ORF28	plasmid carrying ORF28	This study
XL1-Blue pRSET-A-ORF29	plasmid carrying ORF29	This study
XL1-Blue pRSET-A-ORF61	plasmid carrying ORF61	This study
XL1-Blue pRSET-A-ORF71	plasmid carrying ORF71	This study

2.1.2. Plasmids

plasmid	features	source
pBAD24	*bla,* pBR322 ori, *araC*, mcs	Guzman et al., 1995
pBAD24-tnaN	pBAD24 with *N. Magadii* trp promoter	Alte, 2011
pKSII+	*bla,* colE1 ori, *lacZα*, mcs	Stratagene
pKSII+ -Δ*radA*F	*radA* suicide plasmid pKSII+ carrying *gyrB* (NovR)	This study
pKSII+ -Δ*radA*R	*radA* suicide plasmid pKSII+ carrying reversed *gyrB* (NovR)	This study
pKSII+ -Δ*radB*F	*radB* suicide plasmid pKSII+ carrying *gyrB* (NovR)	this study
pKSII+ -Δ*radB*R	*radB* suicide plasmid pKSII+ carrying reversed *gyrB* (NovR)	This study
pNB102	*bla*, colE1 ori, *hmg* (mevR), ϕCh1 derived ori	Zhou et al., 2004
pNB102-ptnaN	pNB102 with *N. Magadii* trp promoter	This study
pNB102-ptnaN-a_*radA*	pNB102-ptnaN with antisense RNA coding *radA*	This study
pNB102-ptnaN-a_*radB*	pNB102-ptnaN with antisense RNA coding *radB*	This study
pRo-5	*bla,* colE1 ori, gyrB (NovR), ϕCh1 derived ori	Mayrhofer-Iro et al., 2013
pRo-5-ptnaN	pRo5 with *N. Magadii* trp promoter	This study
pRo-5-ptnaN-a_*radA*	pRo5-ptnaN with antisense RNA coding *radA*	This study
pRo-5-ptnaN-a_*radB*	pRo5-ptnaN with antisense RNA coding *radB*	This study
pRSET-A	*bla,* pUC ori, T7 promoter, N-terminal 6x His-taq	Invitrogen
pRSET-A-ORF12	pRSET-A with ORF12	This study
pRSET-A-ORF14	pRSET-A with ORF14	This study
pRSET-A-ORF16	pRSET-A with ORF16	This study
pRSET-A-ORF24	pRSET-A with ORF24	This study
pRSET-A-ORF25	pRSET-A with ORF25	This study
pRSET-A-ORF28	pRSET-A with ORF28	This study
pRSET-A-ORF29	pRSET-A with ORF29	This study
pRSET-A-ORF61	pRSET-A with ORF61	This study
pRSET-A-ORF71	pRSET-A with ORF71	This study

plasmid	features	source
pUC19	*bla*, pMB1 ori, mcs, *lac*Za	Yanisch-Perron et al., 1985
pUC19-Nov "forward"	pUC19 carrying *gyrB* (NovR)	Wurzer, 2015
pUC19-Nov "reverse"	pUC19 carrying reversed *gyrB* (NovR)	Wurzer, 2015

2.1.3. Primers

primer	sequence
24-Bam	GACCGGATCCATGACCACAGTCACCATC
24-Hind	CAGGAAGCTTCTACAGCACCCCCGAGA
25-Bam	GACCGGATCCATGGGGGAGATCATCCC
25-Hind	GACCAAGCTTCACTACCACTCATCCGGC
28-Bam	GACCGGATCCATGCCATCAAACCTAATCTCG
28-Hind	CAGCGAAGCTTATTCGTCGGGAGCCTC
29-Bgl	CAGGAGATCTATGAAATTCAAACGAACA
29-Hind	CAGGAAGCTTACACCTCCAGATCGAATC
A-3-1	GCCGCCACGGAGTGAA
A-3-2	GTGCTCGCAGAGAAGGTTCG
A-3-2N	GCGTCCACATTCCCGT
A-5-1	GCTGCAGTTGCTGTGAGAC
A-5-2	GAACCGGTGACCGGCT
A-5-2N	GGCGGCCACGATACTG
a-RadA-1_pNB102	ATCACGAGGCCCTTTCGTCTTCAAGACTGAGGAATCGACCGGTTTTGTTCT
a-RadA-1_pRo-5	GCTCTCGACGATGCCGCGGACCTCGGCTGAGGAATCGACCGGTTTTGTTCT
a-RadA-2	AGGACGAAGGGCTGAAACCAGAGTAATAGCAACTCGAGAACGCCACGCGTGT
a-RadA-3	ACACGCGTGGCGTTCTCGAGTTGCTATTACTCTGGTTTCAGCCCTTCGTCCT
a-RadA-4_pNB102	TGATAAGCTGTCAAACATGAGAATTATGGCAGACGCAGACCTCGAGACACT
a-RadA-4_pRo-5	AGGGCCAGACGAAGACCAAGCTCGGGATGGCAGACGCAGACCTCGAGACACT
a-RadB-1_pNB102	ATCACGAGGCCCTTTCGTCTTCAAGACTGAGGAATCGACCGGTTTTGTTCT

primer	sequence
a-RadB-1_pRo-5	GCTCTCGACGATGCCGCGGACCTCGGCTGAGGAATCGACCGGTTTTGTTCT
a-RadB-2	CCGGTCGGAAGTGCCGCGTCGTTCACTAGCAACTCGAGAACGCCACGCGTGT
a-RadB-3	ACACGCGTGGCGTTCTCGAGTTGCTAGTGAACGACGCGGCACTTCCGACCGG
a-RadB-4_pNB102	TGATAAGCTGTCAAACATGAGAATTTCTATCGCGACGCCGGCTCCGCCCCAC
a-RadB-4_pRo-5	AGGGCCAGACGAAGACCAAGCTCGGGCTATCGCGACGCCGGCTCCGCCCCAC
B-3-1	GTACCTGAAACGCGGCAAC
B-3-2	GCGTGTCCAAGACATCTGGAC
B-5-1	GAACAGCAAGGTGAACAGC
B-5-2	GAGCTACCTGCGATTCCG
Nov-12	GCCGGTGAGTACTTAACGC
Nov-9	GATGTCGGTCATCGCGG
NovR-1p	GATCCTGCAGTGTCGACTGGAACGAGG
NovR-1s	GATCCCCGGGTGTCGACTGGAACGAGG
NovR-2p	GTTACTGCAGGCCGTAATATCCAGCTGA
NovR-2s	GTTACCCGGGCCGTAATATCCAGCTGA
ORF14-3	GATTAAGCTTTAGCTGTCCTCACGAGTCGAG
ORF14-5	GACCGGATCCATGAGCCCGCTTCCATCAT
ORF61-3	GATTAAGCTTTCAGGCATCGTCCTGCC
ORF61-5	GACCGGATCCATGGCGCTGGCCTGTC
ORF71-3	GATTAAGCTTCTAAACATCGTCCTCCTCCACG
ORF71-5	GACCGGATCCATGAACGACGCTGAGACGC
p12-3	GATCAAGCTTACCCCTCGACTTCCG
p12-5	GTACGGATCCATGGCTGAACGCACCA
p16-3	GATCAAGCTTCAGTCGATTACAGCACCC
p16-5	GATCGGACTTATGGTCGAGGACGAGAAC
pNB102-E	GCACATTTCCCCGAAAA
pRo-5-E	GCCTTCGAGATGATGGC
ptnaN-pNB102	TGATAAGCTGTCAAACATGAGAATTTAGCAACTCGAGAACGCCACGCGTGT
ptnaN-pRo-5	AGGGCCAGACGAAGACCAAGCTCGGTAGCAACTCGAGAACGCCACGCGTGT
radA_del1	GACGTCGGTGGCTTCGAAAC
radA_del2	GGTTTCCGACCTTGTCGAGG

primer	sequence
RadA-1	ATCCCCCGGGCTGCAGGAATTCGATGTTTGTAGCCTCTACGCTGATTCTG
RadA-1-1	ATCCCCCGGGCTGCAGGAATTCGATAGGTCGCATCCATTATACCGATTCAG
RadA-2-F	TCGTTCCAGTCGACACCCGGGGATCACTTCTTCGTTATTGTGGACACCCC
RadA-2-R	GCTGGATATTACGGCCTGCAGTAACACTTCTTCGTTATTGTGGACACCCC
RadA-3-F	GCTGGATATTACGGCCTGCAGTAACGCGGCGTCGCAGTCACACCAATACA
RadA-3-R	TCGTTCCAGTCGACACCCGGGGATCGCGGCGTCGCAGTCACACCAATACA
RadA-4	GGTCGACGGTATCGATAAGCTTGATAGTAGCTGGGAGTGACCTCGGGCGGC
RadA-4-1	GGTCGACGGTATCGATAAGCTTGATAGTTCGCCGCCGAGCGTCCGGTTCATC
RadB-1	ATCCCCCGGGCTGCAGGAATTCGATTCTGTCGGGTTCGACCGGTTTCTGC
RadB-2-F	TCGTTCCAGTCGACACCCGGGGATCCGAACCACGCGACGCGAAGACACAC
RadB-2-R	GCTGGATATTACGGCCTGCAGTAACCGAACCACGCGACGCGAAGACACAC
RadB-3-F	GCTGGATATTACGGCCTGCAGTAACTCTGTCCGGGCAAAAAGCCCCCGAA
RadB-3-R	TCGTTCCAGTCGACACCCGGGGATCTCTGTCCGGGCAAAAAGCCCCCGAA
RadB-4	GGTCGACGGTATCGATAAGCTTGATATCACGTCCTCTCCTGGCCGGTCTGC
radB-del1	GAGGACGACCGCCAGATCGT
radB-del2	GTGAACGACGCGGCACTTCC

2.1.4. Media

name	compound	quantity	comment
Lysogeny broth (LB)	peptone	10 g	pH 7.0, ad 1 L dH_2O, for plates add 15 g agar
	yeast extract	5 g	
	NaCl	5 g	
Natrialba rich media (NVM)	casamino acids (CAA) or casamino hydrolysate (CH)	8.80 g	pH 9.5, ad 0.934L dH_2O, for plates add 8g agar, sterilise via autoclaving (uncomplemented media)
	yeast extract	11.70 g	
	sodium citrate tribasic acid	0.80 g	
	KCl	2.35 g	
	NaCl	235 g	
	NaOH	5 tablets	
	0.57 M Na_2CO_3 (dissolved in sterile dH_2O)	63 mL	add after sterilisation (complemented media)
	1 M $MgSO_4$ (autoclaved)	1 mL	
	20 mM $FeSO_4$ x $7H_2O$ (autoclaved)	1 mL	
	trace elements SL-6	1 mL	
Trace elements SL-6	$CoCl_2$ x $6H_20$	0.2 g	pH 3-4 with HCl, ad 1L dH_2O, sterilised via filtration
	$CuCl_2$ x $6H_2O$	10 mg	
	H_3BO_3	0.3 g	
	$MnCl_3$ x $4H_20$	30 mg	
	Na_2MoO x H_2O	30 mg	
	$NiCl_2$ x H_2O	20 mg	
	$ZnSO_4$ x $7H_2O$	0.1 g	

2.1.5. Additives

compound	stock	final	comment
ampicillin	20 mg/mL	20 µg/mL	dissolved in autoclaved dH_2O, sterile filtered, stored at 4 °C
bacitracin	7 mg/mL	70 µg/mL	dissolved autoclaved dH_2O, stored at 4 °C
chloramphenicol	40 mg/mL	20 µg/mL	dissolved in half EtOH and autoclaved dH_2O, stored at -20 °C

compound	stock	final	comment
IPTG	1 M	1 mM	dissolved in dH_20, stored at -20 °C
L-tryptophane	0.6 M	4 mM	dissolved in 1 M NaOH, sterile filtered, stored in aliquots at -20 °C
mevinolin	5 mg/mL	4 µg/mL	lovastatin powder dissolved in 96 % EtOH, stored at -20 °C
novobiocin	3 mg/mL	3 µg/mL	dissolved in autoclaved dH_2O, sterile filtered, stored at -20 °C
tetracycline	10 mg/mL	10 µg/mL	dissolved in half EtOH and autoclaved dH_2O, stored at -20 °C

2.1.6. Enzymes

name	manufacturer	product number
*Eco*RI-HF	New England Biolabs	R3101S
FastAP Thermosensitive Alkaline Phosphatase	Thermo Scientific	EF0652
FastDigest *Bgl*II	Thermo Scientific	FD0084
FastDigest *Hin*dIII	Thermo Scientific	FD0504
GoTaq® G2 Green Master Mix	Promega	M7823
*Hin*dIII-HF	New England Biolabs	R3104S
*Kpn*I-HF	New England Biolabs	R3142S
Phusion Flash High-Fidelity PCR Master Mix	Thermo Scientific	F548L
Phusion® High Fidelity DNA Polymerase	New England Biolabs	M0530S
Proteinase K	Qiagen	19134
Q5 High-Fidelity DNA Polymerase	New England Biolabs	M0491G
T4 DNA	Thermo Scientific	EP0061
T5 Exonuclease	New England Biolabs	M0363S
Taq DNA Ligase	New England Biolabs	M0208S

2.1.7. Kits

name	manufacturer	product number
Promega Wizard® SV Gel and PCR Clean-Up System	Promega	A9281
Wizard® Plus SV Minipreps DNA Purification system	Promega	A1460

2.1.8. Marker

marker	manufacturer	product number
GeneRuler 1 kb Plus DNA Ladder	Thermo Scientific	SM1331
PageRuler™ Plus Prestained Protein Ladder, 10 to 250 kDa	Thermo Scientific	26619 / 26620

2.1.9. Gibson assembly

name	compound	molarity	quantity
5x ISO reaction buffer	PEG-8000	25 % (w/v)	2.5 g
	1 M Tris/HCl pH 7.5	500 mM	5 mL
	1 M $MgCl_2$	50 mM	500 µL
	dl-Dithiothreitol	50 mM	77 mg
	10mM dNTP	10 mM	100 µL
	5 mM NAD	5 mM	33.2 mg
	nuclease-free dH_2O	-	ad 10 mL

name	compound	quantity
Gibson assembly master mix	5x ISO reaction buffer	100 µL
	T5 Exonuclease (10 U/µL)	0.2 µL
	Phusion polymerase	6.25 µL
	Taq DNA ligase	50 µL
	nuclease-free dH_2O	218.55 µL

2.1.10. SDS-Polyacrylamid gels

name	compound	quantity
12 % Separating Gel	Acrylamide solution 30 %	2 mL
	Separating gel buffer	1.25 mL
	dH_20	1.75 mL
	10 % APS	60 µL
	TEMED	10 µL
4 % Stacking gel	Acrylamide solution 30 %	267 µL
	Stacking gel buffer	0.5 mL
	dH_20	1.233 mL
	10 % APS	20 µL
	TEMED	5 µL

2.1.11. Antibodies

Primary antibodies

antibody	target	application	source
α-ϕCh1	ϕCh1	Diluted 1:2500, 1:500 or 1:100 in 1x TBS, 0.3 % BSA, 0.02 % NaN_3, spatula tip of acetone powder	Klein et al., 2000

Secondary antibodies

antibody	target	application	manufacturer	product number
ECL™ Anti-Rabbit IgG, Horseradish Peroxidase linked whole antibody (from donkey)	Rabbit IgG	Diluted 1:5000 or 1:2500 in 1x TBS	GE Healthcare	NA934V
Goat Anti-Rabbit IgG Peroxidase Conjugate	Rabbit IgG	Diluted 1:5000 or 1:2500 in 1x TBS	Calbiochem	DC03L

2.1.12. Membrane

name	manufacturer	product number
Amersham™ Protran™ 0.2 µm NC	Cytiva	10600001

2.1.13. General Buffers and Solutions

Buffers for DNA methods

name	compound	quantities
50x TAE	Tris/HCl pH 8.2	2 M
	acetic acid	1 M
	EDTA	0.1 M
50x Super buffer	boric acid	1.82 M
	NaOH	0.5 M
6x DNA loading dye	glycerol	60 %
	orange G	0.144 % (m/v)
	Tris/HCl pH 8.0	25 mM
	xylene cyanol	0.036 % (m/v)
Ethidium bromide bath	ethidium bromide	10 µg/mL

Buffers for protein methods

name	compound	quantities	comments
10x SDS-running buffer	glycine	1.92 M	
	tris base	50 mM	
	SDS	1 %	
Stacking gel buffer	Tris/HCl pH 6.8	0.5 M	
	SDS	0.4 %	
Separating gel buffer	Tris/HCl pH 8.8	1.5 M	
	SDS	0.4 %	
Acrylamid solution 30 %	acrylamide	29 %	stored at 4 °C
	N,N'-methylenebisacrylamid	1 %	
10 % APS	ammonium persulphate	1 g	stored at 4 °C
	dH_20	10 mL	
2x Laemmli sample buffer	Tris/HCl pH 6.8	125 mM	
	SDS	4 % (v/v)	
	glycerol	20 % (v/v)	
	β-mercaptoethanol	10 % (v/v)	
	bromophenol blue	0.04 % (m/v)	
5 mM Na-Phosphate buffer	1 M Na_2HPO_4	46.4 mL	pH 6.8
	1 M NaH_2PO_4	53.7 mL	
Coomassie staining solution	Coomassie brilliant Blue R 250	0.25 %	dissolve Coomassie Blue R250 in methanol first
	methanol	40%	
	acetic acid	10 %	
Destaining solution	acetic acid	10 %	
10x TBS	Tris/HCl pH 8.0	0.25 M	
	NaCl	1.37 M	
	KCl	27 mM	
Blocking solution	skim milk powder	5 % (m/v)	in 1x TBS
10x Towbin buffer	tris	0.25 M	pH 8.6
	glycine	1.92 M	
Transfer buffer	methanol	100 mL	
	10x Towbin buffer	50 mL	
	dH_2O	350 mL	

name	compound	quantities	comments
ECL buffer	1.5 M Tris pH 8.5	13.3 mL	store at 4 °C protected from light
	luminol	500 µL	
	coumaric acid	250 µL	
	dH2O	ad 200 mL	
Coumaric acid	coumaric acid	0.148 g	250 µL aliquots stored at -20 °C
	DMSO	10 mL	
Luminol	3-Aminophthalhydrazide	0.886 g	500 µL aliquots stored at -20 °C protected from light
	DMSO	20 mL	

Buffers for E. coli methods

name	compound	quantity	comment
MOPS I	MOPS	100 mM	adjust pH to 7.0 with KOH, sterilisation via filtration
	$CaCl_2$	10 mM	
	RbCl	10 mM	
MOPS II	MOPS	100 mM	adjust pH to 6.5 with KOH, sterilisation via filtration
	$CaCl_2$	70 mM	
	RbCl	10 mM	
MOPS IIa	MOPS	100 mM	adjust pH to 6.5 with KOH, sterilisation via filtration
	$CaCl_2$	70 mM	
	RbCl	10 mM	
	glycerol	15 % (v/v)	
Glycerol stock *E. coli*	glycerol	50 % (v/v)	in dH_20

Buffers for N. magadii methods

name	compound	quantity	comment
High salt (HS) buffered spheroplast solution	Tris/HCl pH 9.5	50 mM	after sterilisation add of 15 % (v/v) of sterile filtered sucrose
	NaCl	2 M	
	KCl	27 mM	

name	compound	quantity	comment
High salt (HS) unbuffered spheroplast solution	NaCl	2 M	after sterilisation add 15 % (v/v) of sterile filtered sucrose
	KCl	27 mM	
60% PEG 600	PEG-600	60 % (v/v)	PEG-600 aliquots are stored up to six months at -70 or -80 °C
	High salt (HS) unbuffered spheroplast solution	40% (v/v)	
Glycerol stock halophilic strains	NaCl	4 M	in dH_2O, solution is saturated, NaCl cannot be dissolved completely
	glycerol	50% (v/v)	

Virus isolation

CsCl gradient solution 1.1

name	compound	quantity
CsCl gradient solution 1.1	CsCl	0.6 M
	NaCl	2 M
	Tris/HCl pH 9.5 or HEPES/NaOH pH 8	50 mM 20 mM
CsCl gradient solution 1.3	CsCl	2.7 M
	NaCl	2 M
	Tris/HCl pH 9.5 or HEPES/NaOH pH 8	50 mM 20 mM
CsCl gradient solution 1.5	CsCl	4 M
	NaCl	2 M
	Tris/HCl pH 9.5 or HEPES/NaOH pH 8	50 mM 20 mM
Dialyse buffer	NaCl	4 M
	Tris/HCl pH 9.5 or HEPES/NaOH pH 8	50 mM 20 mM

2.2. Methods

2.2.1. DNA methods

Polymerase chain reaction (PCR)

Preparative PCR

Thermo Scientific Phusion Flash High-Fidelity PCR Master Mix

dH_20	19 µL
primer 1 (100 ng/µL)	2.5 µL
primer 2 (100 ng/µL)	2.5 µL
DNA template	1 µL
Phusion Flash High-Fidelity PCR Master Mix	25 µL
total volume	50 µL

	step	temperature	time
	initial denaturation	98 °C	5 min
35x	denaturation	98 °C	10 s
	annealing	$T_{M\ of\ lower\ primer}$ -4 °C	10 s
	elongation	72 °C	15 s / 1 kbp
	final elongation	72 °C	3x elongation
	hold	4 -16 °C	∞

NEB Q5® Phusion® High Fidelity DNA Polymerase

dH_20	22.5 µL
Q5 Reaction Buffer (B9027S)	10 µL
(optional) Q5 High GC Enhancer (B9028A)	10 µL
dNTPs (10 mM)	1 µL
primer 1 (100 ng/µL)	2.5 µL
primer 2 (100 ng/µL)	2.5 µL
DNA template	1 µL
Phusion Flash High-Fidelity PCR Master Mix	25 µL
total volume	50 µL

	step	temperature	time
	initial denaturation	98 °C	3 min
35x	denaturation	98 °C	10 s
	annealing	$T_{M\ of\ lower\ primer}$ -4 °C	15 s
	elongation	72 °C	30 s / 1 kbp
	final elongation	72 °C	3x elongation
	hold	4 -16 °C	∞

Analytical PCR

Promega GoTaq® G2 Green Master Mix

dH_20	8.5 µL
primer 1 (100 ng/µL)	1.5 µL
primer 2 (100 ng/µL)	1.5 µL
GoTaq® G2 Green Master Mix	12.5 µL
DNA template	1 µL
total volume	25 µL

1 µL of *E. coli* culture can be used directly as a template.

	step	temperature	time
	initial denaturation	95 °C	5 min
35x	denaturation	95 °C	10 s
	annealing	$T_{M\ of\ lower\ primer}$ -4 °C	10 s
	elongation	72 °C	1 min / 1 kbp
	final elongation	72 °C	3x elongation
	hold	4 -16 °C	∞

Template DNA isolation methods

N. magadii crude extract

To obtain DNA as a template from *N. magadii* 40 µL of culture were spin down at 13 krpm for 3 min. The supernatant was removed and the pellet was resuspended in 100 µL dH_2O.

ϕCh1

To obtain ϕCh1 DNA 400 µL of dH_2O was added to 100 µL of isolated virus solution. The DNA was then extracted by adding 250 µL of phenol and the same amount of chloroform. After vortexing followed by centrifugation at 13 krpm for 2 min, the liquid phase was transferred into a fresh tube. This process was repeated at least 3 times until no interphase was visible. Afterwards, the solution was extracted again twice with 500 µL chloroform. The DNA was then precipitated by adding 500 µL of isopropanol to the aqueous phase followed by centrifugation at 13 krpm for 30 min. The pellet was washed with 70 % EtOH and dried via lyophilisation. The pellet was then resuspended in 20 µL dH_20.

Agarose gel electrophoresis and staining

DNA samples were loaded onto a 0.8 % agarose gel in either 1x Super buffer or 1x TAE for separation. If necessary, loading dye was added. The gel was then stained in an ethidium bromide bath.

DNA gel elution

Fragments were detected via UV light after ethidium bromide staining and excised from gel. DNA was then isolated by using Promega Wizard® SV Gel and PCR Clean-Up System according to the manufacturer protocol and eluted in 30 or 50 µL dH_2O.

Plasmid DNA isolation

For plasmid DNA isolation Wizard® Plus SV Minipreps DNA Purification system was used according to their instructions with following modifications:

E. coli cultures were centrifuged in multiple 1.5 mL tubes. After discarding the supernatant, liquid culture was again added and centrifuged to double the pellet. All tubes with same culture were loaded onto one column. Elution was done in 30 or 50 µL dH_2O.

DNA restriction

Restrictions were performed as described by the manufacturer.

DNA dephosphorylation

Dephosphorylation was performed as described by the manufacturer.

DNA ligation

Ligation was performed by T4 ligase as described by the manufacturer. A molar ratio of 1:3 for vector to insert was used. Ligation was performed for 3 h or overnight at room temperature or 4°C, respectively.

Gibson assembly

To ligate fragments into a vector Gibson assembly (GA) was performed. For 50 – 100 ng of vectors, 2 – 3 molar fold excess of inserts was used. If the fragment size was below 200 bp, 5-fold excess was used. Samples were incubated at 50 °C for 15 min for 2 or 3 fragments and up to 60 min for 6 fragments. 10 or 15 µL of this GA mixture were transformed into XL1-Blue.

2.2.2. Protein methods

Crude extract protein sample

1.5 mL of cultures were centrifuged at 13 krpm for 2 min at room temperature and the supernatant was removed. A quick spin was performed and the remaining liquid was pipetted out. Depending on the optical density buffer and sample buffer were added according to given formular: $volume\ [\mu L] = 75 * OD_{600}$. Hence, the pellet was resuspended in 5 mM Na-phosphate-buffer pH 6.8 according to optical density and the same amount of 2x Laemmli sample buffer was added. The samples were heated at 95 °C for 10 min before 10 µL of them were loaded onto a SDS-PAGE.

Aceton Powders

1 L of *E. coli* or 1.5 L of *N. magadii* culture were grown until the stationary phase was reached and were then kept on ice. *E. coli* culture was centrifuged at 4 °C at 10 krpm for 10 min and *N. magadii* culture was centrifuged at 4 °C at 6000 rpm for 15 min. For 1 g pellet, 1 mL of saline for *E. coli* or 4 M NaCl for *N. magadii* was used for resuspension. After incubation at 4 °C for 5 min, 2 mL of acetone (-20 °C) per 8 mL of cell suspension was added. Vigorous mixing was performed and after incubation on ice, the vigorous mixing was repeated occasionally. The precipitate was collected via centrifugation at 10000 g for 10 min at 4 °C. After discarding the supernatant, the pellet was resuspended with 2 mL fresh acetone (-20 °C) per 8 mL of cell suspension. Centrifugation at 10000 g for 10 min at 4 °C followed. The pellet was then spread, dispersed and air dried on Whatman paper overnight. The next day, the dried pellet was broken into fine powder by grinding. A spatula tip was then added to the primary antibodies in 1x TBS and gently stirred overnight at 4 °C.

SDS-PAGE

SDS-PAGE is a method to separate proteins (Laemmli, 1970). Samples were loaded onto a SDS-PAGE. The gel was run at 40 V until samples reached stacking gel, 60 V until samples reached separating gel and 100 V until bromophenol blue eluted into the buffer.

Western Blot

Western Blot is a method to detect proteins and different variants were described by Burnette (1981), Renart et al. (1979) and Towbin et al. (1979).

Blotting

A semi-dry blotting was performed. All membranes and layers except the SDS-PAGE gel were soaked in Transfer buffer. From the anode at the bottom to the cathode on top, the following setup was made: three Whatman papers, nitrocellulose membrane, SDS-PAGE gel and three Whatman papers. Excess liquid and air were removed carefully by roller. The

blotting was performed at 83 V for 15 min for one gel and up to 30 min for four gels. Standards were labelled with pen on the membrane afterwards for better interpretation.

Blocking

The nitrocellulose membrane was incubated in a blocking solution at 4 °C overnight with gentle agitation.

Antibodies

The membrane was washed with 1x TBS for 10 min three times at room temperature. Afterwards, it was incubated with 10 mL of primary antibodies in 1x TBS with acetone powders for 1 h at room temperature. Subsequently, primary antibodies were recycled, and the membrane was washed again three times with 1x TBS. Then, the membrane was incubated with freshly prepared 10 mL of secondary antibodies in 1x TBS for 1 h at room temperature. Afterwards, the membrane was washed another 3 times with 1x TBS.

Detection

3 mL ECL and 3 µL H_2O_2 were added to the membrane 1 min before exposing. Pictures were obtained by BioRad Chemidoc and detection was performed by using High Sensitivity Chemiluminescence by setting the manual configuration of 5 to 180 s exposure time and 30 pictures. Further, a colorimetric picture was taken to visualise the marker, which then was merged into one picture of the detection series.

2.2.3. Virus isolation

N. madadii L11 was grown in three Erlenmeyer flasks with 1.5 L complemented NVM CH media each at 37 °C with agitation. After lysis, the culture was centrifuged with 6 krpm at room temperature for 20 minutes. The supernatant was then stirred gently overnight with 10 % (w/v) PEG 6000. The next day, the culture was centrifuged with 6 krpm at room

temperature for 20 minutes at room temperature. The supernatant was removed and the pellet was dissolved in 4 M NaCl Tris/HCl pH 9.5 or 4 M NaCl HEPES pH 8. The virus was then isolated by a CsCl gradient. Therefore, in Beckmann tubes 3.5 mL of CsCl solution 1.5, followed by 4 mL of CsCl solution 1.3 and 5 mL of virus suspension was pipetted. To balance the different tubes CsCl solution 1.1 or virus suspension was used. The Beckmann tubes were filled until 2mm under the seam to prevent collapsing. The suspension was then centrifuged at 30 krpm for at least 20 hours at room temperature. Consequently, phases appeared and the white shimmering phase was isolated. To purify the virus, this shimmering phase was mixed with CsCl solution 1.3 and centrifuged again in Beckmann tubes with the same setting as mentioned above. Once again, the white shimmering phase was isolated. This phase was then dialysed for one hour and afterwards overnight in 4 M NaCl Tris/HCl pH 9.5 or 4 M NaCl HEPES pH 8. Nucleic acid and protein concentration was measured by Thermo Scientific™ NanoDrop™ 2000/2000c Spectrophotometers (catalog number ND-2000C). The virus was then stored at room temperature.

2.2.4. Generation of competent cells, transformation procedure and inoculation of colonies

E. coli strains

Generation

Strains were inoculated into 100 mL LB media with antibiotics at 37 °C at 165 rpm to an OD_{600} of 0.6. Then the culture was centrifuged at 10 kprm for 10 min. The pellet was resuspended in 40 mL MOPS I and incubated on ice for 10 min. Centrifugation was repeated with the same settings mentioned above and the pellet was resuspended in 40 mL MOPS II. Afterwards, it was left on ice for 30 min and centrifugation was repeated. The pellet was resuspended in 2 mL MOPS IIa and stored in 100 µL aliquots at -70 or -80 °C for up to six months.

Transformation

100 µL aliquots are thawed on ice before use. DNA eluate is added to aliquot (4 µL of vector, 10 or 15 µL Gibson assembly mix, 10 – 15 µL ligation mix or up to 1 µg DNA) and incubated on ice for 30 min. Afterwards, the samples underwent a heat shock at 42 °C for 2 min followed by immediate incubation on ice for another 2 min. Subsequently, 300 µL of LB were added and the cells were regenerated on 37 °C for 30 min. Next, the cells were plated on selective media and incubated at 37 °C overnight.

Inoculation

Single colonies were inoculated in 500 µL selective media and incubated at 37 °C with agitation overnight.

N. magadii strains

Generation

In each Erlenmeyer flask with 50 mL complemented NVM CAA containing 70 µg mL^{-1} bacitracin, either 2, 4 or 6 mL of a *N. magadii* L13 pre-culture were inoculated at 37 °C until OD_{600} 0.6 was reached. The culture closest to this value was then harvested by centrifugation at 6 krpm for 15 min at room temperature. The pellet was resuspended in HS buffered spheroplast solution (20 mL for OD_{600} 0.6) and proteinase K was added to a final concentration of 0.1 % (v/v). Consequently, the cell suspension was incubated at 42 °C for up to 48 h until the S-layer of the organisms was lost, which was screened under the microscope. Competent cells were stored at room temperature for up to one week.

Transformation

1.5 mL of competent cells were centrifuged for 3 min at 10 krpm at room temperature. Then, the pellet was resuspended in 150 µL HS buffered spheroblast solution and DNA was added (0.5 – 3 µg as standard condition or 5 – 30 µg for deletions) up to maximum of 10 µL. After 5 min of incubation at room temperature, 150 µL of 60 % PEG-600 in HS

unbuffered spheroblast solution was added, followed by incubation for 20 to 30 minutes at room temperature. Consequently, 1 mL of complemented media was added to the cells carefully. Then, the volume was transferred into a culture tube (12 mL capacity) and another 1 mL of complemented media was added. Cells were regenerated at 37 °C with agitation for at least one day until their morphology returned to their natural rod shape. Subsequently, 100 µL of cell suspension (undiluted, 1:10 and 1:100 dilutions) were plated on selective NVM media. Plates were sealed into plastic bags to prevent desiccation and incubated at 42 °C for at least one and a half weeks.

Inoculation

Single colonies were inoculated in 500 µL selective media and incubated at 37 °C with agitation for up to one week. Successfully regenerated cultures were identified by visible turbulences when agitated.

2.2.5. General handling of liquid cultures

Liquid cultures were grown with 165 rpm agitation if not indicated otherwise. *E. coli* strains were grown at 37 °C. *N. magadii* strains were grown on 42 or 37 °C, depending on the experimental requirements. For passaging, cultures were inoculated in baffled flasks.

2.2.6. Tools and Resources used

Agarose gel and Western Blot images were obtained by using the software Image Lab (Biorad). Sequences were analysed with Gene Runner and SnapGene. Sanger Sequencing was performed by Microsynth. Sequences were aligned with Nucleotide BLAST (Basic Local Alignment Search Tool):

https://blast.ncbi.nlm.nih.gov/Blast.cgi?PROGRAM=blastn&PAGE_TYPE=BlastSearch&LINK_LOC=blasthome

Figures were edited with Microsoft PowerPoint and Office 365 Excel. DeepL and Grammarly were used to improve the language in this work.

3. Results and discussion

3.1. Recombinase RadA and RadB in *N. magadii*

3.1.1. *radA* and *radB* suicide plasmids

This study aimed to analyse the inversion of the ϕCh1 invertible region. Three enzymes are suggested to cause this: Int1, RadA or RadB and this thesis focuses on the latter two. To obtain homozygous *radA* or *radB N. magadii* L13 deletion mutants, suicide plasmids containing *gyrB* mediating the resistance to novobiocin (Nov) were cloned. As the name indicates, the suicide plasmids cannot replicate in *N. magadii*, therefore, obtaining the resistance requires the Nov cassette to be integrated into the chromosome via homologous recombination. To improve the chance of recombination, the Nov resistance cassette was cloned in forward and reverse directions for both variants. Therefore, *radA* up- and downstream sequences flanking *gyrB* were cloned into *Eco*RI restricted shuttle vector pKSII+ using GA-primers RadA-1, RadA-2-F, RadA-3-F and RadA-4. The principle was the same for reversed *gyrB* (RadA-1, RadA-2-R, RadA-3-R and RadA-4) and for cloning of all *radB* deletion constructs (forward (fw): RadB-1, RadB-2-F, RadB-3-F and RadB-4; reverse (rv): RadB-1, RadB-2-R, RadB-3-R and RadB-4). Template DNA used for recombinases cloning were obtained from chromosomal *N. magadii* L13 DNA, for *gyrB* from plasmid pUC19-Nov “forward” and pUC-19-Nov “reversed”. Table 2 summarises all templates and primers used for each construct. Subsequently, Gibson assembly was performed. Afterwards, the GA mixture was transformed into XL1-Blue and clones were PCR screened by using primers A-5-1 and A-3-1 for *radA* deletion or B-5-1 and B-3-1 for *radB* deletion. From positive clones, plasmid DNA was isolated and transformed into competent L13.

After screening of 115 colonies no positive *N. magadii* L13 clones for *radA* deletions transformants could be obtained, therefore, the *gyrB* flanked by up- and downstream sequences of *radA* were extended to 1332 bp upstream and 988 bp downstream to increase the DNA overlay for homologous recombination (RadA-1-1 and RadA-4-1).

suicide plasmid	templates	primers
pKSII+ -Δ*radA*F	L13	RadA-1-1, RadA-4-1
	pUC19-Nov “forward”	RadA-2-F, RadA-3-F
pKSII+ -Δ*radA*R	L13	RadA-1-1, RadA-4-1
	pUC19-Nov “reverse”	RadA-2-R, RadA-3-R
pKSII+ -Δ*radB*F	L13	RadB-1, RadB-4
	pUC19-Nov “forward”	RadB-2-F, RadB-3-F
pKSII+ -Δ*radB*R	L13	RadB-1, RadB-4
	pUC19-Nov “reverse”	RadB-2-R, RadB-3-R

Table 2: Templates and primers used for constructing suicide plasmids.

3.1.2. Homologous recombination and passaging

The aim was to generate homozygote *radA* or *radB N. magadii* L13 deletion mutants. It is assumed that *N. magadii* contains 50 chromosomes (A. Witte, personal communication). After the exchange of *radA* or *radB* for *gyrB* in forward ($Nov^{R\text{-}fw}$ cassette) or reverse direction ($Nov^{R\text{-}rv}$ cassette) (Figure 3), the cultures were passaged. Upon cell division, the chromosome doubles and the two chromosomes carrying the Nov resistance cassette can be either distributed to two individual cells, or one cell can acquire both. As the Nov resistance gets inherited and thereby deletes the *radA* or *radB* gene over generations, the first homozygous organisms could theoretically occur after six generations as illustrated in Figure 4. However, this case is not very likely to happen with a probability of ~0.001147 %.[1] Nevertheless, in this sixth generation, all daughter cells would carry the antibiotic resistance cassette in multiple copies. Therefore, obtaining a homozygous deletion mutant becomes more and more likely after continuous passaging. The formula for the possible cell distribution in a generation is $P_{n\leq 50}(n) = \frac{n}{2} + 1$ if the number of chromosome carrying the resistance is 50 or underneath. If the dividing cell carries over 50 chromosomes containing the antibiotic resistance cassette the formula is $P_{n>50}(n) = 51 - \frac{n}{2}$. The variable n represents the number of chromosomes with

[1] This was calculated with the formula $p(P) = \frac{1}{P} * 100$, which calculates the probability in percent of the cell carrying the highest amount of the antibiotic resistance cassette. In this case $p_{\Delta\, after\, G6} = \frac{1}{2*3*5*9*17*19} * 100 = \sim 0.001147\ \%$.

resistance genes in the dividing cell. The strains of the passages are referred to as *N. magadii* P(No.) L13 RadA⁻(Nov$^{R\text{-}fw}$), P(No.) L13 RadA⁻(Nov$^{R\text{-}rv}$), P(No.) L13 RadB⁻(Nov$^{R\text{-}fw}$) and P(No.) L13 RadB⁻(Nov$^{R\text{-}rv}$). The acquired homozygous deletion mutants would be named as L13-*ΔradA* or L13-Δ*radB*. Figure 5 shows the primers and fragment length of the PCR screens used for *radA* or *radB* exchange to Nov$^{R\text{-}fw}$ or Nov$^{R\text{-}rv}$ cassette via homologous recombination.

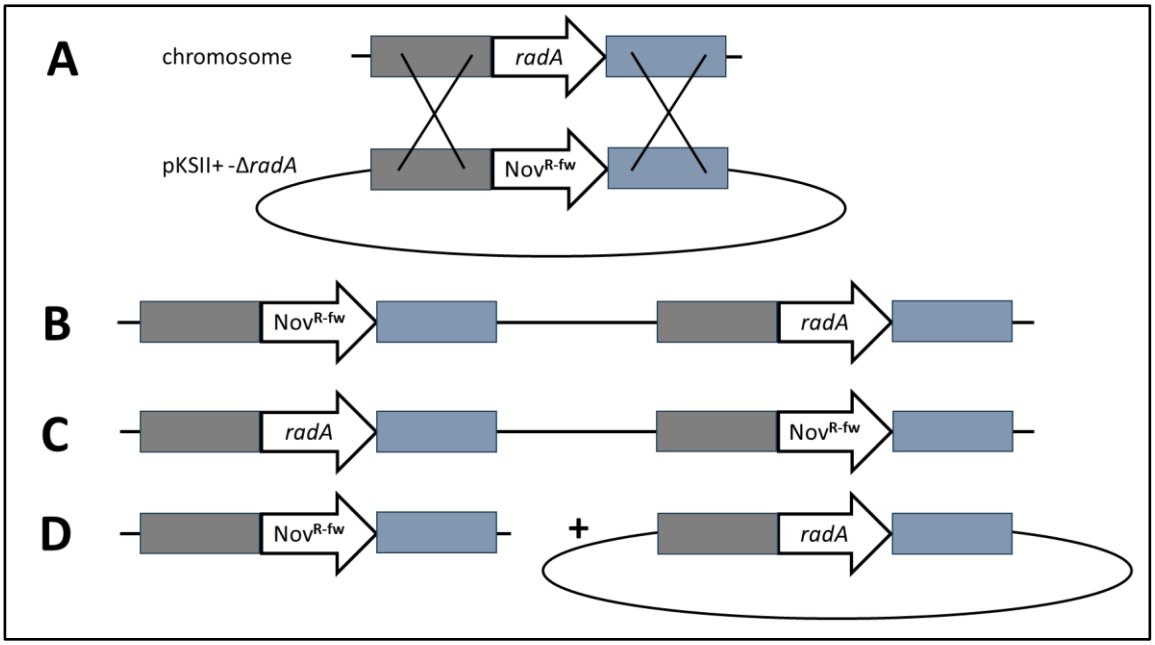

Figure 3: Schematic of gene replacement via homologous recombination. (**A**) Up- and downstream sequences are identical for both dsDNA. Thus, gene exchange via homologous recombination is possible. However, there are different recombination events possible. In case (**B**), the Nov$^{R\text{-}fw}$ cassette and the whole vector are recombined prior to *radA* if only the upstream part, shown in grey, is involved in recombination. In (**C**), only the downstream element, shown in blue, was involved in recombination, resulting in the insertion of the whole vector and Nov$^{R\text{-}fw}$ cassette after *radA*. Only in case (**D**) the up- and downstream elements recombine leading to the exchange of *radA* for Nov$^{R\text{-}fw}$ cassette in forward direction.

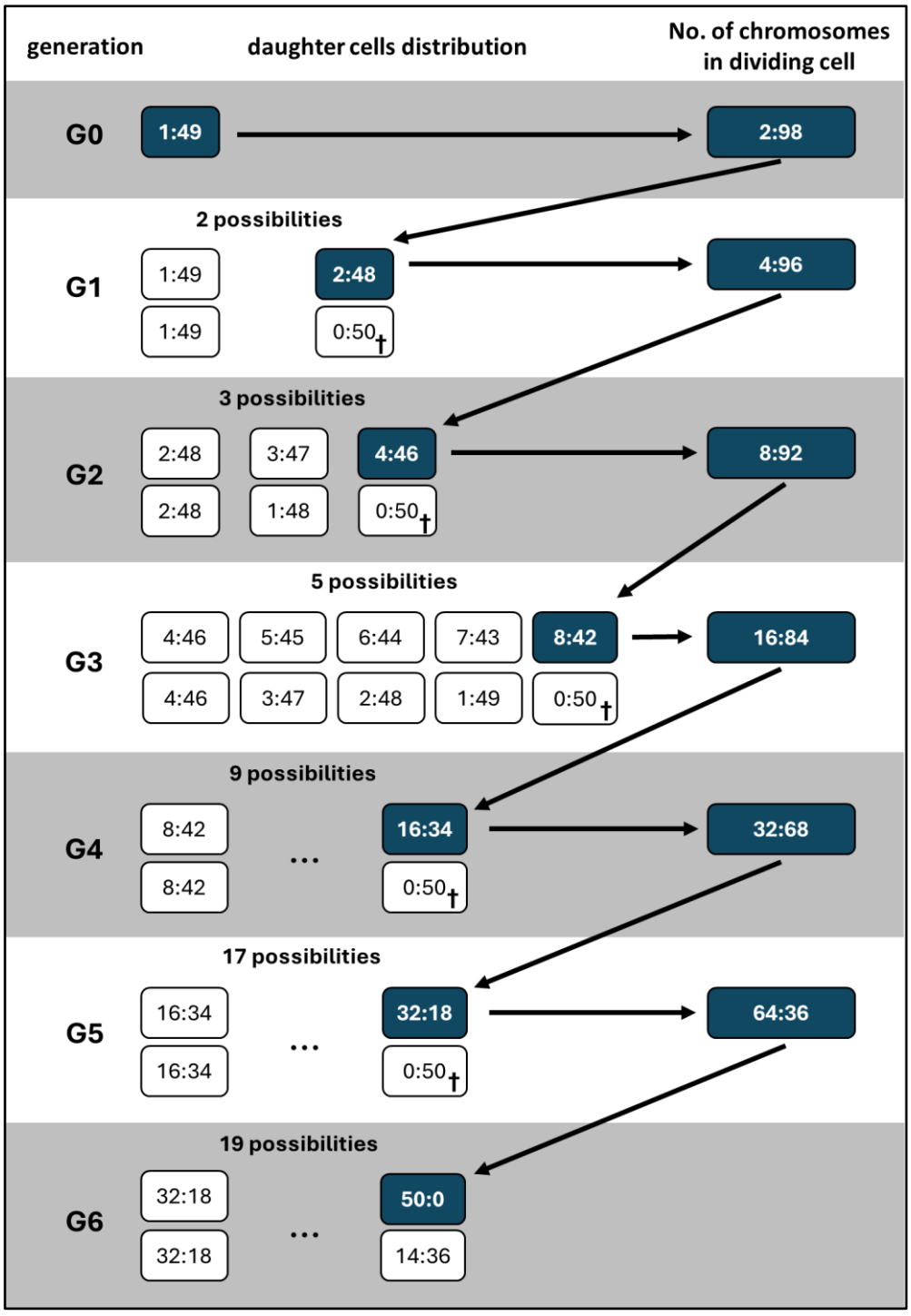

Figure 4: Schematic of hypothetical homozygous deletion by replacement through an antibiotic resistance cassette in a polyploid organism with 50 chromosomes such as likely *N. magadii* is. The rectangles represent a cell and chromosome distribution is given within the cell. The number in the cell on the left side counts the chromosome containing the antibiotic resistance, while the right counts for the wild type chromosomes. This illustration depicts the distribution of chromosomes of dividing cells. Only organisms that carry the antibiotic resistance will survive on selective media. The probability of getting an organism carrying the highest possible recombined chromosomes in the first generation is 50%, for the second generation 33.33 %, for the third 20 %, for the fourth

11.11 %, for the fifth 5.88 % and the sixth 5.26 %. If the cultures are passaged for longer, the higher the outcome of cells starting with a higher number of chromosomes harbouring the antibiotic resistance cassette. In this graph, chromosomes are distributed randomly and putative recombination or mutation are not considered. Further, this model shows only the fastest path (Derntl (2009) with modifications).

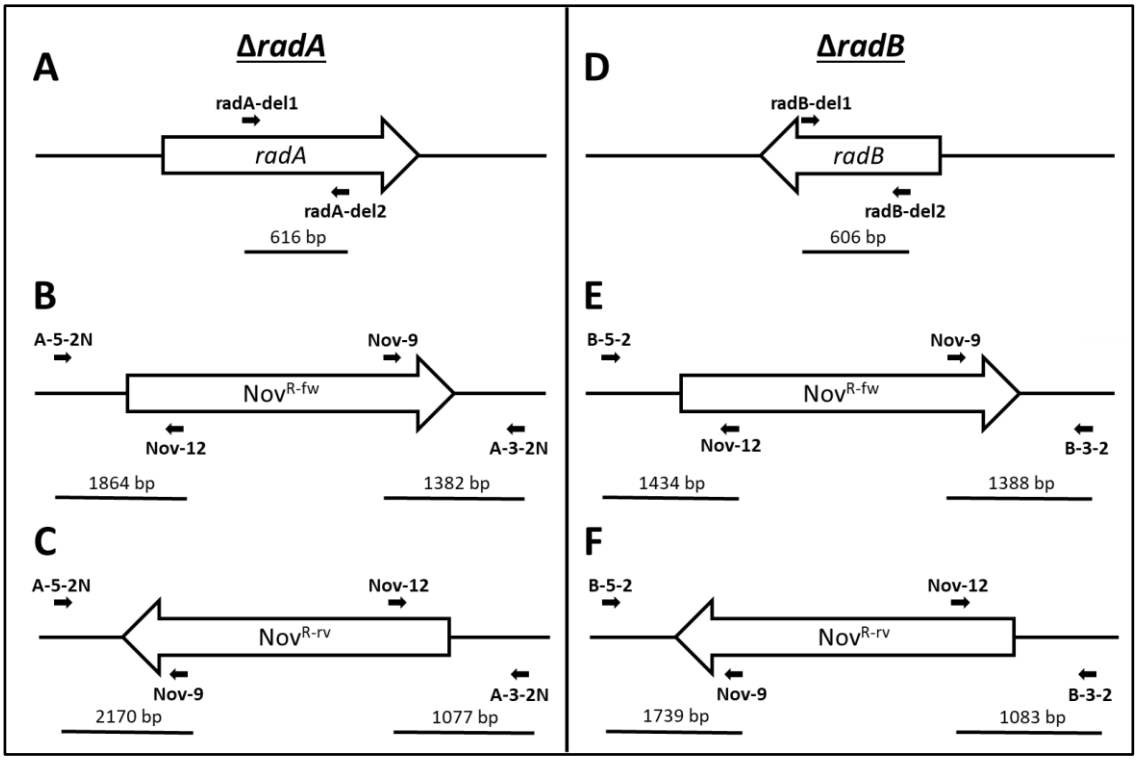

Figure 5: Schematic of the performed recombination PCR screens. Primers are indicated with arrows and the length of amplified DNAs are shown as vertical black line below the gene schematic. On the left side, all constructs with corresponding primers used for PCR screen for Δ*radA* are depicted: (**A**) *radA* deletion screen, (**B**) up- and downstream recombination of Nov$^{R\text{-}fw}$ cassette into *N. magadii* screen and (**C**) up- and downstream recombination of Nov$^{R\text{-}rv}$ cassette into *N. magadii* screen. On the right side, all constructs with corresponding primers used for PCR screen for Δ*radB* are depicted: (**D**) *radB* deletion screen, (**E**) up- and downstream recombination of Nov$^{R\text{-}fw}$ cassette into *N. magadii* screen and (**F**) up- and downstream recombination of Nov$^{R\text{-}rv}$ cassette into *N. magadii* screen.

Before starting the passaging and after every fifth passage, PCR screens were performed. In addition, a dilution streak on complemented NVM CAA Nov plates was done after every fifth passage. As shown in Figure 6, no homozygous *radA* or *radB N. magadii* L13 deletion strain could be obtained. Although the Nov cassette was successfully recombined into the chromosomes, the gene *radA* is still detectable via PCR by using internal primers

radA_del1, radA_del2 in L13 RadA⁻(Nov$^{R\text{-}fw}$) after 23 passages and in L13 RadA⁻(Nov$^{R\text{-}rv}$) after 20 passages. This is also true for the gene *radB* since it was detected by using the internal primers radB-del1, radB-del2 in L13 RadB⁻(Nov$^{R\text{-}fw}$) after 34 passages and in L13 RadB⁻(Nov$^{R\text{-}fw}$) after 37 passages. This is in contrast to previous studies since homozygous deletion mutants could be obtained after 15 passages (Derntl, 2009; Schöner, 2013). Therefore, the question arises as to whether these genes are essential for *N. magadii,* meaning that these genes cannot be replaced in all chromosomes in order to survive. Consequently, new experiments were performed to verify this hypothesis.

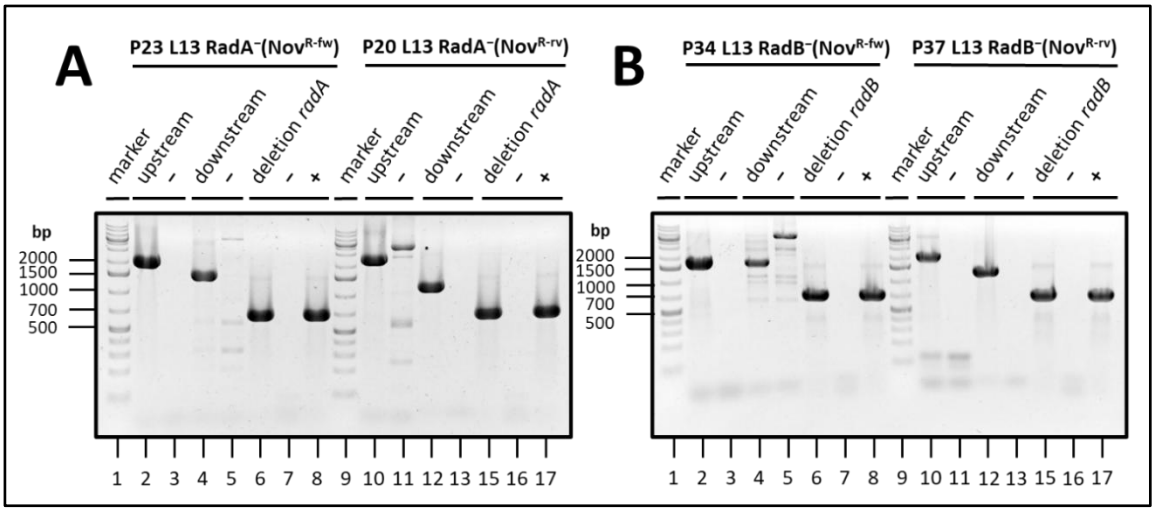

Figure 6: PCR screens of final passages. 0.8 % agarose in 1x Super buffer gel. (**A**) Marker loaded on slots 1 and 9. Upstream, downstream and deletion screen PCRs of passage *N. magadii* P23 L13 RadA⁻(Nov$^{R\text{-}fw}$) and P20 of L13 RadA⁻(Nov$^{R\text{-}rv}$). PCR amplicons of P23 crude extract were loaded on slots 2, 4, 6 and for P20 on slots 10, 12 and 15. As negative controls (indicated with **–**) for up- and downstream PCR screen wildtype L13 was used and loaded onto slots 3, 5, 11 and 13. For deletion screens dH_20 was used as a negative control (indicated as **–**, slot 7) and wildtype L13 was used as the positive control (indicated as +, slot 8). The chromosomal exchange of *radA* against Nov resistance cassette (*gyrB*) was detected for upstream (1864 bp for Nov$^{R\text{-}fw}$ and 2170 bp for Nov$^{R\text{-}rv}$) and downstream (1382 bp for Nov$^{R\text{-}fw}$ and 1070 bp for Nov$^{R\text{-}rv}$) of *radA*. However, *radA* could not be deleted in all chromosomes for both passages in *N. magadii* L13 since the gene is still detectable via PCR using internal primers after 50 cycles (616 bp). (**B**) Same schematic scheme as *radA* for *radB* deletion and equivalent PCR procedures. *N. magadii* P34 L13 RadB⁻(Nov$^{R\text{-}fw}$) PCR amplicons were loaded on slots 2, 4, 6 and P37 L13 RadB⁻(Nov$^{R\text{-}fw}$) PCR amplicons were loaded onto slots 10, 12 and 15. The same controls as described for (**A**) were used. Upstream signals were detected at 1434 bp for Nov$^{R\text{-}fw}$ and 1739 bp for Nov$^{R\text{-}rv}$. Downstream signals are located at 1388 bp for Nov$^{R\text{-}fw}$ and 1083 bp for Nov$^{R\text{-}rv}$. The gene *radB* is also detectable via PCR using internal primers after 50 cycles. After over 30 passages, *radB* is still discernible at 606 bp in both passage strains.

3.1.3. Antisense *radA* and *radB* RNA codon plasmids

To test if *radA* or *radB* are essential genes, plasmids encoding for antisense *radA* or *radB* genes under the control of the tryptophan inducible promoter ptnaN were constructed. In the absence of tryptophan, the *tna* gene was nearly inactive and, thus, the *tna* promoter was shown to be appropriate for transcription induction in *H. volcanii* (Large et al., 2007). Selb et al. (2017) showed the inducibility of the *tnaA* promoter by using the *bgaH* reporter gene in *N. magadii* upon addition of tryptophan to minimal media. Therefore, anti-*radA* encoding RNA fragments were amplified via PCR by using GA-primers a-RadA-1_pRo-5, a-RadA-2, a-RadA-3 and a-RadA-4_pRo-5 for shuttle vector pRo-5 and a-RadA-1_pNB102, a-RadA-2, a-RadA-3 and a-RadA-4_pNB102 for shuttle vector pNB102. As a template, *N. magadii* L13 chromosomal DNA and pBAD24-tnaN were used. The plasmid pRo-5 carries Nov resistance while pNB102 harbours mevinolin resistance (Mev). Nov inhibits DNA gyrase (Holmes et al., 1991) while the synthesis of side chains of isoprenoid lipid is inhibited through Mev (Lam & Doolittle, 1992). Fragments for anti-*radB* encoding RNA were amplified via PCR by using GA-primers a-RadB-1_pRo-5, a-RadB-2, a-RadB-3 and a-RadB-4_pRo-5 for pRo-5 and a-RadB-1_pNB102, a-RadB-2, a-RadB-3 and a-RadB-4_pNB102 for pNB102. Further, control constructs with the ptnaN promoter only were amplified by using GA-primers a-RadA-1_pRo-5, ptnaN-pRo5 for pRo-5 and a-RadA-1_pNB102, ptnaN_pNB102 for pNB102. A summary of all templates and primers used for each construct is provided in Table 3. All constructs were cloned into *Eco*RI restricted pRo-5 and pNB102 by Gibson Assembly. Afterwards, 10 µL of this GA mixture was transformed into XL1-Blue and from positive clones, the plasmid was isolated from an overnight culture. Consequently, the vector was then transformed into *N. magadii* L13. Crude extracts of transformants were then screened by PCR using primers Tna-N-1, Tna-N-2, radA_del1 and radB_del1 as shown in Figure 7.

construct	templates	primers
pRo-5-ptnaN	pBAD24-tnaN	a-RadA-1_pRo-5, ptnaN-pRo5
pRo-5-ptnaN-a_*radA*	pBAD24-tnaN	a-RadA-1_pRo-5, a-RadA-2

construct	templates	primers
	L13	a-RadA-3, a-RadA-4_pRo-5
pRo-5-ptnaN-a_*radB*	pBAD24-tnaN	a-RadB-1_pRo-5, a-RadB-2
	L13	a-RadB-3, a-RadB-4_pRo-5
pNB102-ptnaN	pBAD24-tnaN	a-RadA-1_pNB102, ptnaN_pNB102
pNB102-ptnaN-a_*radA*	pBAD24-tnaN	RadA-1_pNB102, a-RadA-2,
	L13	a-RadA-3, a-RadA-4_pNB102
pNB102-ptnaN-a_*radB*	pBAD24-tnaN	RadB-1_pNB102, a-RadB-2,
	L13	a-RadB-3, a-RadB-4_pNB102

Table 3: Templates and primers used for antisense RNA coding constructs.

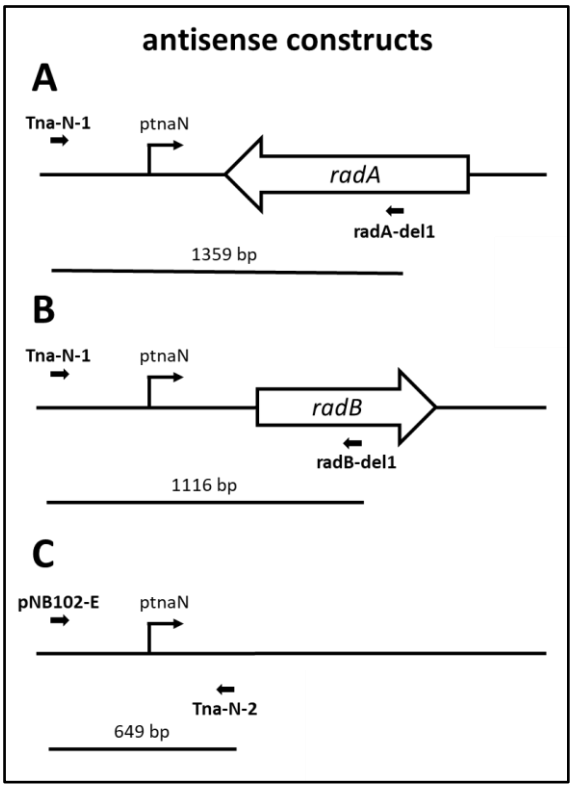

Figure 7: Schematic of the antisense constructs. Primers used for PCR screens and fragment length are indicated. (**A**) shows promoter ptnaN and antisense *radA* construct, (**B**) promoter and antisense *radB* and (**C**) ptnaN promoter only in pNB102.

While all constructs for pNB102 could be obtained, this was only true for antisense *radA* encoding RNA for pRo-5 (Figure 8). After multiple cloning of pRo-5 antisense constructs and transformations into L13, crude extract of 79 picked colonies of antisense *radB* and

87 picked colonies of control construct (harbouring only the ptnaN promoter) were PCR screened if they carry the construct. Unfortunately, no positive strain could be detected. This is in contrast to the antisense *radA* construct where one positive out of 24 tested could be obtained. Thus, pRo-5 constructs were no longer taken into consideration.

These results were unexpected because Mayrhofer-Iro et al. (2013) showed that pRo-5 has a high transformation efficiency.

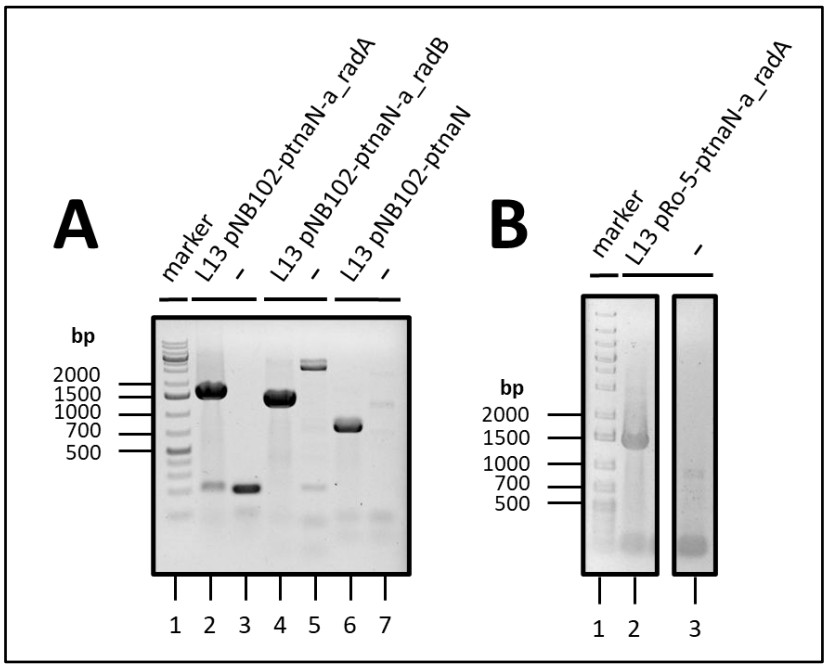

Figure 8: PCR screens of antisense constructs. (**A**) 0.8 % agarose in 1x Super buffer gel. As negative control, indicated with **–**, wildtype L13 was used. The fragments length of the PCR screens of pNB102 carrying antisense *radA* coding is 1359 bp (slot 2), of antisense *radB* coding is 1116 bp (slot 4) and the plasmid carrying only the promoter is 649 bp (slot 6). (**B**) 0.8 % agarose in 1x TAE gel. As negative control, indicated with **–**, wildtype L13 was used. Only the antisense coding *radA* was obtained with a PCR screen fragment of 1359 bp (slot 2).

3.1.4. Time kinetics with antisense *radA* and *radB*

To analyse now the influence of *radA* or *radB*, precultures of strains L13 pNB102-ptnaN, L13 pNB102-ptnaN-a_*radA* and L13 pNB102-ptnaN-a_*radB* were inoculated in selective media. Upon reaching the stationary phase, each strain was inoculated in 50 mL of complemented NVM CAA without yeast extract and Mev with a start OD_{700} of 0.05 in

parallels. Three cultures of each strain were then induced around OD_{700} of 0.3 with 4 mM L-tryptophan. Two cultures of non-induced strains served as a reference. The strains that carried the promoter only (L13 pNB102-ptnaN) served as the control. The optical density was measured daily for 12 days. As Figure 9 and Figure 10 illustrate, few differences between the induced and uninduced cultures can be seen. The depicted values of the induced and uninduced control strain are the same for both figures. However, the colour of the uninduced culture changed during the growth kinetics (Figure 11). The strain harbouring the antisense *radA* RNA codon turned red (Figure 11, A), the strain containing antisense *radB* turned orange (Figure 11, B) and the control strain (carrying the ptnaN promoter only) light yellow (Figure 11, C). This is in contrast to the induced ones, where all strains had a dark yellow to brownish colour (Figure 11, D-F).

These results conclude that neither *radA* nor *radB* would be essential for *N. magadii*. Nevertheless, large RNAs are likely not very stable because they can form secondary structures. Further, the host could have some defence mechanisms to avoid the genes from silencing.

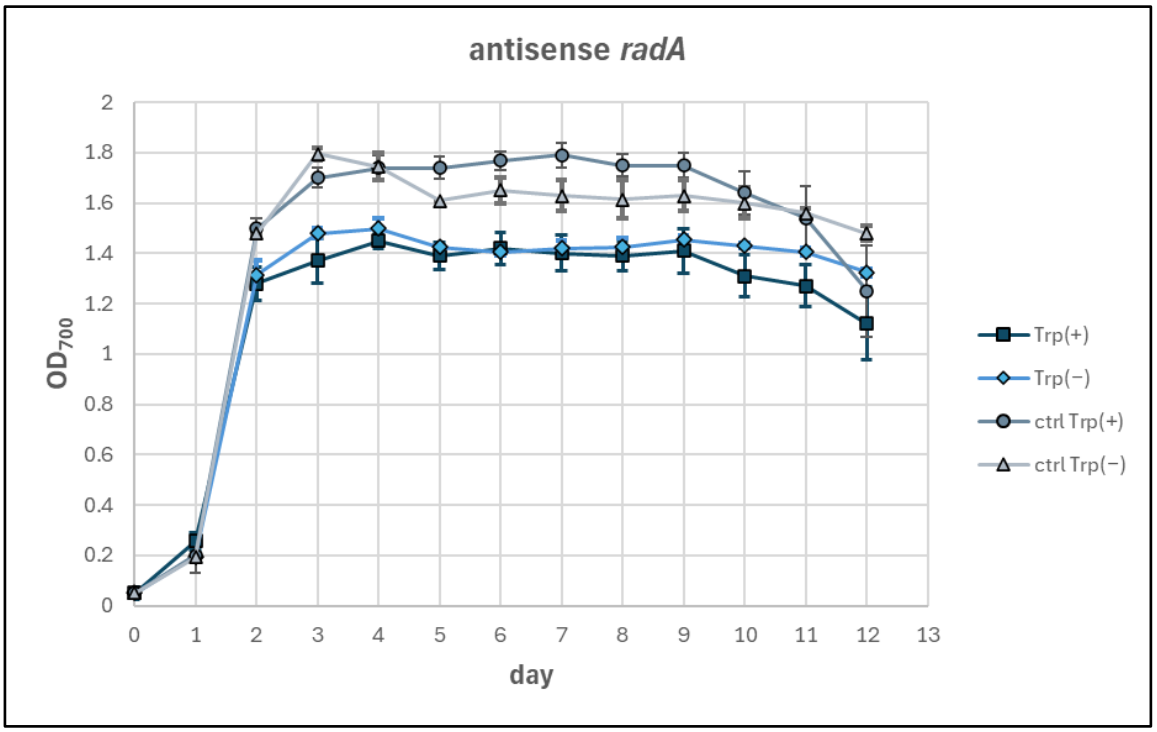

Figure 9: Growth kinetic of L13 pNB102-ptnaN-a_*radA*. Results from induced cultures were derived from triplicates and results from uninduced cultures from duplicates.

Cultures were induced one day after inoculation at around OD_{700} 0.3. The control strains appear to have a higher population density as the antisense *radA* constructs. However, little discrepancies are visible for the induced and uninduced antisense *radA*. With day 10, the OD values drop slightly for the induced strains compared to the non-induced ones.

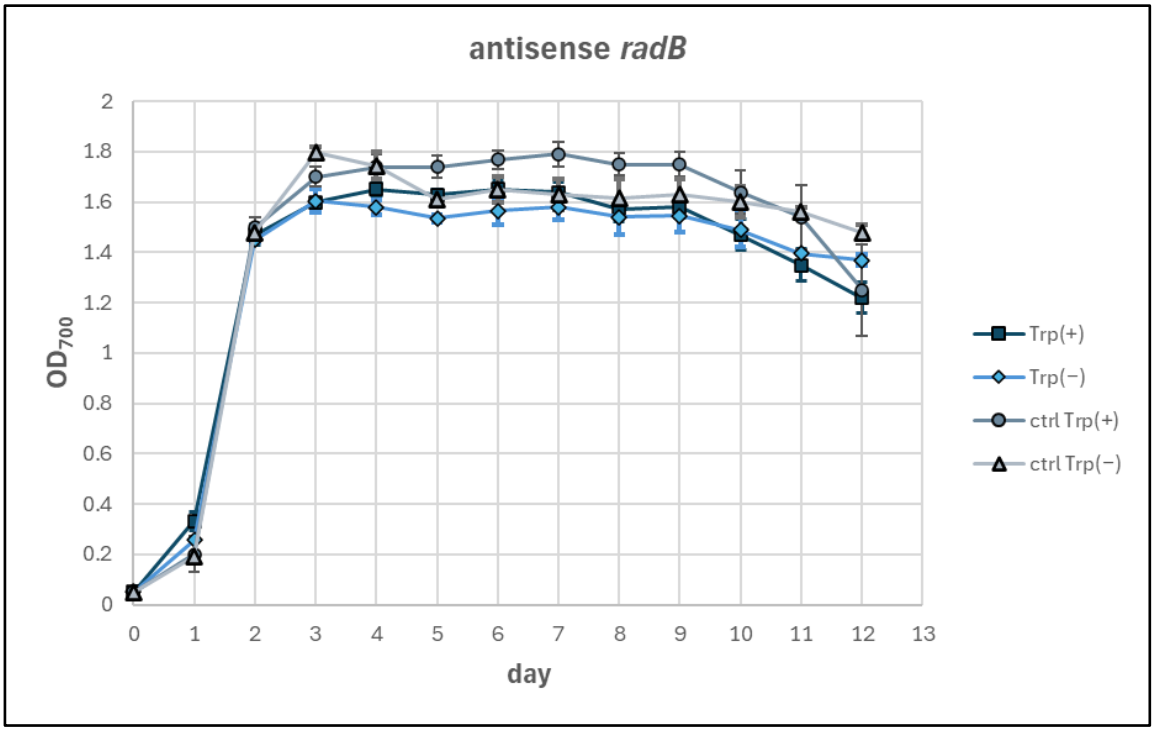

Figure 10: Growth kinetic of L13 pNB102-ptnaN-a_*radB*. Results from induced cultures were derived from triplicates and results from uninduced cultures from duplicates. Cultures were induced one day after inoculation at around OD_{700} 0.3. The control strains appear to have a higher population density as the antisense *radB* constructs. However, little discrepancies are visible for the induced and uninduced antisense *radB*. With day 11, the OD values of the induced strains drop faster than the non-induced ones.

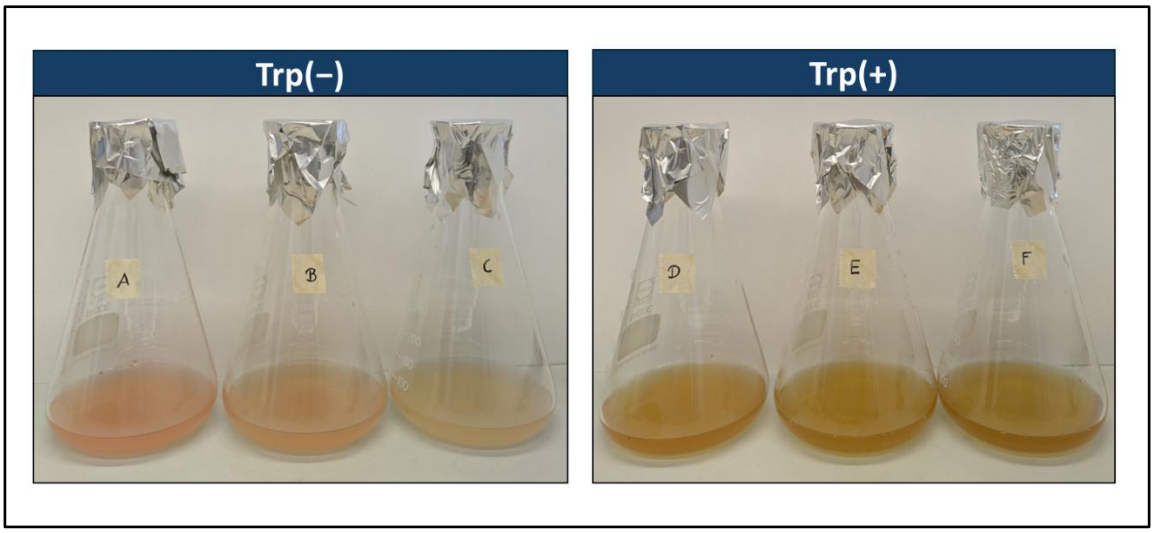

Figure 11: Cultures after 12 days of incubation in complemented NVM CAA with Mev (control) or complemented NVM CAA with Mev Trp (induced) at 37 °C. (**A**) L13 pNB102-ptnaN-a_*radA*, (**B**) L13 pNB102-ptnaN-a_*radB*, (**C**) L13 pNB102-ptnaN, (**D**) induced L13 pNB102-ptnaN-a_*radA*, (**E**) induced L13 pNB102-ptnaN-a_*radB* and (**F**) induced L13 pNB102-ptnaN-a_*radA*. While (**A**-**C**) were grown without induction, (**D**-**F**) were induced with 4 mM Trp. Colour of the uninduced strains varied.

3.1.5. Spot test

Since the results for the growth kinetics did not show any difference, a spot test was performed. Therefore, on a plate triplets of 5 µL of cultures with an OD_{700} of 1 and dilutions were spotted. The plate was wrapped in aluminium foil and incubated at 37 °C until spots appeared. As depicted in Figure 12, the sizes of the spots of the antisense constructs (L13 pNB102-ptnaN-a_*radA* and L13 pNB102-ptnaN-a_*radB*) for the undiluted spots (1:1) do not significantly vary from the control constructs (L13 pNB102-ptnaN). For the 1:10 dilutions, no spot appeared at all for the control on the top. Generally, the controls did not grow as well as the strains with the antisense constructs. Another interesting observation is that the spots on the edge for the 1:10 dilutions also did not grow as well as the spots in the middle of the plate. This was also experienced on a previous spot assay plate (data not shown). One possible explanation could be that there was a pipetting error. However, it seems unlikely that pipetting errors happen twice on similar spots on different plates. Hence, the reasons why no spots could be obtained on the edges for the dilutions remains unclear.

Interestingly, the colours of the different strains varied. The colour of the antisense *radA* RNA codon construct was red, for antisense *radB* the colour was dark orange and for the control construct it was orange. These results are in contrast to the prior growth kinetics experiments because the colour resembles the not induced strains.

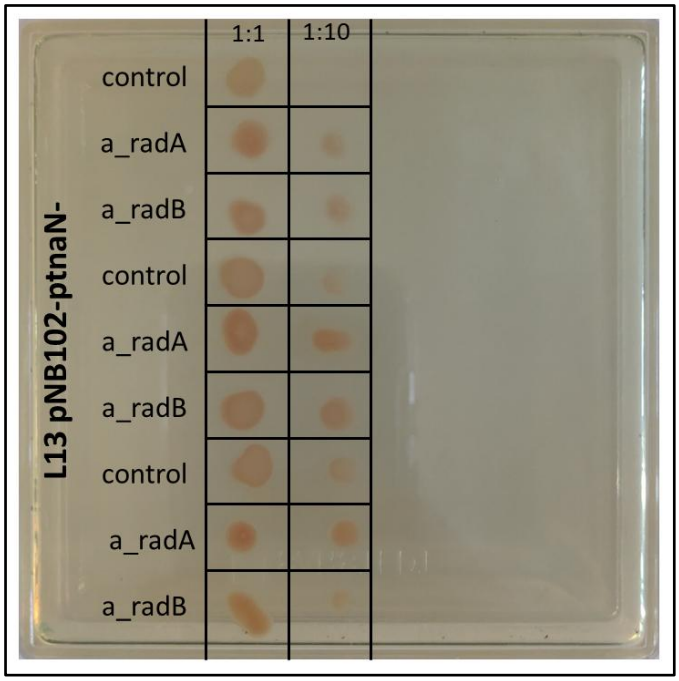

Figure 12: Spot test of L13 pNB102-ptnaN (control), L13 pNB102-ptnaN-a_*radA* and L13 pNB102-ptnaN-a_*radB* on a plate with complemented NVM CAA without yeast extract with Mev and Trp.

3.2. ΦCh1 nucleoside capsid proteins

The purpose of this experiment is to identify novel nucleocapsids of virus ϕCh1. Therefore, *N. magadii* L11 strain was grown in Erlenmeyer upon lysis. Then, ϕCh1 was isolated as described in Material and Methods.

3.2.1. Mass spectroscopy analysis

To analyse the different proteins which are part of the capsid structure of ϕCh1, mass spectroscopy was performed with an isolated virus suspension. The mass spectroscopy was performed by IMC University of Applied Sciences Krems by Reinhard Klein and colleagues. The suspension using either Tris/HCl or HEPES as a buffer system was analysed separately by MS. Since it is known that Tris can interfere with the proteins and can lead to adducts, which could result in peaks in the spectra, this experiment was also performed with HEPES (*FAQ: Core Facility Hohenheim - Modul 1 Massenspektrometrie*, 2018; Kabadi et al., 2016). The data were obtained as Microsoft Office Excel files (see Supplementary Table 1 and Supplementary Table 2). In these documents, all the found proteins were listed with the corresponding ORFs through accession numbers (see Supplementary Table 1 and Supplementary Table 2). The results of the MS indicated that Tris was a feasible buffer. The comparison of the data of the virus suspension in the different buffers showed nine ORFs of ϕCh1 in common, namely ORF14, ORF16, ORF24, ORF25, ORF28, ORF29, ORF36, ORF61 and ORF71. According to Klein et al. (2012), RNA of ORF36 could not be detected in L11 during time kinetics of 225 h. Hence, this ORF was not considered as part of the viral particles. Nevertheless, ORF36 is part of the ϕCh1 invertible region (Klein et al., 2012). ORF12 was only found in the analysis where HEPES was used as buffer but since it's an early gene surrounded by other capsid encoding ORFs, it was chosen for further study.

3.2.2. Cloning of ORFs into pRSET-A and transformation into *E. coli* strains

In order to demonstrate that these proteins are actually components of the virus, or are present there in a corresponding number of copies, they were cloned and the ORFs were expressed in *E. coli*.

ORF12, ORF14, ORF16, ORF24, ORF25, ORF28, ORF61 and ORF71 were amplified by PCR and restricted with *Bam*HI and *Hin*dIII. ORF29 was restricted with *Bgl*II and *Hin*dIII after PCR amplification. Primers used for cloning for the different ORFs have the corresponding number in their name: p12-5, p12-3, ORF14-5, ORF14-3, p16-5, p16-3, 24-Hind, 24-Bam, 25-Hind, 25-Bam, 28-Hind, 28-Bam, 29-Hind, 29-Bgl, ORF61-5, ORF61-3, ORF71-5 and ORF71-3 (see Table 4). Afterwards, the fragments were cloned into *Bam*HI and *Hin*dIII restricted pRSET-A via T4 ligase and transformed into XL1-Blue. *Bgl*II restricted ORF29 amplicons have the same overhang as *Bam*HI restricted ORFs. All cloned ORFs are under the control of the T7 promoter (Milligan et al., 1987; Milligan & Uhlenbeck, 1989). Positive PCR screened clones were inoculated in 15 mL LB ampicilin (Amp) tetracycline (Tet) to obtain plasmid DNA. 4 µL of isolated plasmid DNA were then transformed into BL21(DE3).

ORF	template	primers
ORF12	ϕCh1	p12-5, p12-3
ORF14	ϕCh1	ORF14-5, ORF14-3
ORF16	ϕCh1	p16-5, p16-3
ORF24	ϕCh1	24-Hind, 24-Bam
ORF25	ϕCh1	25-Hind, 25-Bam
ORF28	ϕCh1	28-Hind, 28-Bam
ORF29	ϕCh1	29-Hind, 29-Bgl
ORF61	ϕCh1	ORF61-5, ORF61-3
ORF71	ϕCh1	ORF71-5, ORF71-3

Table 4: Templates and primers used for the predicted ϕCh1 ORFs encoding nucleocapsid proteins.

3.2.3. Time series of selected ORF in BL21(DE3)

A BL21(DE3) pRSET-A strain carrying one of the ϕCh1 ORFs constructs was inoculated with an overnight culture to a start OD_{600} of 0.1 in 25 mL LB chloramphenicol (Cam) Tet. At OD_{600} 0.3, IPTG was added and samples were taken before induction (0 min) and 15, 30, 45, 60, 90, 120 min after induction. IPTG enables the transcription of T7 RNA polymerase and consequently, this leads to the expression of the cloned ORF (Studier & Moffatt, 1986). As control, BL21(DE3) pRSET-A was used and samples were taken before induction (0 min) and 120 min after induction. The samples were loaded onto a SDS-PAGE and stained with Coomassie afterwards. Destaining was done overnight (data not shown).

3.2.4. Western Blot analysis of selected ORFs

Samples of the time series were loaded again onto a SDS-PAGE for the Western Blot. As shown in Figure 13, signals were detected for ORF12, ORF14, ORF24, ORF25, ORF28 and ORF29. This strongly suggests that these genes encode for ϕCh1 nucleocapsids and are, therefore, part of the viral-structure. While most of the ORFs could be detected from time sample 0', this is not the case for ORF25 and the signals at the first two time points for ORF14 were also faint. ORF12 seems to be more synthesised at the beginning but in the end signals fade out. For ORF14, ORF28 and ORF29 signals became intensive over time. Protein synthesis for ORF24 and ORF25 appears to be overall stable. However, the differences seen in the expression rates are based on the *E. coli* system rather than given a hit how they are expressed in *N. magadii*.

Do these results mean that not all predicted ORFs are part of the ϕCh1 viral-structure? Not necessarily, because it could also be possible that the not detected ORFs have a lower copy number compared to the detected ORFs. Consequently, the previously produced α-ϕCh1 antiserum is only specific for the nucleocapsids encoded by highly transcribed ORFs.

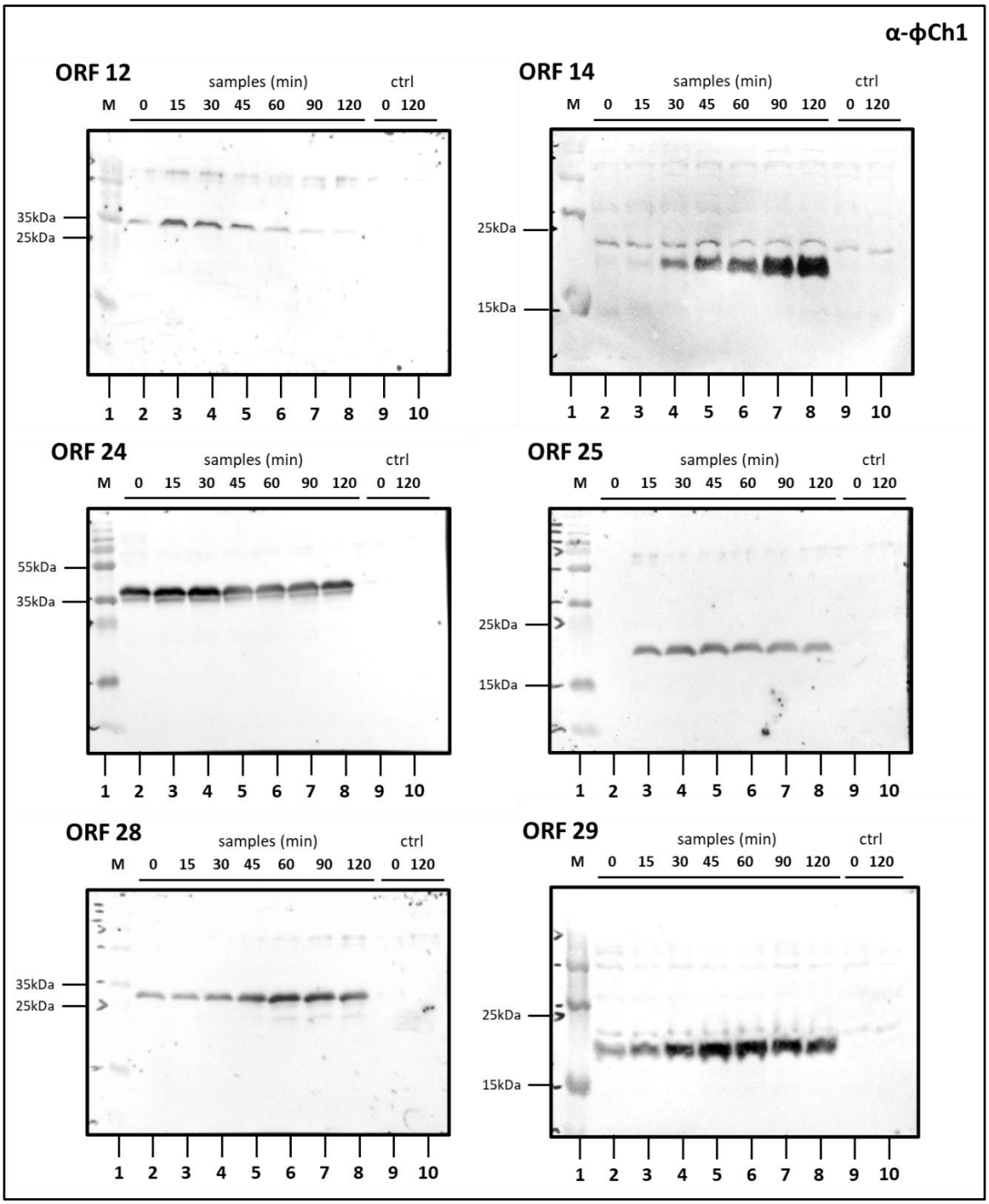

Figure 13: Western Blots of novel identified ϕCh1 nucleosidcapsids. 10 µL of each time sample were loaded into slots. ORF12, ORF14, ORF24, ORF25, ORF28 and ORF29 were identified with α-ϕCh1 antibodies and are, therefore, considered to be part of the viral-structure. ORF12 was expected at 20.548 kDa but the band appeared at ~35 kDa. ORF14 was expected at 17.548 kDa. ORF24 was expected at 23.848 kDa but double bands appeared above 35 kDa. ORF25 was expected at 17.548 kDa. ORF28 was expected at 24.848 kDa but the band appeared between 25 and 35 kDa. ORF29 was expected at 16.548 kDa.

As the ORFs are cloned between *Bam*HI and *Hin*dIII restriction sites of pRSET-A, upstream fragments including a 6x His-Taq with a total length of 4.148 kDa are also synthesised. Thus, this weight was included in the expected size of the different ORFs in the Western Blots. A summary is provided by Table 5 and as can be seen, the molecular weights as they appeared form the Western blots differ from the calculated ones. A potential reason behind this is that haloalkaliphilic proteins contain acidic amino acids (Lanyi, 1974; Larsen, 1967). Therefore, these proteins move slower in SDS gels.

ORF	theoretical MW [kDa]	expected MW with upstream Taq [kDa]	MW as in Western Blot [kDa]
ORF12	16.4	20.548	~35
ORF14	13.4	17.548	15 - 25
ORF16	15.7	19.848	N/A
ORF24	19.7	23.858	35 - 55
ORF25	13.4	17.548	15 - 25
ORF28	20.7	24.848	25 - 35
ORF29	12.4	16.548	16 - 25
ORF61	7.9	12.048	N/A
ORF71	16.4	20.558	N/A

Table 5: Molecular weights of the analysed ORFs. This table provides information on the molecular weight of the designated ORFs.

4. Conclusion

4.1. *N. magadii* recombinases RadA and RadB

This part of the study attempted to delete either *N. magadii* L13 *radA* or *radB* to analyse the responsible proteins for the inversion of the ϕCh1 invertible region comprising ORF34, *int*1 (ORF35) and ORF36. Upon successful uptake of the suicide plasmid pKSII+ containing the resistance gene and recombination of the Nov resistance cassette, the strain inherits the antibiotic cassette to their daughter cells upon doubling chromosomes during replication. Since the cultures faced antibiotic selection pressure, the distribution of the chromosome carrying the resistance gene is likely advantageous. As Figure 4 illustrates, a minimum of six generations are needed to obtain the very first homozygote. The approximate doubling time of 8 h indicates that at least 48 h are required. Hence, after one passage, which normally takes two to three days, a homozygous deletion mutant could emerge in the best case. However, this scenario with 0.001147 % is statistically very unlikely. Nevertheless, with continuous passages the probability increases to obtain cells carrying a higher chromosome number with replaced gene. Prior studies showed that homozygous deletion mutants are obtained after the 15th passage (Derntl, 2009; Schöner, 2013). Yet, *radA* was still detectable via PCR by using internal primers after 50 cycles and over 20 passages in L13 RadA^{-}Nov$^{R\text{-}fw}$ and L13 RadA^{-}Nov$^{R\text{-}rv}$, resulting in a 616 bp fragment (Figure 6, A, slot 6 and 15). The same is true for strains L13 RadB^{-}Nov$^{R\text{-}fw}$ and L13 RadB^{-}Nov$^{R\text{-}rv}$ where *radB* was still detectable via PCR by using internal primers after 50 cycles, resulting in a 606 bp fragment (Figure 6, B, slot 6 and 15). As a result, no homozygous deletion mutant could be obtained. This concludes that *radA* and *radB* appear to be essential for *N. magadii*. Hence, these genes cannot be replaced in all chromosomes by Nov resistance cassette in L13 in order to survive. To test this hypothesis, plasmids carrying either inducible antisense *radA* or *radB* RNA were cloned and time course experiments were performed. Cultures were induced with 4 mM Trp when they were close to OD_{700} 0.3. The growth kinetics showed that induction does not interfere with growth (Figure 9 and Figure 10). An interpretation is that neither *radA* nor *radB* would be essential. This is in contrast to the prior performed deletion experiment. An explanation why the strains were not affected by the antisense coding *radA* or *radB* RNA

could be that the antisense RNAs were not stable. Not only can RNA form secondary structures, but the host could also have defence mechanisms protecting the genes from silencing. However, the putative defence mechanisms behind this remains unclear. To further analyse the living organisms within a culture upon and after Trp induction, a cell count experiment could be performed. Therefore, dilution streaks of 10^{-2}, 10^{-4}, 10^{-6} and 10^{-8} of every time measure point are suggested. Future studies could focus on cloning inducible specific small antisense *radA* or *radB* coding RNA.

4.2. ΦCh1 viral-structure

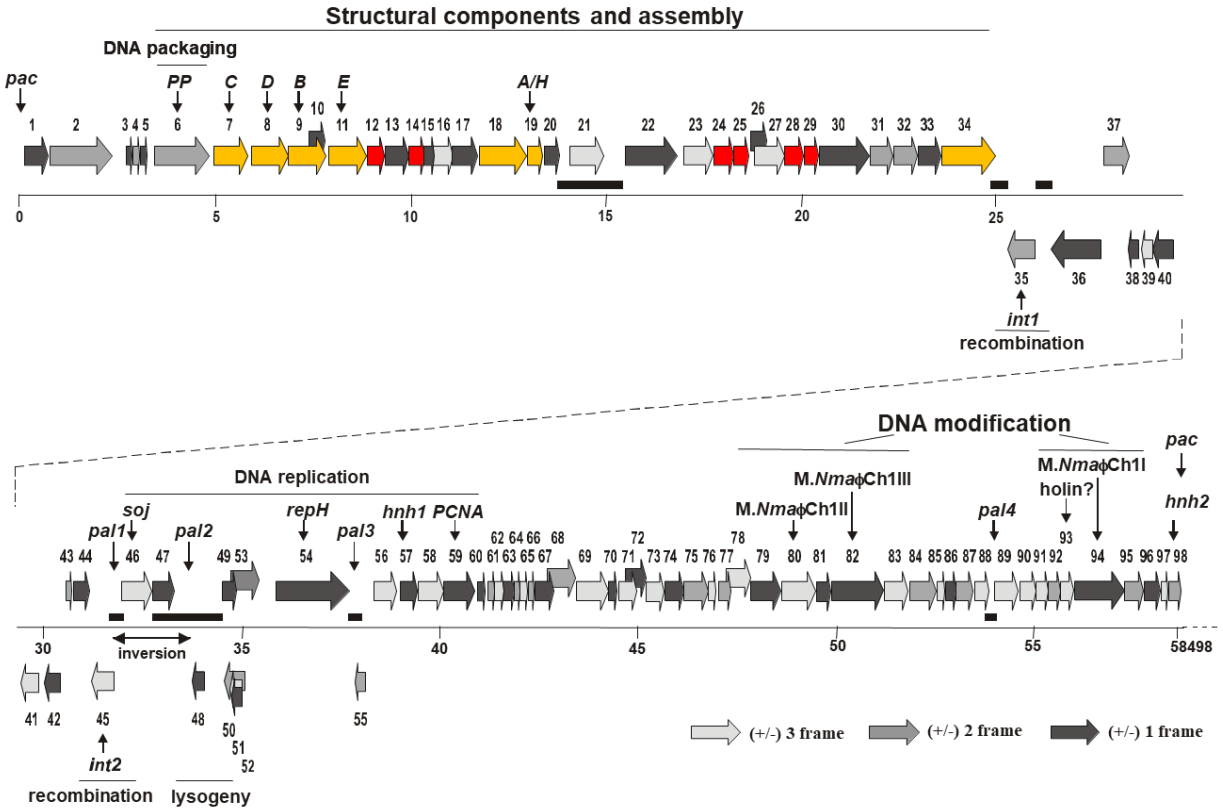

Figure 14: Gene map of ϕCh1 with marked ORFs encoding for nucleocapsids. Novel identified are marked in red and previously identified in yellow. Adapted from Klein et al. (2002).

The second part of this study aimed to identify further ϕCh1 nucleocapsid encoding ORFs. Thus, *N. magadii* strain L11 was grown until no lysis was detectable via optical density. The virus was then isolated and purified by a discontinuous followed by a continuous CsCl

gradient. Tris/HCl or HEPES were used as buffer and samples were then sent for MS analysis to IMC University of Applied Sciences Krems. However, Tris can cause problems with MS even though it is a commonly used buffer (*FAQ: Core Facility Hohenheim - Modul 1 Massenspektrometrie*, 2018; Kabadi et al., 2016). The data of these two performed MS analyses were then compared and ten ORFs putatively appeared to encode for nucleocapsids. One of these, ORF36, was not considered for further analysis because Klein et al. (2012) showed that this ORF was never transcribed. Hence, the ORF12, ORF14, ORF16, ORF24, ORF25, ORF28, ORF29, ORF61 and ORF71 were cloned into pRSET-A. Consequently, a time series was performed and after IPTG induction, samples were collected at different time points. These were then loaded onto a SDS-PAGE and a Western Blot was performed. The detection with α-ϕCh1 antibodies revealed that ORF12, ORF14, ORF24, ORF25, ORF28 and ORF29 encode for nucleocapsids (Figure 13). A summary of all structural encoding ORFs is provided in Figure 14. The not detected proteins could also be part of the ϕCh1 viral-structure because their encoding ORFs may have a lower copy number compared to the detected ones. Future studies could clone the putative nucleocapsid encoding ORF fused with the green fluorescence protein (GFP) gene under the control of an inducible promoter in a vector. Upon viral-assembly, the GFP labelled protein may get incorporated and, therefore, should be detectable on the outside of the virus. Nomura & Harada (1998) fused two recombinants of GFPs with bacteriorhodopsin and showed by the expression in *H. salinarum* and its detection that this reporter system is suitable for organisms which requires high salt concentrations.

5. List of abbreviations, figures and tables

5.1. Abbreviations

‘	minutes(s)
°C	Degree Celsius
µ	micro
µm	micrometre
Å	Ångström
Amp	ampicillin
BLAST	Basic Local Alignment Search Tool
bp	base pair(s)
Cam	chloramphenicol
DNA	deoxyribonucleic acid
fw	forward
G	generation
g	Earth’s gravitational force
GA	Gibson Assembly
GFP	green fluorescence protein
h	hour(s)
HMG-CoA	3-hydroxy-3-methylglutaryl coenzyme A
IPTG	isopropyl β-d-1-thiogalactopyranoside
k	kilo
kDa	kilo Dalton
krpm	kilo rounds per minutes
L	liter
LB	Lysogenic broth
M	molarity [mol L^{-1}]
m	milli
Mev	mevinolin (lovastatin)
min	minute(s)
mol	mole
MS	mass spectroscopy
n	nano
N/A	not available
Nov	novobiocin
nt	nucleotide(s)
NVM CAA	Natrialba rich media with casamino acids
NVM CH	Natrialba rich media with casamino hydrolysate
ORF	open reading frame
pH	potential of hydrogen
R	resistance
RNA	ribonucleic acid
rv	reversed

S	sensitive
Tet	tetracycline
Trp	tryptophan

5.2. Figures

5.3. Tables

6. References

Adams, M. W. W., & Kelly, R. M. (1995). ENZYMES FROM MICROORGANISMS IN EXTREME ENVIRONMENTS. *Chemical & Engineering News Archive*, *73*(51), 32–42. https://doi.org/10.1021/cen-v073n051.p032

Alte, B. (2011). *Konstruktion einer Flagellum-Deletionsmutante in Natrialba magadii und Charakterisierung bestehender Natrialba magadii Mutanten* [Diploma thesis, Universität Wien]. https://doi.org/10.25365/thesis.16361

Baquero, D. P., Liu, Y., Wang, F., Egelman, E. H., Prangishvili, D., & Krupovic, M. (2020). Chapter Four—Structure and assembly of archaeal viruses. In M. Kielian, T. C. Mettenleiter, & M. J. Roossinck (Eds.), *Advances in Virus Research* (Vol. 108, pp. 127–164). Academic Press. https://doi.org/10.1016/bs.aivir.2020.09.004

Baranyi, U., Klein, R., Lubitz, W., Krüger, D. H., & Witte, A. (2000). The archaeal halophilic virus-encoded Dam-like methyltransferase M.ϕCh1-I methylates adenine residues and complements dam mutants in the low salt environment of Escherichia coli. *Molecular Microbiology*, *35*(5), 1168–1179. https://doi.org/10.1046/j.1365-2958.2000.01786.x

Beer, C. (2024). *Influence of Int1 and the repeat clusters on the inversion of the central region of PhiCh1* [Master's thesis, Universität Wien]. https://doi.org/10.25365/thesis.76228

Bishop, D. K., Park, D., Xu, L., & Kleckner, N. (1992). DMC1: A meiosis-specific yeast homolog of E. coli recA required for recombination, synaptonemal complex formation, and cell cycle progression. *Cell*, *69*(3), 439–456. https://doi.org/10.1016/0092-8674(92)90446-J

Breuert, S., Allers, T., Spohn, G., & Soppa, J. (2006). Regulated Polyploidy in Halophilic Archaea. *PLOS ONE*, *1*(1), e92. https://doi.org/10.1371/journal.pone.0000092

Brown, M. S., & Goldstein, J. L. (1980). Multivalent feedback regulation of HMG CoA reductase, a control mechanism coordinating isoprenoid synthesis and cell growth. *Journal of Lipid Research*, *21*(5), 505–517.

Burnette, W. N. (1981). "Western Blotting": Electrophoretic transfer of proteins from sodium dodecyl sulfate-polyacrylamide gels to unmodified nitrocellulose and radiographic detection with antibody and radioiodinated protein A. *Analytical Biochemistry*, *112*(2), 195–203. https://doi.org/10.1016/0003-2697(81)90281-5

Cabrera, J. A., Bolds, J., Shields, P. E., Havel, C. M., & Watson, J. A. (1986). Isoprenoid synthesis in Halobacterium halobium. Modulation of 3-hydroxy-3-methylglutaryl coenzyme a concentration in response to mevalonate availability. *The Journal of Biological Chemistry*, *261*(8), 3578–3583.

Cavicchioli, R., Curmi, P. M. G., Saunders, N., & Thomas, T. (2003). Pathogenic archaea: Do they exist? *BioEssays*, *25*(11), 1119–1128. https://doi.org/10.1002/bies.10354

Cavicchioli, R., & Thomas, T. (2000). Extremophiles. In *Encylopedia of Microbiology* (2nd edition, Vol. 2, p. pp 317-337). Academic Press.

Clark, A. J., & Margulies, A. D. (1965). Isolation and characterization of recombination-deficient mutants of escherichia coli k12*. *Proceedings of the National Academy of Sciences*, *53*(2), 451–459. https://doi.org/10.1073/pnas.53.2.451

Cromie, G. A., Connelly, J. C., & Leach, D. R. F. (2001). Recombination at Double-Strand Breaks and DNA Ends: Conserved Mechanisms from Phage to Humans. *Molecular Cell*, *8*(6), 1163–1174. https://doi.org/10.1016/S1097-2765(01)00419-1

DeLong, E. (1998). Archaeal Means and Extremes. *Science*, *280*(5363), 542–543. https://doi.org/10.1126/science.280.5363.542

Derntl, C. (2009). *Construction of the first deletion mutant of a haloalkaliphilic archaeon and analysis of gene expression of the methyltransferase M.NmaϕCh1I of the halophage ϕCh1* [Diploma thesis]. Universität Wien.

Donovan, R. S., Robinson, C. W., & Glick, B. R. (1996). Review: Optimizing inducer and culture conditions for expression of foreign proteins under the control of thelac promoter. *Journal of Industrial Microbiology*, *16*(3), 145–154. https://doi.org/10.1007/BF01569997

Egelman, E. H. (2001). Does a Stretched DNA Structure Dictate the Helical Geometry of RecA-like Filaments? *Journal of Molecular Biology*, *309*(3), 539–542. https://doi.org/10.1006/jmbi.2001.4686

FAQ: Core Facility Hohenheim—Modul 1 Massenspektrometrie. (2018, September 6). [Educational Website]. Universität Hohenheim. https://ms-service.uni-hohenheim.de/84277

Friedberg, E. C., Walker, G. C., & Siede, W. (1995). *DNA Repair and Mutagenesis*. ASM Press.

George, D. G., Yeh, L.-S. L., & Barker, W. C. (1983). Unexpected relationships between bacteriophage lambda hypothetical proteins and bacteriophage T4 tail-fiber proteins. *Biochemical and Biophysical Research Communications*, *115*(3), 1061–1068. https://doi.org/10.1016/S0006-291X(83)80043-6

Grant, W. D. (2004). Life at low water activity. *Philosophical Transactions of the Royal Society of London. Series B: Biological Sciences*, *359*(1448), 1249–1267. https://doi.org/10.1098/rstb.2004.1502

Grant, W. D., Kamekura, M., Mcgenity, T., & Ventosa, A. (2001). Halobacteria (Class). In *Bergey's manual of systematic bacteriology* (2nd ed., Vol. 1, pp. 294–334). Springer-Verlag.

Guzman, L. M., Belin, D., Carson, M. J., & Beckwith, J. (1995). Tight regulation, modulation, and high-level expression by vectors containing the arabinose

PBAD promoter. *Journal of Bacteriology*, *177*(14), 4121–4130. https://doi.org/10.1128/jb.177.14.4121-4130.1995

Haldenby, S., White, M. F., & Allers, T. (2009). RecA family proteins in archaea: RadA and its cousins. *Biochemical Society Transactions*, *37*(1), 102–107. https://doi.org/10.1042/BST0370102

Hayashi, I., Morikawa, K., & Ishino, Y. (1999). Specific interaction between DNA polymerase II (PolD) and RadB, a Rad51/Dmc1 homolog, in Pyrococcus furiosus. *Nucleic Acids Research*, *27*(24), 4695–4702.

Hiestand-Nauer, R., & Iida, S. (1983). Sequence of the site-specific recombinase gene cin and of its substrates serving in the inversion of the C segment of bacteriophage P1. *The EMBO Journal*, *2*(10), 1733–1740. https://doi.org/10.1002/j.1460-2075.1983.tb01650.x

Holmes, M. L., Nuttall, S. D., & Dyall-Smith, M. L. (1991). Construction and use of halobacterial shuttle vectors and further studies on Haloferax DNA gyrase. *Journal of Bacteriology*, *173*(12), 3807–3813. https://doi.org/10.1128/jb.173.12.3807-3813.1991

Iranzo, J., Koonin, E. V., Prangishvili, D., & Krupovic, M. (2016). Bipartite Network Analysis of the Archaeal Virosphere: Evolutionary Connections between Viruses and Capsidless Mobile Elements. *Journal of Virology*, *90*(24), 11043. https://doi.org/10.1128/JVI.01622-16

Ito, N., Phillips, S. E. V., Stevens, C., Ogel, Z. B., McPherson, M. J., Keen, J. N., Yadav, K. D. S., & Knowles, P. F. (1991). Novel thioether bond revealed by a 1.7 Å crystal structure of galactose oxidase. *Nature*, *350*(6313), 87–90. https://doi.org/10.1038/350087a0

Kabadi, P. G., Sankaran, P. K., Palanivelu, D. V., Adhikary, L., Khedkar, A., & Chatterjee, A. (2016). Mass Spectrometry Based Mechanistic Insights into Formation of Tris Conjugates: Implications on Protein Biopharmaceutics. *Journal of the American Society for Mass Spectrometry*, *27*(10), 1677–1685. https://doi.org/10.1007/s13361-016-1447-4

Kamekura, M., Dyall-Smith, M. L., Upasani, V., Ventosa, A., & Kates, M. (1997). Diversity of Alkaliphilic Halobacteria: Proposals for Transfer of Natronobacterium vacuolatum, Natronobacterium magadii, and Natronobacterium pharaonis to Halorubrum, Natrialba, and Natronomonas gen. nov., Respectively, as Halorubrum vacuolatum comb. nov., Natrialba magadii comb. nov., and Natronomonas pharaonis comb. nov., Respectively. *International Journal of Systematic and Evolutionary Microbiology*, *47*(3), 853–857. https://doi.org/10.1099/00207713-47-3-853

Karner, M. B., DeLong, E. F., & Karl, D. M. (2001). Archaeal dominance in the mesopelagic zone of the Pacific Ocean. *Nature*, *409*(6819), 507–510. https://doi.org/10.1038/35054051

Klein, R., Baranyi, U., Rössler, N., Greineder, B., Scholz, H., & Witte, A. (2002). Natrialba magadii virus ϕCh1: First complete nucleotide sequence and functional organization of a virus infecting a haloalkaliphilic archaeon.

Molecular Microbiology, *45*(3), 851–863. https://doi.org/10.1046/j.1365-2958.2002.03064.x

Klein, R., Greineder, B., Baranyi, U., & Witte, A. (2000). The Structural Protein E of the Archaeal Virus ϕCh1: Evidence for Processing in Natrialba magadii during Virus Maturation. *Virology*, *276*(2), 376–387. https://doi.org/10.1006/viro.2000.0565

Klein, R., Rössler, N., Iro, M., Scholz, H., & Witte, A. (2012). Haloarchaeal myovirus ϕCh1 harbours a phase variation system for the production of protein variants with distinct cell surface adhesion specificities. *Molecular Microbiology*, *83*(1), 137–150. https://doi.org/10.1111/j.1365-2958.2011.07921.x

Komori, K., Miyata, T., DiRuggiero, J., Holley-Shanks, R., Hayashi, I., Cann, I. K. O., Mayanagi, K., Shinagawa, H., & Ishino, Y. (2000). Both RadA and RadB Are Involved in Homologous Recombination inPyrococcus furiosus *. *Journal of Biological Chemistry*, *275*(43), 33782–33790. https://doi.org/10.1074/jbc.M004557200

Koonin, E. V., Senkevich, T. G., & Dolja, V. V. (2006). The ancient Virus World and evolution of cells. *Biology Direct*, *1*(1), 29. https://doi.org/10.1186/1745-6150-1-29

Krupovic, M., Cvirkaite-Krupovic, V., Iranzo, J., Prangishvili, D., & Koonin, E. V. (2018). Viruses of archaea: Structural, functional, environmental and evolutionary genomics. *Virus Research*, *244*, 181–193. https://doi.org/10.1016/j.virusres.2017.11.025

Kushner, D. (1978). Life in high salt and solute concentrations: Halophilic bacteria. In *Microbial life in extreme environments* (pp. 317–368). Academic Press.

Ladurner, A. (2008). *Characterization of the inversion reaction of ϕCh1 and the establishment of a transformation system for Natrialba magadii* [Universität Wien]. https://doi.org/10.25365/thesis.695

Laemmli, U. K. (1970). Cleavage of Structural Proteins during the Assembly of the Head of Bacteriophage T4. *Nature*, *227*(5259), 680–685. https://doi.org/10.1038/227680a0

Lam, W. L., & Doolittle, W. F. (1992). Mevinolin-resistant mutations identify a promoter and the gene for a eukaryote-like 3-hydroxy-3-methylglutaryl-coenzyme A reductase in the archaebacterium Haloferax volcanii. *The Journal of Biological Chemistry*, *267*(9), 5829–5834.

Lanyi, J. K. (1974). Salt-dependent properties of proteins from extremely halophilic bacteria. *Bacteriological Reviews*, *38*(3), 272–290.

Large, A., Stamme, C., Lange, C., Duan, Z., Allers, T., Soppa, J., & Lund, P. A. (2007). Characterization of a tightly controlled promoter of the halophilic archaeon Haloferax volcanii and its use in the analysis of the essential cct1 gene. *Molecular Microbiology*, *66*(5), 1092–1106. https://doi.org/10.1111/j.1365-2958.2007.05980.x

Larsen, H. (1967). Biochemical Aspects of Extreme Halophilism. In A. H. Rose & J. F. Wilkinson (Eds.), *Advances in Microbial Physiology* (Vol. 1, pp. 97–132). Academic Press. https://doi.org/10.1016/S0065-2911(08)60251-9

Liu, Y., Du, S., Chen, X., Dyall-Smith, M., Jalasvuori, M., Oksanen, H. M., & ICTV Report Consortium. (2023). ICTV Virus Taxonomy Profile: Simuloviridae 2023. *Journal of General Virology*, *104*(4), 001841. https://doi.org/10.1099/jgv.0.001841

Lodwick, D., Ross, H. N. M., Harris, J. E., Almond, J. W., & Grant, W. D. (1986). Dam Methylation in the Archaebacteria. *Microbiology*, *132*(11), 3055–3059. https://doi.org/10.1099/00221287-132-11-3055

Lostroh, P. (2019). In *Molecular and Cellular Biology of Viruses* (pp. 11–13). Garland Science.

Mayrhofer-Iro, M., Ladurner, A., Meissner, C., Derntl, C., Reiter, M., Haider, F., Dimmel, K., Rössler, N., Klein, R., Baranyi, U., Scholz, H., & Witte, A. (2013). Utilization of Virus ϕCh1 Elements To Establish a Shuttle Vector System for Halo(alkali)philic Archaea via Transformation of Natrialba magadii. *Applied and Environmental Microbiology*, *79*(8), 2741–2748. https://doi.org/10.1128/AEM.03287-12

Mevarech, M., Frolow, F., & Gloss, L. M. (2000). Halophilic enzymes: Proteins with a grain of salt. *Biophysical Chemistry*, *86*(2), 155–164. https://doi.org/10.1016/S0301-4622(00)00126-5

Milligan, J. F., Groebe, D. R., Witherell, G. W., & Uhlenbeck, O. C. (1987). Oligoribonucleotide synthesis using T7 RNA polymerase and synthetic DNA templates. *Nucleic Acids Research*, *15*(21), 8783–8798. https://doi.org/10.1093/nar/15.21.8783

Milligan, J. F., & Uhlenbeck, O. C. (1989). [5] Synthesis of small RNAs using T7 RNA polymerase. In *Methods in Enzymology* (Vol. 180, pp. 51–62). Academic Press. https://doi.org/10.1016/0076-6879(89)80091-6

Montag, D., Hashemolhosseini, S., & Henning, U. (1990). Receptor-recognizing proteins of T-even type bacteriophages: The receptor-recognizing area of proteins 37 of phages T4 TuIa and TuIb. *Journal of Molecular Biology*, *216*(2), 327–334. https://doi.org/10.1016/S0022-2836(05)80324-9

Ng, W. L., & DasSarma, S. (1993). Minimal replication origin of the 200-kilobase Halobacterium plasmid pNRC100. *Journal of Bacteriology*, *175*(15), 4584–4596. https://doi.org/10.1128/jb.175.15.4584-4596.1993

Nomura, S., & Harada, Y. (1998). Functional expression of green fluorescent protein derivatives in *Halobacterium salinarum*. *FEMS Microbiology Letters*, *167*(2), 287–293. https://doi.org/10.1111/j.1574-6968.1998.tb13241.x

Oren, A. (1994). The ecology of the extremely halophilic archaea. *FEMS Microbiology Reviews*, *13*(4), 415–439. https://doi.org/10.1111/j.1574-6976.1994.tb00060.x

Oren, A. (1999). Bioenergetic Aspects of Halophilism. *Microbiology and Molecular Biology Reviews*, *63*(2), 334–348. https://doi.org/10.1128/mmbr.63.2.334-348.1999

Oren, A. (2002). Diversity of halophilic microorganisms: Environments, phylogeny, physiology, and applications. *Journal of Industrial Microbiology and Biotechnology*, *28*(1), 56–63. https://doi.org/10.1038/sj/jim/7000176

Pellegrini, L., Yu, D. S., Lo, T., Anand, S., Lee, M., Blundell, T. L., & Venkitaraman, A. R. (2002). Insights into DNA recombination from the structure of a RAD51–BRCA2 complex. *Nature*, *420*(6913), 287–293. https://doi.org/10.1038/nature01230

Pina, M., Bize, A., Forterre, P., & Prangishvili, D. (2011). The archeoviruses. *FEMS Microbiology Reviews*, *35*(6), 1035–1054. https://doi.org/10.1111/j.1574-6976.2011.00280.x

Plasterk, R. H., Brinkman, A., & van de Putte, P. (1983). DNA inversions in the chromosome of Escherichia coli and in bacteriophage Mu: Relationship to other site-specific recombination systems. *Proceedings of the National Academy of Sciences*, *80*(17), 5355–5358. https://doi.org/10.1073/pnas.80.17.5355

Prangishvili, D., Forterre, P., & Garrett, R. A. (2006). Viruses of the Archaea: A unifying view. *Nature Reviews Microbiology*, *4*(11), 837–848. https://doi.org/10.1038/nrmicro1527

Prangishvili, D., Vestergaard, G., Häring, M., Aramayo, R., Basta, T., Rachel, R., & Garrett, R. A. (2006). Structural and Genomic Properties of the Hyperthermophilic Archaeal Virus ATV with an Extracellular Stage of the Reproductive Cycle. *Journal of Molecular Biology*, *359*(5), 1203–1216. https://doi.org/10.1016/j.jmb.2006.04.027

Rashid, N., Morikawa, M., & Imanaka, T. (1996). A RecA / RAD51 homologue from a hyperthermophilic archaeon retains the major RecA domain only. *Molecular and General Genetics MGG*, *253*(3), 397–400. https://doi.org/10.1007/s004380050337

Renart, J., Reiser, J., & Stark, G. R. (1979). Transfer of proteins from gels to diazobenzyloxymethyl-paper and detection with antisera: A method for studying antibody specificity and antigen structure. *Proceedings of the National Academy of Sciences of the United States of America*, *76*(7), 3116–3120.

Rensen, E. I., Mochizuki, T., Quemin, E., Schouten, S., Krupovic, M., & Prangishvili, D. (2016). A virus of hyperthermophilic archaea with a unique architecture among DNA viruses. *Proceedings of the National Academy of Sciences*, *113*(9), 2478–2483. https://doi.org/10.1073/pnas.1518929113

Sandler, S. J., Satin, L. H., Samra, H. S., & Clark, A. J. (1996). recA -Like Genes From Three Archaean Species with Putative Protein Products Similar to Rad51 and Dmcl Proteins of the Yeast Saccharomyces Cerevisiae. *Nucleic Acids Research*, *24*(11), 2125–2132. https://doi.org/10.1093/nar/24.11.2125

Sandmeier, H. (1994). Acquisition and rearrangement of sequence motifs in the evolution of bacteriophage tail fibres. *Molecular Microbiology*, *12*(3), 343–350. https://doi.org/10.1111/j.1365-2958.1994.tb01023.x

Schnabel, H., Zillig, W., Pfäffle, M., Schnabel, R., Michel, H., & Delius, H. (1982). Halobacterium halobium phage øH. *The EMBO Journal*, *1*(1), 87–92. https://doi.org/10.1002/j.1460-2075.1982.tb01129.x

Schöner, L. (2013). *Construction of different mutants of Natrialba magadii and the influence of different ϕCh1 ORFs on N. magadii* [Master's thesis, Universität Wien]. https://doi.org/10.25365/thesis.30718

Selb, R., Derntl, C., Klein, R., Alte, B., Hofbauer, C., Kaufmann, M., Beraha, J., Schöner, L., & Witte, A. (2017). The Viral Gene ORF79 Encodes a Repressor Regulating Induction of the Lytic Life Cycle in the Haloalkaliphilic Virus ϕCh1. *Journal of Virology*, *91*(9), e00206-17. https://doi.org/10.1128/JVI.00206-17

Sensevdi, E. R., Sourrouille, Z. A., & Quax, T. E. (2024). Host range and cell recognition of archaeal viruses. *Current Opinion in Microbiology*, *77*, 102423. https://doi.org/10.1016/j.mib.2023.102423

Shinohara, A., Ogawa, H., & Ogawa, T. (1992). Rad51 protein involved in repair and recombination in S. cerevisiae is a RecA-like protein. *Cell*, *69*(3), 457–470. https://doi.org/10.1016/0092-8674(92)90447-K

Studier, F. W., & Moffatt, B. A. (1986). Use of bacteriophage T7 RNA polymerase to direct selective high-level expression of cloned genes. *Journal of Molecular Biology*, *189*(1), 113–130. https://doi.org/10.1016/0022-2836(86)90385-2

Tindall, B. J., Ross, H. N. M., & Grant, W. D. (1984). *Natronobacterium* gen. Nov. And *Natronococcus* gen. Nov., Two New Genera of Haloalkaliphilic Archaebacteria. *Systematic and Applied Microbiology*, *5*(1), 41–57. https://doi.org/10.1016/S0723-2020(84)80050-8

Torsvik, T., & Dundas, I. D. (1974). Bacteriophage of Halobacterium salinarium. *Nature*, *248*(5450), 680–681. https://doi.org/10.1038/248680a0

Towbin, H., Staehelin, T., & Gordon, J. (1979). Electrophoretic transfer of proteins from polyacrylamide gels to nitrocellulose sheets: Procedure and some applications. *Proceedings of the National Academy of Sciences of the United States of America*, *76*(9), 4350–4354.

Wais, A. C., Kon, M., Macdonald, R. E., & Stollar, B. D. (1975). Salt-dependent bacteriophage infecting Halobacterium cutirubrum and H. halobium. *Nature*, *256*(5515), 314–315. https://doi.org/10.1038/256314a0

Weaver, G. A., Krause, J. A., Miller, T. L., & Wolin, M. J. (1986). Incidence of methanogenic bacteria in a sigmoidoscopy population: An association of methanogenic bacteria and diverticulosis. *Gut*, *27*(6), 698–704. https://doi.org/10.1136/gut.27.6.698

Williams, T. A., Cox, C. J., Foster, P. G., Szöllősi, G. J., & Embley, T. M. (2020). Phylogenomics provides robust support for a two-domains tree of life. *Nature*

Ecology & Evolution, *4*(1), 138–147. https://doi.org/10.1038/s41559-019-1040-x

Witte, A., Baranyi, U., Klein, R., Sulzner, M., Luo, C., Wanner, G., Kru¨ger, D. H., & Lubitz, W. (1997). Characterization of Natronobacterium magadii phage ΦCh1, a unique archaeal phage containing DNA and RNA. *Molecular Microbiology*, *23*(3), 603–616. https://doi.org/10.1046/j.1365-2958.1997.d01-1879.x

Woese, C. R., & Fox, G. E. (1977). Phylogenetic structure of the prokaryotic domain: The primary kingdoms. *Proceedings of the National Academy of Sciences*, *74*(11), 5088–5090. https://doi.org/10.1073/pnas.74.11.5088

Woese, C. R., Kandler, O., & Wheelis, M. L. (1990). Towards a natural system of organisms: Proposal for the domains Archaea, Bacteria, and Eucarya. *Proceedings of the National Academy of Sciences*, *87*(12), 4576–4579. https://doi.org/10.1073/pnas.87.12.4576

Wu, Y., He, Y., Moya, I. A., Qian, X., & Luo, Y. (2004). Crystal Structure of Archaeal Recombinase RadA: A Snapshot of Its Extended Conformation. *Molecular Cell*, *15*(3), 423–435. https://doi.org/10.1016/j.molcel.2004.07.014

Wurzer, A. (2015). *Constructing a deletion cassette of ϕCh1 ORF44 infecting Natrialba magadii*. [Bachelor thesis]. Universität Wien.

Yang, S., VanLoock, M. S., Yu, X., & Egelman, E. H. (2001). Comparison of bacteriophage T4 UvsX and human Rad51 filaments suggests that RecA-like polymers may have evolved independently11Edited by M. Belfort. *Journal of Molecular Biology*, *312*(5), 999–1009. https://doi.org/10.1006/jmbi.2001.5025

Yang, S., Yu, X., Seitz, E. M., Kowalczykowski, S. C., & Egelman, E. H. (2001). Archaeal RadA protein binds DNA as both helical filaments and octameric rings. *Journal of Molecular Biology*, *314*(5), 1077–1085. https://doi.org/10.1006/jmbi.2000.5213

Yanisch-Perron, C., Vieira, J., & Messing, J. (1985). Improved M13 phage cloning vectors and host strains: Nucleotide sequences of the M13mpl8 and pUC19 vectors. *Gene*, *33*(1), 103–119. https://doi.org/10.1016/0378-1119(85)90120-9

Yu, X., & Egelman, E. H. (1993). DNA Conformation Induced by the Bacteriophage T4 UvsX Protein Appears Identical to the Conformation Induced by the *Escherichia coli* RecA Protein. *Journal of Molecular Biology*, *232*(1), 1–4. https://doi.org/10.1006/jmbi.1993.1363

Yu, X., Jacobs, S. A., West, S. C., Ogawa, T., & Egelman, E. H. (2001). Domain structure and dynamics in the helical filaments formed by RecA and Rad51 on DNA. *Proceedings of the National Academy of Sciences*, *98*(15), 8419–8424. https://doi.org/10.1073/pnas.111005398

Zaigler, A., Schuster, S. C., & Soppa, J. (2003). Construction and usage of a onefold-coverage shotgun DNA microarray to characterize the metabolism of the archaeon Haloferax volcanii. *Molecular Microbiology*, *48*(4), 1089–1105. https://doi.org/10.1046/j.1365-2958.2003.03497.x

Zhou, M., Xiang, H., Sun, C., & Tan, H. (2004). Construction of a novel shuttle vector based on an RCR-plasmid from a haloalkaliphilic archaeon and transformation into other haloarchaea. *Biotechnology Letters*, *26*(14), 1107–1113. https://doi.org/10.1023/B:BILE.0000035493.21986.20

Supplementary Table 1
MS with Tris/HCl

Comment	Protein ID	Organism	Description	PhiCh1_Trypsin_1 Intensity	PhiCh1_Trypsin_2 Intensity	PhiCh1_Chymotrypsin_1 Intensity	PhiCh1_Chymotrypsin_2 Intensity	PhiCh1_Chymotrypsin_Urea_1 Intensity	PhiCh1_Chymotrypsin_Urea_2 Intensity	Average Intensity	Coverage
	NP_665929.1	Natrialba phage PhiCh1	virion structural protein [Natrialba phage PhiCh1]	38.36380351	38.45679857	36.36268376	36.30964205	38.09765539	38.10693412	37.6162529	0.996884735
	NP_665936.1	Natrialba phage PhiCh1	head protein [Natrialba phage PhiCh1]	36.46614543	35.93902755	37.80336018	37.55557714	37.89066358	38.03888735	37.28227687	0.96713615
	WP_004268256.1	Natrialba magadii	hypothetical protein [Natrialba magadii]	36.42317747	36.06082421					36.24200084	0.98989899
	NP_665948.1	Natrialba phage PhiCh1	baseplate J/gp47 family protein [Natrialba phage PhiCh1]	35.07530157	35.0474047	34.44587821	34.41118097	34.97457038	34.96235443	34.81944838	0.822695035
	NP_665924.1	Natrialba phage PhiCh1	portal protein [Natrialba phage PhiCh1]	36.9132617	36.89848718	32.48726228	32.64904879	35.10855795	34.83223119	34.81480818	0.824411135
	WP_004268245.1	Natrialba magadii	hypothetical protein [Natrialba magadii]	34.65947781	34.99687237	33.71983153	33.69886445	35.06654811	34.8635632	34.50085958	0.366758242
	NP_665952.1	Natrialba phage PhiCh1	hypothetical protein PhiCh1p35 [Natrialba phage PhiCh1]	35.04367367	35.20683536	33.341741	33.87517939	34.36839975	34.01947892	34.30921801	0.524122807
ORF24	NP_665942.1	Natrialba phage PhiCh1	hypothetical protein PhiCh1p25 [Natrialba phage PhiCh1]	35.33917788	35.42883603	33.02506215	32.56889699	33.42498816	33.2613337	33.84138248	0.902173913
ORF36	NP_665954.1	Natrialba phage PhiCh1	hypothetical protein PhiCh1p37 [Natrialba phage PhiCh1]	33.71379406	30.73229445	34.26991696	34.06679625	33.76301963	34.30414714	33.47499475	0.549065421
	NP_665951.1	Natrialba phage PhiCh1	hypothetical protein PhiCh1p34 [Natrialba phage PhiCh1]	33.53342206	33.01281325	33.47952582	32.05474688	33.098115	33.21449344	33.06551941	0.915841584
	NP_665940.1	Natrialba phage PhiCh1	hypothetical protein PhiCh1p23 [Natrialba phage PhiCh1]	33.16057884	33.04397663	33.29663115	32.91824663	32.95267496	32.98997313	33.06034689	0.847345133
	NP_665937.1	Natrialba phage PhiCh1	head protein [Natrialba phage PhiCh1]	35.50489475	35.7117974	28.6364495	28.54782392	33.46175583	34.84232857	32.78417499	1
	NP_665976.1	Natrialba phage PhiCh1	hypothetical protein PhiCh1p59 [Natrialba phage PhiCh1]	34.00373938	33.73645572	31.59175767	31.46157262	32.1480281	32.11884557	32.51006651	0.511961722
	NP_665931.1	Natrialba phage PhiCh1	hypothetical protein PhiCh1p14 [Natrialba phage PhiCh1]			31.46336372	30.3077371	34.16966143	34.07235409	32.50327908	0.611111111
ORF28	NP_665946.1	Natrialba phage PhiCh1	hypothetical protein PhiCh1p29 [Natrialba phage PhiCh1]	33.29207402	32.87214344	30.74260333	30.90444003	33.22273448	32.96879869	32.333799	0.967741935
	NP_665949.1	Natrialba phage PhiCh1	baseplate protein [Natrialba phage PhiCh1]	32.52928577	32.75754322	31.66646631	31.63247232	31.87920976	32.13333869	32.09971934	0.410628019
ORF14	NP_665932.1	Natrialba phage PhiCh1	hypothetical protein PhiCh1p15 [Natrialba phage PhiCh1]	31.81340485	31.85125503	29.55851274	29.80727846	34.07422691	33.95411198	31.84313166	0.888888889
ORF25	NP_665943.1	Natrialba phage PhiCh1	hypothetical protein PhiCh1p26 [Natrialba phage PhiCh1]	33.39155919	33.97622112	25.9172914	33.34077945	29.91112451	34.28386792	31.80347393	0.815789474
	NP_665945.1	Natrialba phage PhiCh1	hypothetical protein PhiCh1p28 [Natrialba phage PhiCh1]	29.885251	30.39727223	32.08417418	31.81729754	32.09846474	32.17566772	31.4096879	0.884422111
ORF29	NP_665947.1	Natrialba phage PhiCh1	hypothetical protein PhiCh1p30 [Natrialba phage PhiCh1]	32.73714882	31.86282358	30.07015568	29.83195838	31.56358092	31.52047457	31.26435699	0.796610169
	NP_665935.1	Natrialba phage PhiCh1	hypothetical protein PhiCh1p18 [Natrialba phage PhiCh1]	32.88552957	32.90939808	29.72989763	28.40446219	30.40971657	30.61476162	30.82562761	0.772727273
ORF17	NP_665934.1	Natrialba phage PhiCh1	tail completion or Neck1 protein [Natrialba phage PhiCh1]	32.99116646	33.16116125	28.16423332	27.65217056	28.33729305	29.26685644	29.92881351	0.882758621
	NP_665925.1	Natrialba phage PhiCh1	head morphogenesis [Natrialba phage PhiCh1]	32.1729736	32.30709168	28.84439114	27.54737903	28.60062902	28.79731045	29.71162916	0.596825397
	WP_004213981.1	Natrialba magadii	ribonuclease J [Natrialba magadii]	30.66512064	30.89727687	28.02809475	27.92439291	28.43596612	28.61214689	29.09383303	0.795555556
	NP_665941.1	Natrialba phage PhiCh1	hypothetical protein PhiCh1p24 [Natrialba phage PhiCh1]	29.60391856	30.03991253	28.34908425	28.26875857	29.05423831	28.69765324	29.00226091	0.434042553
	WP_004216669.1	Natrialba magadii	surface glycoprotein [Natrialba magadii]	25.91661043	26.60372956	30.09405786	29.88362559	29.82122686	29.57196323	28.64853559	0.314465409
	WP_012996540.1	Natrialba magadii	thioredoxin domain-containing protein [Natrialba magadii]	29.02416827	28.76603588	26.63542509	26.63877351	27.10717828	27.41060287	27.59703065	0.72
	WP_191219368.1	Natrialba magadii	ABC transporter substrate-binding protein [Natrialba magadii]	27.193924	27.06283438	26.25178866	25.85734397	26.99113272	27.27316343	26.77169786	0.397341211
	WP_241432090.1	Natrialba magadii	metal-dependent transcriptional regulator [Natrialba magadii]	26.65980671	26.18798992					26.42389831	0.461538462
	WP_004268244.1	Natrialba magadii	hypothetical protein [Natrialba magadii]	26.16795388	26.20749847					26.18772617	0.609756098
	WP_004216961.1	Natrialba magadii	hypothetical protein [Natrialba magadii]	26.03135559	26.06525867					26.04830713	0.426751592
	WP_004217450.1	Natrialbaceae	MULTISPECIES: stress response translation initiation inhibitor YciH [Natrialbaceae]	25.92921993	25.82641717					25.87781855	0.536082474
	WP_004213862.1	Natrialba magadii	TIR domain-containing protein [Natrialba magadii]	25.66556189	25.79711291					25.7313374	0.346153846
	NP_665950.1	Natrialba phage PhiCh1	hypothetical protein PhiCh1p33 [Natrialba phage PhiCh1]	30.04345022	29.72693479	24.62490431	20.12472564	24.68776843	24.88334928	25.68185544	0.639175258
	WP_004216661.1	Natrialba magadii	hypothetical protein [Natrialba magadii]	25.18162727	25.67362233					25.4276248	0.081632653
	WP_004216048.1	Natrialba magadii	YhbY family RNA-binding protein [Natrialba magadii]	25.36902924	25.29084585					25.32993754	0.365853659
	WP_004214909.1	Natrialba magadii	hypothetical protein [Natrialba magadii]	25.24503995	25.40361983					25.32432989	0.453608247
	WP_004267139.1	Natrialba magadii	peptidylprolyl isomerase [Natrialba magadii]	26.67104288	26.91503495	24.38776309	22.41880832	24.68885419	25.28260376	25.06068453	0.575581395
	WP_004216743.1	Natrialba magadii	hypothetical protein [Natrialba magadii]	25.83378081	26.20286933	21.20136925	24.4653006	26.15394007	26.16224625	25.00325105	0.342105263
	WP_012996986.1	Natrialba magadii	nitrous oxide reductase accessory protein NosL [Natrialba magadii]			23.98341526	24.47687275	25.17750805	25.28942597	24.73180551	0.118997912
	WP_012996892.1	Natrialba magadii	hypothetical protein [Natrialba magadii]	0	21.34067949	30.5376271	32.05099514	31.64196914	31.56915795	24.5234048	0.445783133
	WP_004267190.1	Natrialba magadii	flagellin B1 [Natrialba magadii]			24.4191991	24.21453153	24.24723826	24.61497702	24.37398648	0.243781095
	WP_004217006.1	Natrialbaceae	MULTISPECIES: transcription elongation factor Spt5 [Natrialbaceae]	23.69014764	24.72967312					24.20991038	0.172413793
	WP_012996356.1	Natrialba magadii	thioredoxin-dependent thiol peroxidase [Natrialba magadii]	23.78961672	24.29766609					24.04364141	0.358974359
	WP_012996745.1	Natrialba magadii	chemotaxis protein CheY [Natrialba magadii]	23.64960276	24.43067765					24.04014021	0.220338983
	WP_004267426.1	Natrialba magadii	hypothetical protein [Natrialba magadii]	23.91621934	23.86429271					23.89025603	0.247191011
	WP_004215584.1	Natrialba magadii	PadR family transcriptional regulator [Natrialba magadii]	22.24839349	25.2130103					23.7307019	0.208791209
	WP_004267622.1	Natrialba magadii	50S ribosomal protein L31e [Natrialba magadii]	23.58253987	23.75722203					23.66988095	0.391304348
	WP_004267441.1	Natrialba magadii	group 1 truncated hemoglobin [Natrialba magadii]			22.11913222	21.60064606	21.56595808	28.96167216	23.56185213	0.280991736
	WP_004215031.1	Natrialba magadii	NOB1 family endonuclease [Natrialba magadii]			23.15783524	22.85231005	24.14487603	23.64542118	23.45011062	0.171052632
	WP_004267256.1	Natrialba magadii	poly-gamma-glutamate hydrolase family protein [Natrialba magadii]	24.30162639	24.16131444	23.19660633	22.17087526	23.4300108	23.36045544	23.43681478	0.230769231
	WP_004267570.1	Natrialba	MULTISPECIES: translation initiation factor eIF-1A [Natrialba]	24.1267563	24.70010058	19.21437083	22.29902603	24.14778377	24.40852489	23.14942706	0.59375
	WP_004215791.1	Natrialba magadii	signal recognition particle subunit SRP19 [Natrialba magadii]	23.052136	22.83511449					22.94362525	0.161290323
	WP_004214831.1	Natrialba magadii	type II methionyl aminopeptidase [Natrialba magadii]	22.62843531	23.21079127					22.91961329	0.036789298
	WP_004216024.1	Natrialba magadii	hypothetical protein [Natrialba magadii]	22.73686629	23.03149509					22.88418069	0.316831683
	WP_237076783.1	Natrialba magadii	S8 family serine peptidase [Natrialba magadii]			23.14123466	22.47770034	21.46997065	24.40974441	22.87466252	0.066757493
	WP_004215800.1	Natrialba magadii	BolA family transcriptional regulator [Natrialba magadii]			23.09815548	22.33162702	22.34918929	23.528748	22.82692995	0.25
	WP_237076804.1	Natrialba magadii	hypothetical protein [Natrialba magadii]	23.71324061	21.3439121	22.96398966	19.67993448	24.62896276	24.21187701	22.7569861	0.310502283
	WP_004216022.1	Natrialba	MULTISPECIES: UPF0058 family protein [Natrialba]	23.25695556	22.08338486					22.67017021	0.260869565
	WP_004267383.1	Natrialba magadii	translation initiation factor [Natrialba magadii]	23.12824831	22.17783512					22.65304171	0.489795918
ORF61	NP_665979.1	Natrialba phage PhiCh1	hypothetical protein PhiCh1p62 [Natrialba phage PhiCh1]	22.37305749	22.83823938					22.60564844	0.14084507
	WP_004217325.1	Natrialba magadii	DUF5611 family protein [Natrialba magadii]	22.47790695	22.56063487					22.51927091	0.181102362
	WP_004213960.1	Natrialba magadii	30S ribosomal protein S9 [Natrialba magadii]	22.27157145	22.56379106					22.41768126	0.257575758
	WP_004214575.1	Natrialba magadii	redoxin domain-containing protein [Natrialba magadii]	22.27812003	22.51930919					22.39871461	0.062893082
	WP_004213721.1	Natrialba magadii	adenylate kinase [Natrialba magadii]	22.23581456	22.2021461					22.21898033	0.052132701
	WP_004215640.1	Natrialba magadii	ferredoxin Fer [Natrialba magadii]	22.67514676	22.73790469	20.75916585	18.55369783	23.31124858	23.97839381	22.00259292	0.527131783
	WP_006166884.1	Natrialba	MULTISPECIES: 4a-hydroxytetrahydrobiopterin dehydratase [Natrialba]	21.1540628	22.58108953					21.86757617	0.279569892
ORF71	NP_665989.1	Natrialba phage PhiCh1	hypothetical protein PhiCh1p72 [Natrialba phage PhiCh1]	21.0265148	22.62447688					21.82549584	0.208333333
	NP_665957.1	Natrialba phage PhiCh1	hypothetical protein PhiCh1p40 [Natrialba phage PhiCh1]	22.07920431	21.5079659					21.79358511	0.180851064
	WP_004215035.1	Natrialba magadii	DUF5812 family protein [Natrialba magadii]	21.50662986	21.93396693					21.72029839	0.264705882
	WP_004267771.1	Natrialba magadii	DNA starvation/stationary phase protection protein DpsA [Natrialba magadii]	27.87636968	27.79015577	0	22.07065409	26.12235992	26.31613732	21.69594613	0.790055249
	WP_004213683.1	Natrialba magadii	30S ribosomal protein S8 [Natrialba magadii]	21.72899283	21.60463159					21.66681221	0.146153846

Supplementary Table 1
MS with Tris/HCl

Comment	Protein ID	Organism	Description	PhiCh1_Trypsin_1 Intensity	PhiCh1_Trypsin_2 Intensity	PhiCh1_Chymotrypsin_1 Intensity	PhiCh1_Chymotrypsin_2 Intensity	PhiCh1_Chymotrypsin_Urea_1 Intensity	PhiCh1_Chymotrypsin_Urea_2 Intensity	Average Intensity	Coverage
	WP_004213957.1	Natrialba	MULTISPECIES: 50S ribosomal protein L18e [Natrialba]	21.69843762	21.59434192					21.64638977	0.111111111
	WP_004216896.1	Natrialba magadii	hypothetical protein [Natrialba magadii]	21.41049545	21.8203168					21.61540613	0.1
	WP_004216339.1	Natrialba magadii	hypothetical protein [Natrialba magadii]	22.17624362	21.02231227					21.59927795	0.146666667
	WP_004216567.1	Natrialba magadii	nitrous oxide reductase accessory protein NosL [Natrialba magadii]	21.59946169	21.56575048					21.58260609	0.039473684
	WP_004215373.1	Natrialba magadii	cobalamin B12-binding domain-containing protein [Natrialba magadii]	21.73158773	21.42108376					21.57633575	0.105263158
	WP_012996932.1	Natrialba magadii	S8 family serine peptidase [Natrialba magadii]			21.77764052	20.98526146	21.40379003	21.64595926	21.45316282	0.007602339
	WP_004216483.1	Natrialba magadii	winged helix-turn-helix domain-containing protein [Natrialba magadii]	21.25216115	21.60588359					21.42902237	0.198275862
	WP_004268125.1	Natrialba magadii	aldo/keto reductase [Natrialba magadii]	21.35538148	20.9544334					21.15490744	0.051282051
	WP_004267637.1	Natrialba	MULTISPECIES: hypothetical protein [Natrialba]			20.55971587	21.55723721	21.61502901	20.86350656	21.14887216	0.551724138
	WP_004266954.1	Natrialba magadii	Rrf2 family transcriptional regulator [Natrialba magadii]	21.15795687	21.12369076					21.14082381	0.069364162
	WP_004267698.1	Natrialba magadii	hypothetical protein [Natrialba magadii]	20.98442764	21.01873334					21.00158049	0.074074074
	WP_004267302.1	Natrialbaceae	MULTISPECIES: 30S ribosomal protein S12 [Natrialbaceae]	20.94469648	20.98962387					20.96716017	0.077464789
	WP_004267615.1	Natrialba magadii	DUF424 family protein [Natrialba magadii]	20.79989066	20.91284483					20.85636775	0.103092784
	WP_004214958.1	Natrialba	MULTISPECIES: bis(5'-nucleosyl)-tetraphosphatase [Natrialba]	20.62081924	21.02849777					20.8246585	0.105633803
	WP_004214652.1	Natrialba magadii	peptide-methionine (S)-S-oxide reductase MsrA [Natrialba magadii]			20.34240134	20.15566084	21.24127795	21.05816102	20.69937529	0.146892655
	WP_004217290.1	Natrialba magadii	RNA-binding protein [Natrialba magadii]	20.47849858	20.76440683					20.6214527	0.088050314
	NP_665944.1	Natrialba phage PhiCh1	hypothetical protein PhiCh1p27 [Natrialba phage PhiCh1]	27.23022219	27.15043465	23.18758148	22.89981418	0	21.83875914	20.38446861	0.307017544
	WP_004217211.1	Natrialba magadii	GNAT family N-acetyltransferase [Natrialba magadii]			20.146555	19.51221674	20.96079534	20.84012035	20.36492186	0.073684211
	WP_004267950.1	Natrialba magadii	30S ribosomal protein S6e [Natrialba magadii]			20.43303982	20.37149995	19.90368212	20.35053771	20.2646899	0.089552239
	NP_665975.1	Natrialba phage PhiCh1	HNH endonuclease [Natrialba phage PhiCh1]	20.24842505	20.07356355					20.1609943	0.047945205
	WP_049916358.1	Natrialba magadii	CoA-binding protein [Natrialba magadii]	19.9738648	20.12852932					20.05119706	0.077464789
	NP_665980.1	Natrialba phage PhiCh1	hypothetical protein PhiCh1p63 [Natrialba phage PhiCh1]	25.70480812	25.72357179	20.22052523	0	23.37916165	23.20604226	19.70568484	0.475
	WP_004215577.1	Natrialba magadii	hypothetical protein [Natrialba magadii]	19.30546596	19.73113106					19.51829851	0.084745763
	WP_148221940.1	Natrialba magadii	hypothetical protein [Natrialba magadii]	26.3515274	26.57296038	18.72836365	0	20.5194777	23.83538507	19.33461903	0.974137931
	WP_012996289.1	Natrialba magadii	universal stress protein [Natrialba magadii]	25.59977871	25.59910071	0	20.69813922	21.92745536	21.7158776	19.25672527	0.458333333
	WP_004214225.1	Natrialba magadii	cytochrome c oxidase subunit II [Natrialba magadii]			19.96439996	19.05705966	19.0015209	18.84202095	19.21625037	0.046666667
	WP_004217072.1	Natrialba magadii	hypothetical protein [Natrialba magadii]	19.58550742	18.72918703					19.15734723	0.034615385
	WP_004214151.1	Natrialba	MULTISPECIES: cold-shock protein [Natrialba]			24.25753877	25.06593459	0	26.01269853	18.83404297	0.421875
	WP_004267634.1	Natrialba magadii	DUF1917 domain-containing protein [Natrialba magadii]	21.99689306	22.58042604	21.15813764	0	23.00908299	22.88647395	18.60516895	0.322222222
	WP_004214097.1	Natrialba magadii	archaeal proteasome endopeptidase complex subunit alpha [Natrialba magadii]	18.73051724	18.46658554					18.59855139	0.028571429
	WP_049916406.1	Natrialba magadii	DUF655 domain-containing protein [Natrialba magadii]	24.71962257	24.65167922	19.34444667	20.24762045	19.86561237	0	18.13816355	0.409090909
	WP_012996683.1	Natrialba magadii	ABC transporter substrate-binding protein [Natrialba magadii]			22.58516795	0	24.47802154	24.30471157	17.84197527	0.189189189
	WP_004214671.1	Natrialba magadii	MTH865 family protein [Natrialba magadii]	18.69701268	23.04467227	20.33588632	20.28729585	20.4136363	0	17.12975057	0.421686747
	WP_012996684.1	Natrialba magadii	ABC transporter substrate-binding protein [Natrialba magadii]			20.7926332	0	22.81319306	22.66479523	16.56765537	0.07907743
	WP_004216475.1	Natrialba magadii	glycine cleavage system protein GcvH [Natrialba magadii]			0	21.39715245	22.32708098	20.92830793	16.16313534	0.078125
	WP_237076787.1	Natrialba magadii	hypothetical protein [Natrialba magadii]			20.67128	18.86176998	0	22.57357658	15.52665664	0.041474654
	WP_004267565.1	Natrialba magadii	twin-arginine translocation signal domain-containing protein [Natrialba magadii]	23.48627615	23.49647457	0	0	23.10838918	22.4679346	15.42651242	0.127272727
	WP_076609512.1	Natrialbaceae	MULTISPECIES: translation initiation factor eIF-1A [Natrialbaceae]	23.51803562	22.92765284	0	0	21.28088243	22.91828822	15.10747652	0.382978723
	WP_004217095.1	Natrialba magadii	translation initiation factor IF-5A [Natrialba magadii]	22.14557522	22.9230808	0	0	20.8280145	21.0843721	14.49684044	0.330645161
	WP_004214879.1	Natrialba magadii	MGMT family protein [Natrialba magadii]	22.18109219	22.3906989	0	20.24450019	0	21.78161145	14.43298379	0.371794872
	WP_004215545.1	Natrialba magadii	SRPBCC family protein [Natrialba magadii]	20.91928744	21.2906157	0	0	21.64391717	19.77080169	13.937437	0.229166667
	WP_004216963.1	Natrialba	MULTISPECIES: elongation factor 1-beta [Natrialba]	0	24.04997365					12.02498682	0.113636364
	WP_004214767.1	Natrialba magadii	thioredoxin family protein [Natrialba magadii]			22.69850936	0	23.45199031	0	11.53762492	0.292682927
	WP_004266949.1	Natrialba magadii	hypothetical protein [Natrialba magadii]	21.09842828	0	0	0	22.76193982	23.56556512	11.23765554	0.376344086
	WP_012996744.1	Natrialba magadii	flagellin [Natrialba magadii]	0	22.33330715					11.16665358	0.032911392
	WP_004215841.1	Natrialba	MULTISPECIES: ribbon-helix-helix domain-containing protein [Natrialba]	22.02892131	23.44787298	0	0	21.46877889	0	11.15759553	0.283783784
	NP_666013.1	Natrialba phage PhiCh1	hypothetical protein PhiCh1p96 [Natrialba phage PhiCh1]	0	22.24741691					11.12370845	0.213483146
	WP_004213890.1	Natrialba magadii	hypothetical protein [Natrialba magadii]	0	22.01393974					11.00696987	0.141732283
	WP_012996287.1	Natrialba magadii	iron-sulfur cluster assembly accessory protein [Natrialba magadii]	0	21.21131352					10.60565676	0.14516129
	WP_004267454.1	Natrialba magadii	NifU family protein [Natrialba magadii]	21.17350025	0					10.58675013	0.109243697
	WP_004215447.1	Natrialba	MULTISPECIES: peptidyl-tRNA hydrolase Pth2 [Natrialba]	21.15084863	0					10.57542431	0.080357143
	WP_004267315.1	Natrialba magadii	HVO_0476 family zinc finger protein [Natrialba magadii]	21.05459319	0					10.52729659	0.046082949
	WP_004216526.1	Natrialba magadii	phage tail protein [Natrialba magadii]	0	20.78403611					10.39201805	0.06
	WP_004217036.1	Natrialba magadii	multiprotein-bridging factor 1 family protein [Natrialba magadii]	0	20.26142811					10.13071406	0.051724138
	WP_004215683.1	Natrialba magadii	non-histone chromosomal MC1 family protein [Natrialba magadii]			20.57194869	0	0	19.31659187	9.97213514	0.098039216
	WP_004214079.1	Natrialba magadii	phosphopantetheine adenylyltransferase [Natrialba magadii]	0	18.22636233					9.113181164	0.063583815
	WP_004268078.1	Natrialba magadii	Tfx family DNA-binding protein [Natrialba magadii]	0	17.84407263					8.922036316	0.084415584
	WP_004213647.1	Natrialba magadii	heavy-metal-associated domain-containing protein [Natrialba magadii]			0	0	0	21.50293982	5.375734955	0.376811594
	NP_666006.1	Natrialba phage PhiCh1	hypothetical protein PhiCh1p89 [Natrialba phage PhiCh1]			0	0	0	20.73252569	5.183131422	0.102564103
	WP_004267482.1	Natrialba magadii	ferredoxin [Natrialba magadii]			0	0	0	19.5383049	4.884576224	0.172839506
	WP_004216765.1	Natrialba	MULTISPECIES: 50S ribosomal protein L15e [Natrialba]	0	0					0	0.051020408
	WP_004217298.1	Natrialba magadii	GTP-dependent dephospho-CoA kinase family protein [Natrialba magadii]			0	0	0	0	0	0.235
	WP_049916085.1	Natrialba magadii	transcriptional regulator [Natrialba magadii]	0	0					0	0.088435374
	WP_004268029.1	Natrialba magadii	DUF6276 family protein [Natrialba magadii]	0	0					0	0.072847682
	WP_004217246.1	Natrialba	MULTISPECIES: 50S ribosomal protein L40e [Natrialba]	0	0					0	0.183673469

Supplementary Table 2

MS with HEPES (1/2)

Comment	PG.ProteinAccessions	PG.ProteinNames	PG.Organisms	PhiCh1_profiling.raw.PG.Label-Free Quant	PhiCh1_profiling_20240227193201.raw.PG.Label-Free Quant	PhiCh1_profiling.raw.PG.Coverag	PhiCh1_profiling_20240227193201.raw.PG.Coverag	PhiCh1_profiling.raw.PG.UniquePeptidesForQuantInRun
	WP_004268251.1	XkdF-like putative serine protease domain-containing protein	Natrialba magadii	261494300	157268430	31.50%	20.40%	5
	WP_004217347.1	MULTISPECIES: DNA-binding protein	Natrialba	37346.125	48817.74	12.10%	12.10%	1
	NP_665952.1	hypothetical protein PhiCh1p35	Natrialba phage PhiCh1	405211420	161703800	37.90%	37.70%	5
	WP_004214144.1	FAD-dependent oxidoreductase	Natrialba magadii	91183.82	121358.65	5.60%	5.60%	1
	WP_004268256.1	hypothetical protein	Natrialba magadii	674529800	295241400	93.40%	65.70%	5
	NP_665951.1;WP_004268282.1	hypothetical protein PhiCh1p34;hypothetical protein	Natrialba phage PhiCh1;Natrialba magadii	261501500	93517496	43.1%;43.1%	40.1%;40.1%	5
ORF36	NP_665954.1	hypothetical protein PhiCh1p37	Natrialba phage PhiCh1	104076456	27310216	31.80%	11.40%	5
	WP_004213683.1	30S ribosomal protein S8	Natrialba magadii	272018.38	243918.84	23.80%	14.60%	3
	WP_012997004.1	phage tail tape measure protein	Natrialba magadii	37188650	10756624	29.20%	22.60%	5
	NP_665936.1;WP_004268262.1	head protein;hypothetical protein	Natrialba phage PhiCh1;Natrialba magadii	5.04E+09	431479330	45.1%;45.1%	45.1%;45.1%	5
ORF16	NP_665934.1;WP_004268260.1	tail completion or Neck1 protein;phage virion morphogenesis protein	Natrialba phage PhiCh1;Natrialba magadii	150721700	57815470	49.7%;49.7%	49.7%;49.7%	5
	WP_004213780.1	Rrf2 family transcriptional regulator	Natrialba magadii	31698.064	39108.58	6.80%	14.10%	1
	NP_665929.1;WP_004268254.1	virion structural protein;phage major capsid protein	Natrialba phage PhiCh1;Natrialba magadii	8.90E+09	3.69E+09	77.6%;77.6%	76.3%;76.3%	5
	WP_004267139.1	peptidylprolyl isomerase	Natrialba magadii	1569845.2	35988.42	23.30%	9.30%	2
	WP_237076867.1	hypothetical protein	Natrialba magadii	6495190	1870943.8	62.50%	34.50%	5
	WP_004267426.1	hypothetical protein	Natrialba magadii	920494.4	506734.75	22.50%	22.50%	2
	WP_004268244.1	hypothetical protein	Natrialba magadii	1891560.2	104842.59	90.20%	56.10%	4
ORF24	NP_665942.1;WP_004268270.1	hypothetical protein PhiCh1p25;hypothetical protein	Natrialba phage PhiCh1;Natrialba magadii	211779500	42369930	64.7%;64.7%	42.4%;42.4%	5
	NP_665925.1;WP_004268250.1	head morphogenesis;phage minor head protein	Natrialba phage PhiCh1;Natrialba magadii	7081956	1244450.2	55.6%;55.6%	40.3%;40.3%	5
	WP_004267771.1	DNA starvation/stationary phase protection protein DpsA	Natrialba magadii	2395418.2	1154834.6	17.70%	17.10%	4
	WP_004216526.1	phage tail protein	Natrialba magadii	155337	78777.85	8%	8%	1
	WP_004216961.1	hypothetical protein	Natrialba magadii	1263351.8	1212972.9	35%	26.80%	5
	WP_004215791.1	signal recognition particle subunit SRP19	Natrialba magadii	111925.56	32661.088	14%	14%	1
	WP_004216567.1	nitrous oxide reductase accessory protein NosL	Natrialba magadii	14627.9795	0.16626677	3.90%	3.90%	1
ORF61	NP_665979.1;WP_004217566.1	hypothetical protein PhiCh1p62;hypothetical protein	Natrialba phage PhiCh1;Natrialba magadii	61970.492	NaN	14.1%;14.1%	NaN	1
	WP_049939279.1	isocitrate dehydrogenase (NADP(+))	Natrialba magadii	0.21206382	862.9652	2.60%	1.70%	1
	NP_665948.1;WP_004268277.1	baseplate J/gp47 family protein	Natrialba phage PhiCh1;Natrialba magadii	198202960	79499640	50.4%;50.4%	50.1%;50.1%	5
	WP_012996540.1	thioredoxin domain-containing protein	Natrialba magadii	2980909.5	1478772.8	44%	44%	3
	WP_004214879.1	MGMT family protein	Natrialba magadii	307543.3	202050.83	22.40%	16%	3
ORF25	NP_665943.1;WP_004268271.1	hypothetical protein PhiCh1p26;hypothetical protein	Natrialba phage PhiCh1;Natrialba magadii	26926628	7418513.5	36.8%;36.8%	36.8%;36.8%	5
	WP_004215312.1	translation elongation factor EF-1 subunit alpha	Natrialba magadii	88184.08	95572.1	2.40%	6.90%	1
ORF72	NP_665989.1;WP_004268185.1	hypothetical protein PhiCh1p72;DUF4326 domain-containing protein	Natrialba phage PhiCh1;Natrialba magadii	37668.977	NaN	8.3%;8.3%	NaN	1
ORF28	NP_665946.1;WP_004268274.1	hypothetical protein PhiCh1p29;Gp138 family membrane-puncturing spike protein	Natrialba phage PhiCh1;Natrialba magadii	170182060	51560530	61.8%;61.8%	48.9%;48.9%	5
	WP_004213862.1	TIR domain-containing protein	Natrialba magadii	2032099.9	835631.44	34%	19.20%	4
	WP_004267256.1	poly-gamma-glutamate hydrolase family protein	Natrialba magadii	7830160	1136527.9	35.70%	24.50%	5
	WP_004217450.1	MULTISPECIES: stress response translation initiation inhibitor YciH	Natrialbaceae	1464310	1139931.2	32%	19.60%	3
	WP_004214831.1	type II methionyl aminopeptidase	Natrialba magadii	0.19681546	NaN	3.70%	NaN	1
	WP_004268248.1	phage portal protein	Natrialba magadii	1.06E+09	562706370	55.50%	56.10%	5
	WP_004267482.1	ferredoxin	Natrialba magadii	469508.2	492469.47	13.60%	13.60%	1
	WP_004216669.1	surface glycoprotein	Natrialba magadii	6160683.5	4845748.5	4.30%	4.30%	1
	WP_004214273.1	FAD-dependent oxidoreductase	Natrialba magadii	507236.66	NaN	17.60%	NaN	2
	WP_004215031.1	NOB1 family endonuclease	Natrialba magadii	31012.484	136540.34	9.20%	9.20%	1
	WP_012996745.1	chemotaxis protein CheY	Natrialba magadii	64640.086	NaN	11%	NaN	1
	WP_004214182.1	hypothetical protein	Natrialba magadii	35309.195	12719.458	6.40%	6.40%	1
	WP_004267622.1	50S ribosomal protein L31e	Natrialba magadii	173857.14	43829.5	25%	8.70%	2
	NP_665935.1;WP_004268261.1	hypothetical protein PhiCh1p18;hypothetical protein	Natrialba phage PhiCh1;Natrialba magadii	18285906	899133	40.4%;40.4%	22.2%;22.2%	4
	WP_012996718.1	nascent polypeptide-associated complex protein	Natrialba magadii	34238.004	42734.695	8.10%	8.10%	1
	NP_665937.1;WP_004268265.1	head protein;hypothetical protein	Natrialba phage PhiCh1;Natrialba magadii	73741220	78679336	100%;100%	100%;100%	5
	WP_257719839.1	catalase/peroxidase HPI	Natrialba magadii	128565.33	20037.475	1.90%	1.90%	1
	NP_665949.1;WP_004268278.1	baseplate protein;hypothetical protein	Natrialba phage PhiCh1;Natrialba magadii	35015652	10558604	33.3%;34.2%	15%;15.3%	5
	WP_004215841.1	MULTISPECIES: ribbon-helix-helix domain-containing protein	Natrialba	55929.96	NaN	25.70%	NaN	1
	WP_004214958.1	MULTISPECIES: bis(5'-nucleosyl)-tetraphosphatase	Natrialba	85513.89	63440.207	10.60%	10.60%	1
	WP_237076804.1	hypothetical protein	Natrialba magadii	166050.94	24682.623	5%	5%	2
	WP_004216896.1	hypothetical protein	Natrialba magadii	10964.76	4965.4746	10%	10%	1
	WP_004216022.1	MULTISPECIES: UPF0058 family protein	Natrialba	0.30011526	75951.91	13%	13%	1
ORF14	NP_665932.1;WP_012997003.1	hypothetical protein PhiCh1p15;hypothetical protein	Natrialba phage PhiCh1;Natrialba magadii	194892640	90178504	36.5%;36.5%	19.8%;19.8%	3
	WP_004216423.1	glutaredoxin family protein	Natrialba magadii	0.1142857	110441.266	10.50%	10.50%	1
	WP_148221940.1	hypothetical protein	Natrialba magadii	28987280	897529.06	20.70%	7.80%	2
	WP_004216661.1	hypothetical protein	Natrialba magadii	291965.22	62471.855	8.20%	8.20%	1
	WP_004267359.1	hypothetical protein	Natrialba magadii	0.3966287	26554.049	18.30%	18.30%	1
	WP_004216963.1	MULTISPECIES: elongation factor 1-beta	Natrialba	91429.02	237571.08	29.50%	29.50%	3
	WP_004216339.1	hypothetical protein	Natrialba magadii	121813.08	NaN	8.70%	NaN	1
	WP_006166884.1	MULTISPECIES: 4a-hydroxytetrahydrobiopterin dehydratase	Natrialba	7114.4604	NaN	25.80%	NaN	1
	WP_004215584.1;WP_0042669	PadR family transcriptional regulator	Natrialba magadii	178905.62	45434.547	12.1%;11.8%	12.1%;11.8%	1
	WP_004267570.1	MULTISPECIES: translation initiation factor eIF-1A	Natrialba	481653.56	59231.246	28.10%	8.30%	2
	WP_004214171.1	molecular chaperone DnaK	Natrialba magadii	625.8292	5245.264	1.40%	1.40%	1
	WP_004215335.1	50S ribosomal protein L44e	Natrialba magadii	8256.682	NaN	10.80%	NaN	1
	WP_004217246.1	MULTISPECIES: 50S ribosomal protein L40e	Natrialba	21268.758	31511.035	18.40%	18.40%	1
ORF29	NP_665947.1;WP_004268276.1	hypothetical protein PhiCh1p30;hypothetical protein	Natrialba phage PhiCh1;Natrialba magadii	64212300	9986264	76.3%;76.3%	75.4%;75.4%	5
	WP_012997006.1	hypothetical protein	Natrialba magadii	21902650	8176683.5	4.50%	4.50%	1
	WP_004217290.1	RNA-binding protein	Natrialba magadii	108760.914	50500.793	8.80%	8.80%	1
	WP_004214909.1	hypothetical protein	Natrialba magadii	107936.79	259956.12	28.90%	51.50%	2
	WP_004216048.1	YhbY family RNA-binding protein	Natrialba magadii	773554	NaN	25.60%	NaN	1
	WP_004213930.1	DUF2150 family protein	Natrialba magadii	117747.6	108376.73	6.20%	6.20%	1
	WP_004267454.1	NifU family protein	Natrialba magadii	623638.25	223638.47	16.80%	10.90%	2
	NP_665944.1	hypothetical protein PhiCh1p27	Natrialba phage PhiCh1	357465.66	755658.5	17.50%	17.50%	1
	WP_004215487.1	thiamine pyrophosphate-dependent enzyme	Natrialba magadii	52365.777	686.754	3.20%	3.20%	1
	WP_004215913.1	archaeal proteasome endopeptidase complex subunit alpha	Natrialba magadii	183237.1	81950.19	9.20%	9.20%	2
	WP_004215447.1	MULTISPECIES: peptidyl-tRNA hydrolase Pth2	Natrialba	141232.44	23895.52	8%	8%	1
	NP_665950.1;WP_004268280.1	hypothetical protein PhiCh1p33;hypothetical protein	Natrialba phage PhiCh1;Natrialba magadii	35660144	10402026	56.2%;56.2%	15.5%;15.5%	5
	WP_004213797.1	DUF371 domain-containing protein	Natrialba magadii	19074.838	2944.0625	5.80%	5.80%	1
	WP_004267531.1	DUF1684 domain-containing protein	Natrialba magadii	8094.6685	12107.9795	5.60%	5.60%	1

Supplementary Table 2

MS with HEPES (1/2)

Comment	PG.ProteinAccessions	PG.ProteinNames	PG.Organisms	PhiCh1_profiling.raw.PG.Label-Free Quant	PhiCh1_profiling_20240227193201.raw.PG.Label-Free Quant	PhiCh1_profiling.raw.PG.Coverage	PhiCh1_profiling_20240227193201.raw.PG.Coverage	PhiCh1_profiling.raw.PG.UniquePeptidesForQuantInRun
	WP_004213981.1	ribonuclease J	Natrialba magadii	58251.03	25383.203	2.40%	2.40%	1
	WP_004268078.1	Tfx family DNA-binding protein	Natrialba magadii	53336.39	25408.676	8.40%	8.40%	1
ORF12	NP_665930.1;WP_004268255.1	hypothetical protein PhiCh1p13;hypothetical protein	Natrialba phage PhiCh1;Natrialba magadii	18700.428	18780.41	14.3%;14.3%	14.3%;14.3%	1
	WP_004214766.1	Glu/Leu/Phe/Val dehydrogenase dimerization domain-containing protein	Natrialba magadii	NaN	25770.713	NaN	3.40%	NaN
	WP_004215737.1	2-oxo acid dehydrogenase subunit E2	Natrialba magadii	NaN	105813.16	NaN	2.60%	NaN
	WP_004214961.1	DUF5797 family protein	Natrialba magadii	NaN	15400.208	NaN	16.20%	NaN
	WP_004215577.1	hypothetical protein	Natrialba magadii	NaN	13382.342	NaN	8.50%	NaN
	WP_004267565.1	twin-arginine translocation signal domain-containing protein	Natrialba magadii	NaN	31674.768	NaN	12.10%	NaN
	WP_004267063.1	CBS domain-containing protein	Natrialba magadii	NaN	8288.607	NaN	4.40%	NaN
	WP_004267478.1	malate dehydrogenase	Natrialba magadii	NaN	36371.324	NaN	2.30%	NaN
	WP_004267120.1	DUF5817 domain-containing protein	Natrialba magadii	NaN	9113.619	NaN	4.60%	NaN
	WP_049916406.1	DUF655 domain-containing protein	Natrialba magadii	NaN	682.68066	NaN	5.60%	NaN
	WP_004267908.1	UPF0179 family protein	Natrialba magadii	NaN	40788.55	NaN	7.40%	NaN
	WP_004267135.1	hypothetical protein	Natrialba magadii	NaN	20938.957	NaN	8.70%	NaN
	WP_241432090.1	metal-dependent transcriptional regulator	Natrialba magadii	NaN	123611.984	NaN	16%	NaN

Supplementary Table 2
MS with HEPES (2/2)

Comment	PG.ProteinAccessions	PhiCh1_profiling_20240227193201.raw.PG.UniquePeptidesForQuantInRur	PhiCh1_profiling.raw.PG.QValue	PhiCh1_profiling_20240227193201.raw.PG.QValue	PhiCh1_profiling.raw.PG.UniquePeptide	PhiCh1_profiling_20240227193201.raw.PG.UniquePeptides	PhiCh1_profiling.raw.PG.UniquePeptidesForQuan	PhiCh1_profiling_20240227193201.raw.PG.UniquePeptidesForQuant
	WP_004268251.1	5	0	0	13	13	7	7
	WP_004217347.1	1	0	0	1	1	1	1
	NP_665952.1	5	0	0	19	19	5	5
	WP_004214144.1	1	0	0	1	1	1	1
	WP_004268256.1	5	0	0	18	18	6	6
	NP_665951.1;WP_004268282.1	4	0	0	6	6	6	6
ORF36	NP_665954.1	3	0	0	8	8	6	6
	WP_004213683.1	2	0	0	3	3	3	3
	WP_012997004.1	5	0	0	19	19	6	6
	NP_665936.1;WP_004268262.1	5	0	0	11	11	6	6
ORF16	NP_665934.1;WP_004268260.1	5	0	0	7	7	5	5
	WP_004213780.1	2	0	0	2	2	2	2
	NP_665929.1;WP_004268254.1	5	0	0	25	25	6	6
	WP_004267139.1	1	0	0	2	2	2	2
	WP_237076867.1	5	0	0	10	10	6	6
	WP_004267426.1	2	0	0	2	2	2	2
	WP_004268244.1	2	0	0	4	4	4	4
ORF24	NP_665942.1;WP_004268270.1	5	0	0	9	9	6	6
	NP_665925.1;WP_004268250.1	5	0	0	8	8	5	5
	WP_004267771.1	3	0	0	4	4	4	4
	WP_004216526.1	1	0	0	1	1	1	1
	WP_004216961.1	4	0	0	5	5	5	5
	WP_004215791.1	1	0	0	1	1	1	1
	WP_004216567.1	1	0	0	1	1	1	1
ORF61	NP_665979.1;WP_004217566.1	NaN	0	NaN	1	NaN	1	NaN
	WP_049939279.1	1	0	0	2	2	2	2
	NP_665948.1;WP_004268277.1	5	0	0	24	24	8	8
	WP_012996540.1	3	0	0	3	3	3	3
	WP_004214879.1	2	0	0	3	3	3	3
ORF25	NP_665943.1;WP_004268271.1	5	0	0	7	7	5	5
	WP_004215312.1	3	0	0	3	3	3	3
ORF72	NP_665989.1;WP_004268185.1	NaN	0	NaN	1	NaN	1	NaN
ORF28	NP_665946.1;WP_004268274.1	5	0	0	13	13	5	5
	WP_004213862.1	3	0	0	4	4	4	4
	WP_004267256.1	4	0	0	7	7	5	5
	WP_004217450.1	2	0	0	3	3	3	3
	WP_004214831.1	NaN	0.009345794	NaN	1	NaN	1	NaN
	WP_004268248.1	5	0	0	30	30	7	7
	WP_004267482.1	1	0	0	1	1	1	1
	WP_004216669.1	1	0	0	1	1	1	1
	WP_004214273.1	NaN	0	NaN	2	NaN	2	NaN
	WP_004215031.1	1	0	0	1	1	1	1
	WP_012996745.1	NaN	0.009345794	NaN	1	NaN	1	NaN
	WP_004214182.1	1	0	0	1	1	1	1
	WP_004267622.1	1	0	0	2	2	2	2
	NP_665935.1;WP_004268261.1	2	0	0	4	4	4	4
	WP_012996718.1	1	0	0	1	1	1	1
	NP_665937.1;WP_004268265.1	5	0	0	12	12	7	7
	WP_257719839.1	1	0	0	1	1	1	1
	NP_665949.1;WP_004268278.1	4	0	0	6	6	5	5
	WP_004215841.1	NaN	0	NaN	1	NaN	1	NaN
	WP_004214958.1	1	0	0	1	1	1	1
	WP_237076804.1	2	0	0	2	2	2	2
	WP_004216896.1	1	0	0	1	1	1	1
	WP_004216022.1	1	0	0	1	1	1	1
ORF14	NP_665932.1;WP_012997003.1	2	0	0	3	3	3	3
	WP_004216423.1	1	0	0	1	1	1	1
	WP_148221940.1	1	0	0	2	2	2	2
	WP_004216661.1	1	0	0	1	1	1	1
	WP_004267359.1	1	0	0	1	1	1	1
	WP_004216963.1	2	0	0	3	3	3	3
	WP_004216339.1	NaN	0	NaN	1	NaN	1	NaN
	WP_006166884.1	NaN	0	NaN	1	NaN	1	NaN
	WP_004215584.1;WP_00426692	1	0	0	1	1	1	1
	WP_004267570.1	1	0	0	2	2	2	2
	WP_004214171.1	1	0	0	1	1	1	1
	WP_004215335.1	NaN	0.009345794	NaN	1	NaN	1	NaN
	WP_004217246.1	1	0	0	1	1	1	1
ORF29	NP_665947.1;WP_004268276.1	5	0	0	9	9	6	6
	WP_012997006.1	1	0	0	1	1	1	1
	WP_004217290.1	1	0	0	1	1	1	1
	WP_004214909.1	3	0	0	3	3	3	3
	WP_004216048.1	NaN	0	NaN	1	NaN	1	NaN
	WP_004213930.1	1	0	0	1	1	1	1
	WP_004267454.1	1	0	0	2	2	2	2
	NP_665944.1	1	0	0	1	1	1	1
	WP_004215487.1	1	0	0	1	1	1	1
	WP_004215913.1	2	0.009345794	0.009345794	2	2	2	2
	WP_004215447.1	1	0	0	1	1	1	1
	NP_665950.1;WP_004268280.1	4	0	0	6	6	5	5
	WP_004213797.1	1	0	0	1	1	1	1
	WP_004267531.1	1	0	0	1	1	1	1
	WP_004213981.1	1	0	0	1	1	1	1
	WP_004268078.1	1	0	0	1	1	1	1

Supplementary Table 2
MS with HEPES (2/2)

Comment	PG.ProteinAccessions	PhiCh1_profiling_20240227193201.raw.PG.UniquePeptidesForQuantInRun	PhiCh1_profiling.raw.PG.QValue	PhiCh1_profiling_20240227193201.raw.PG.QValue	PhiCh1_profiling.raw.PG.UniquePeptide	PhiCh1_profiling_20240227193201.raw.PG.UniquePeptides	PhiCh1_profiling.raw.PG.UniquePeptidesForQuan	PhiCh1_profiling_20240227193201.raw.PG.UniquePeptidesForQuant
ORF12	NP_665930.1;WP_004268255.1	1	0	0	1	1	1	1
	WP_004214766.1	1	NaN	0	NaN	1	NaN	1
	WP_004215737.1	1	NaN	0	NaN	1	NaN	1
	WP_004214961.1	1	NaN	0	NaN	1	NaN	1
	WP_004215577.1	1	NaN	0	NaN	1	NaN	1
	WP_004267565.1	1	NaN	0	NaN	1	NaN	1
	WP_004267063.1	1	NaN	0	NaN	1	NaN	1
	WP_004267478.1	1	NaN	0	NaN	1	NaN	1
	WP_004267120.1	1	NaN	0	NaN	1	NaN	1
	WP_049916406.1	1	NaN	0	NaN	1	NaN	1
	WP_004267908.1	1	NaN	0	NaN	1	NaN	1
	WP_004267135.1	1	NaN	0	NaN	1	NaN	1
	WP_241432090.1	1	NaN	0.009345794	NaN	1	NaN	1